GRAZIELA DOS SANTOS PAULINO

MATERIAIS CELULÓSICOS: ISOLAMENTO DE NANOCRISTAIS A PARTIR DA BIOMASSA DE CAFÉ E FUNCIONALIZAÇÃO DE MEMBRANAS PARA REMOÇÃO DE CONTAMINANTES EM ÁGUAS RESIDUAIS

Tese apresentada à Universidade Federal de Viçosa, como parte das exigências do Programa de Pós-Graduação em Bioquímica Aplicada, para obtenção do título de Doctor Scientiae.

Orientador: Tiago Antônio de Oliveira Mendes
Coorientadora: Deusanilde de Jesus Silva

VIÇOSA - MINAS GERAIS
2023

Ficha catalográfica elaborada pela Biblioteca Central da Universidade Federal de Viçosa - Campus Viçosa

T
P328m
2023

Paulino, Graziela dos Santos, 1996-
Materiais celulósicos: isolamento de nanocristais a partir da biomassa de café e funcionalização de membranas para remoção de contaminantes em águas residuais / Graziela dos Santos Paulino. – Viçosa, MG, 2023.
1 tese eletrônica (79 f.): il. (algumas color.).

Texto em português e inglês.
Inclui anexo.
Orientador: Tiago Antônio de Oliveira Mendes.
Tese (doutorado) - Universidade Federal de Viçosa, Departamento de Bioquímica e Biologia Molecular, 2023.
Inclui bibliografia.
DOI: https://doi.org/10.47328/ufvbbt.2023.777
Modo de acesso: World Wide Web.

1. Celulose. 2. Nanocristais de celulose. 3. Café. 4. Biomassa. 5. Águas residuais - Purificação - Filtração. I. Mendes, Tiago Antônio de Oliveira, 1986-. II. Universidade Federal de Viçosa. Departamento de Bioquímica e Biologia Molecular. Programa de Pós-Graduação em Bioquímica Aplicada. III. Título.

CDD 22. ed. 572.56682

Bibliotecário(a) responsável: Bruna Silva CRB-6/2552

GRAZIELA DOS SANTOS PAULINO

MATERIAIS CELULÓSICOS: ISOLAMENTO DE NANOCRISTAIS A PARTIR DA BIOMASSA DE CAFÉ E FUNCIONALIZAÇÃO DE MEMBRANAS PARA REMOÇÃO DE CONTAMINANTES EM ÁGUAS RESIDUAIS

Tese apresentada à Universidade Federal de Viçosa, como parte das exigências do Programa de Pós-Graduação em Bioquímica Aplicada, para obtenção do título de Doctor Scientiae.

APROVADA: 28 de agosto de 2023.

Assentimento:

gov.br Documento assinado digitalmente
GRAZIELA DOS SANTOS PAULINO
Data: 21/12/2023 16:51:09-0300
Verifique em https://validar.iti.gov.br

Graziela dos Santos Paulino
Autor

gov.br Documento assinado digitalmente
TIAGO ANTONIO DE OLIVEIRA MENDES
Data: 20/12/2023 18:56:55-0300
Verifique em https://validar.iti.gov.br

Tiago Antônio de Oliveira Mendes
Orientador

"O correr da vida embrulha tudo. A vida é assim: esquenta e esfria, aperta e daí afrouxa, sossega e depois desinquieta. O que ela quer da gente é coragem"

(Guimarães Rosa)

À minha família e amigos.

AGRADECIMENTOS

Agradecer é um ato de expressar todo o amor e alegria que sentimos pelas pessoas e pela nossa jornada. Agradeço ao Autor da vida, por ser a minha fonte de amor inesgotável, força e alegria.

A minha mãe (Maria Aparecida) que na sua simplicidade me mostrou que o amor é algo que doa tudo que há de bom, que o amor é a força que nos move, que nos coloca de joelho se necessário e nos faz rezar com todo o coração pelos que amamos, é a energia que nos levanta e nos faz continuar, é o dilatar do coração que sente compaixão pelos os que não nos pode retribuir e que nada no mundo se compara ao valor de ter a consciência e coração tranquilos. Obrigada, Mamãe!

Aos meus irmãos e amigos, que foram a alegria e a distração de todos os dias, que me aconselharam mesmo quando eram eles que precisavam de conselhos, que compartilharam cafés e risadas, almoços, passeios e piadas ruins. Que me fizeram entender que o amor é simples e despretensioso. Obrigada, "meus xuxuzinhos!"

Aos meus orientadores, o professor Tiago e a professora Deusanilde, que estiveram sempre presentes, e que fizeram crescer ainda mais meu carinho e respeito pela ciência, que me aconselharam profissionalmente e foram compreensivos sempre que precisei. Que são referências, modelos e inspirações para a profissional que quero tornar-me. E dos quais eu terei orgulho em dizer que tive o prazer de trabalhar e ser orientada, a vocês minha gratidão!

Aos amigos de pesquisa, colegas de trabalho, aos técnicos e aos laboratórios que me receberam com toda a disposição do mundo e me auxiliaram em todas as etapas desse trabalho, sem vocês não seria possível concluir essa tese! Obrigada, vocês são e foram incríveis.

À Universidade Federal de Viçosa, pela oportunidade de realizar a pós-graduação e por toda a estrutura oferecida.

O presente trabalho foi realizado com apoio da Coordenação de Aperfeiçoamento de Pessoal de Nível Superior – Brasil (CAPES) – Código de Financiamento 001.

À Coordenação de Aperfeiçoamento de Pessoal de Nível Superior (CAPES), pela concessão da bolsa de estudos.

"O saber contra a ignorância, a saúde contra a doença, a vida contra a morte… Mil reflexos da Batalha Permanente em que todos estamos envolvidos."
(Oswaldo Cruz)

"Estou entre aqueles que pensam que a ciência tem uma grande beleza."

(Marie Curie)

RESUMO

Paulino, Graziela dos Santos, D.Sc., Universidade Federal de Viçosa, agosto de 2023. **Materiais celulósicos: isolamento de nanocristais a partir da biomassa de café e funcionalização de membranas para remoção de contaminantes em águas residuais**. Orientador: Tiago Antônio de Oliveira Mendes. Coorientadora: Deusanilde de Jesus Silva.

Esta tese é apresentada em forma de artigo e divide-se em dois capítulos distintos. Assim sendo, são apresentados neste trabalho na secção "resumo" dois resumos de artigos, cada resumo refere-se a um artigo em específico desta tese.

Grãos de café de baixa qualidade como nova fonte de biomassa de nanocristais de celulose: extração e aplicação em embalagens

Resíduos vegetais gerados a partir de processos industriais ou agroindustriais podem resultar em produtos de alto valor agregado. Devido à presença de compostos funcionais com grande potencial tecnológico, como celulose, lignina, hemicelulose, metabólitos secundários, entre outros. Além disso, o reaproveitamento da biomassa contribui para a criação de alternativas verdes para o descarte do grande volume de biomassa gerado. Neste trabalho, foram extraídos nanocristais de celulose a partir de grãos de café arábica de baixa qualidade descartados durante o processamento de grãos de café na agroindústria. Os grãos de café arábica foram coletados, higienizados, triturados, clarificados por tratamento alcalino e submetidos à hidrólise ácida com ácido sulfúrico 65% m/v. Os nanocristais de celulose extraídos apresentaram formato de agulha, com altura e comprimento médios de 7,27 nm e 221,34 nm, respectivamente. Esses nanocristais mostraram-se estáveis em meio aquoso em pH 7 e 8, com um potencial elétrico de 22,5 mV e 20,5 mV, nessa ordem. O seu índice de cristalinidade foi de 67,75% e a sua taxa de degradação térmica de apenas 8%. Por fim, os nanocristais de celulose de café produzidos neste trabalho foram adicionados a matriz polimérica de metil celulose para avaliar sua capacidade como agente de fortalecimento térmico. Os resultados demonstraram que a presença de nanocristais de celulose de café não afetou significativamente a resistência à degradação térmica dos filmes produzidos. No entanto, foram capazes de diminuir o teor de umidade desses filmes, não afetou o grau de transparência dos mesmos, e ainda, agiram como barreira de proteção contra a luz ultravioleta.

Palavras-chave: nanocristais de celulose, café, reaproveitamento de resíduos, cristalinidade, hidrólise ácida, bioplásticos, metil-celulose.

Otimizando a eficiência da remoção de material genético de SARS-CoV-2 de águas residuais sintéticas usando UVC e membranas de celulose derivadas

Os SARS-CoV-2 são transmitidos principalmente por gotículas respiratórias e partículas de aerossóis. No entanto, como para outros CoVs, esse vírus também pode ser eliminado de pacientes sintomáticos ou assintomáticos por meio das fezes, uma excreção comumente descartada em águas residuais. Assim, neste trabalho foi avaliada a capacidade de remoção de material genético SARS-CoV-2 de efluentes sintéticos usando um protótipo de baixo custo contendo uma membrana de celulose funcionalizada com grupos alquilamônia e alquilamina acoplada à luz UVC. O protótipo utilizado mostra que um curto tempo de exposição ao UVC (5 min) já é possível degradar mais de 60% do gene N-SARS-CoV-2. Além disso, observamos uma remoção de aproximadamente 100% do material genético avaliado quando a membrana de celulose foi derivatizada com $QASN^{+}(CH_2)_3$. Portanto, esse protótipo pode ser utilizado tanto para a remoção de material genético de microrganismos patogênicos, quanto para a retirada dos próprios microorganismos patogênicos viáveis, de águas residuárias. Especialmente, em áreas onde o saneamento básico é deficiente ou inexistente, além disso, sua aplicação em efluentes hospitalares pode minimizar o risco de contaminação em épocas de surtos epidêmicos, garantindo a segurança da população.

Palavras-chaves: membrana de celulose, Covid, tratamento de efluente, UV, aminas quaternárias.

ABSTRACT

Paulino, Graziela dos Santos, D.Sc., Universidade Federal de Viçosa, agosto de 2023. **Cellulosic materials: isolation of nanocrystals from coffee biomass and functionalization of membranes to remove contaminants in wastewater.** advisor: Tiago Antônio de Oliveira Mendes. Co-advisor: Deusanilde de Jesus Silva.

This thesis is presented in the form of an article and is divided into two distinct chapters. Therefore, two article summaries are presented in this work, each summary refers to a specific article from this thesis.

Low quality coffee beans as a new source of cellulose nanocrystal biomass: extraction and application in packaging

Plant residues generated from industrial or agro-industrial processes can result in products with high added value. Due to the presence of functional compounds with great technological potential, such as cellulose, lignin, hemicellulose, secondary metabolites, among others. Furthermore, the reuse of biomass contributes to the creation of green alternatives for disposing of the large volume of biomass generated. In this work, cellulose nanocrystals were extracted from low-quality Arabica coffee beans discarded during the processing of coffee beans in the agribusiness. Arabica coffee beans were collected, sanitized, crushed, clarified by alkaline treatment and subjected to acid hydrolysis with sulfuric acid 65% w/v. The extracted cellulose nanocrystals were needle-shaped, with an average height and length of 7.27 nm and 221.34 nm, respectively. These nanocrystals were stable in aqueous media at pH 7 and 8, with an electrical potential of 22.5 mV and 20.5 mV, in that order. Its crystallinity index was 67.75% and its thermal degradation rate was only 8%. Finally, the coffee cellulose nanocrystals produced in this work were added to the methyl cellulose polymeric matrix to evaluate their capacity as a thermal strengthening agent. The results demonstrated that the presence of coffee cellulose nanocrystals did not significantly affect the resistance to thermal degradation of the films produced. However, they were able to reduce the moisture content of these films, did not affect their degree of transparency, and also acted as a protective barrier against ultraviolet light.

Keywords: cellulose nanocrystals, crystallinity, acid hydrolysis, thermogravimetry.

Optimizing the Efficiency of Removal of SARS-CoV-2 Genetic Material from Synthetic Wastewater Using UVC and Derived Cellulose Membranes

SARS-CoV-2 is mainly transmitted by respiratory droplets and aerosol particles. However, as for other CoVs, this virus can also be shed from symptomatic or asymptomatic patients through feces, an excretion commonly discarded in wastewater. Thus, in this work, the ability to remove SARS-CoV-2 genetic material from synthetic effluents was evaluated using a low-cost prototype containing a cellulose membrane functionalized with alkylammonium and alkylamine groups coupled to UVC light. The prototype used shows that a short exposure time to UVC (5 min) is already possible to degrade more than 60% of the N-SARS-CoV-2 gene. Furthermore, we observed a removal of approximately 100% of the genetic material evaluated when the cellulose membrane was derivatized with $QASN^{+}(CH_2)_3$. Therefore, this prototype can be used both for the removal of genetic material from pathogenic microorganisms, and for the removal of viable pathogenic microorganisms themselves, from wastewater. Especially in areas where basic sanitation is deficient or non-existent, in addition, its application in hospital effluents can minimize the risk of contamination in times of epidemic outbreaks, ensuring the safety of the population.

Keywords: cellulose membrane, Covid, effluent treatment, UV, quaternary amines.

Sumário

1. INTRODUÇÃO GERAL

Nas últimas décadas pesquisas em diversas áreas envolvendo biomateriais, energia renovável e química verde ganharam destaque. Os três ramos de pesquisas visam desenvolver tecnologias capazes de suprir parcialmente ou totalmente as diferentes demandas de mercado, e ao mesmo tempo diminuir o uso de matérias-primas não renováveis e seu impacto ambiental (Bozell,2001). O **gráfico 1** mostra a evolução em números de pesquisas envolvendo fontes renováveis. Uma das aplicações mais recorrentes, é a troca de moléculas de fontes não renováveis por moléculas de fontes renováveis. Por exemplo, produção de etanol de segunda geração pela fermentação do bagaço de cana-de-açúcar; uso de óleo vegetal para produzir moléculas de interesse industrial como o ácido palmítico; uso de celulose para a produção de moléculas como xilose e glicose; produção de biosurfactantes por microorganismos; uso de polímeros advindos de biomassa vegetal, animal ou de microorganismos para produção de bioembalagens, materiais condutores e implante tecidual, entre muitas outras aplicações emergentes (Cherubini, 2010; Reshmy et al., 2021).

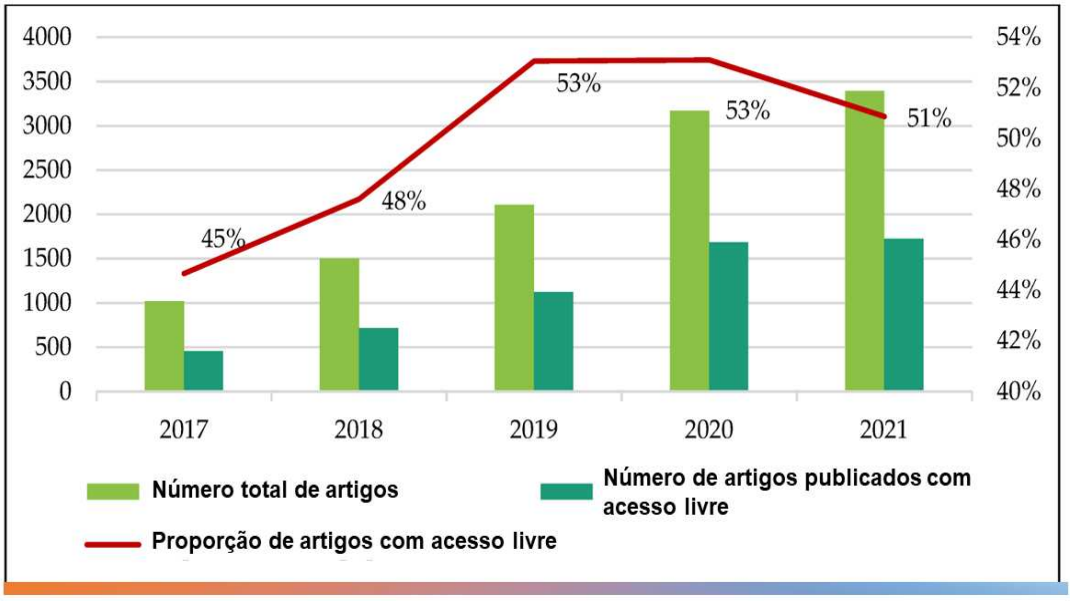

Gráfico 1: Números de artigos publicados entre os anos de 2017 até 2021 relacionados aos temas" Bioecnomia" e "Produto de base ecológica". A pesquisa foi realizada por D'Adamo e colaboradores, 2022. A base de dados foi a Web of Science e as informações foram acessadas em 27 de outubro de 2021. **Fonte:** Gráfico adaptado de D'Adamo e colaboradores, 2022.

Biomassa é uma das principais fontes de biomoléculas com viés sustentável, sendo definida como toda e qualquer fonte carbônica e renovável de origem vegetal, animal, ou

microbiológica que pode ser utilizada para fins tecnológicos. Tais como, produção de energia, fabricação ou extração de insumos bioquímicos, fabricação de biomateriais, entre outros (Ning et al., 2021)). Nesse cenário, a biomassa vegetal é que mais se destaca, para se ter uma ideia, a fixação de carbono pelas copas das árvores amazônicas é cerca de 1 tC ha $^{-1}$ ano^{-1} e por árvores de florestas secundárias com mais de 20 anos é cerca 3 tC ha^{-1}ano^{-1} (Boina,2008 apud grace, et al., 1996; Ortiz, 1997), acrescentada a produção de biomassa pelas florestas, existe a produção agrícola de biomassa vegetal, assim a biomassa vegetal é abundante.

Esforços para a utilização de biomassa vegetal vem aumentando gradativamente em todo mundo, principalmente devido ao forte apelo econômico e ambiental. A biomassa vegetal possui grande flexibilidade de utilização, podendo ser usada para a produção de combustíveis verdes, tais como, bioetanol, biodiesel, carvão e gás; na produção de produtos biodegradáveis a partir de fibras vegetais, como é o caso dos biopolímeros aplicados nas indústrias de embalagens, farmacêutica, automobilísticas e médica; na produção de derivados e percursores químicos de interesse industrial como: O ácido levulínico, glicose, sorbitol, ácido linoleico, surfactantes, derivados de furanos, celulose, lignina e seus aromáticos, aminoácidos e muitas outras moléculas (Isikgor & Becer, 2015).

As moléculas lignoceluloticas recebem grande destaque nesse contexto, a diversidade química e a complexidade estrutural das moléculas que formam a biomassa lignoceluloticas podem ser aplicadas em diversos campos da biotecnologia gerando produtos de valor agregado. No geral a biomassa lignoceluloticas é composta por 10–25% de lignina, 20–40% de hemicelulose e 40–60% de celulose, a estrutura química básica dessas biomoléculas são mostradas na **figura 1** (Ning, et al.2021). O estudo e o emprego biotecnológico de biomassa lignoceluloticas é amplo e variado. Sua aplicação pode ser encontrada em: produtos farmacêuticos e alimentícios; produção de plásticos, tintas e adesivos; nanomateriais; biomedicina e biorremediação. A **tabela 1** sumariza os principais produtos obtidos de biomassa lignoceluloticas.

Dentre as macromoléculas das fibras lignoceluloticas, a celulose é mais valorizada. Seu uso é datado desde 105 d.C na China, quando o papel foi criado pelo inventor T'sai Lun e sua fórmula química foi determinada 1838 pelo químico francês Anselme Payen. As primeiras aplicações da celulose focam em sua estrutura macroscópica, especialmente devido a sua flexibilidade e resistência (Trache et al., 2020). No entanto, o uso tradicional da celulose não é capaz de responder as altas demandas e as complexidades tecnológicas

exigidas pela sociedade moderna.

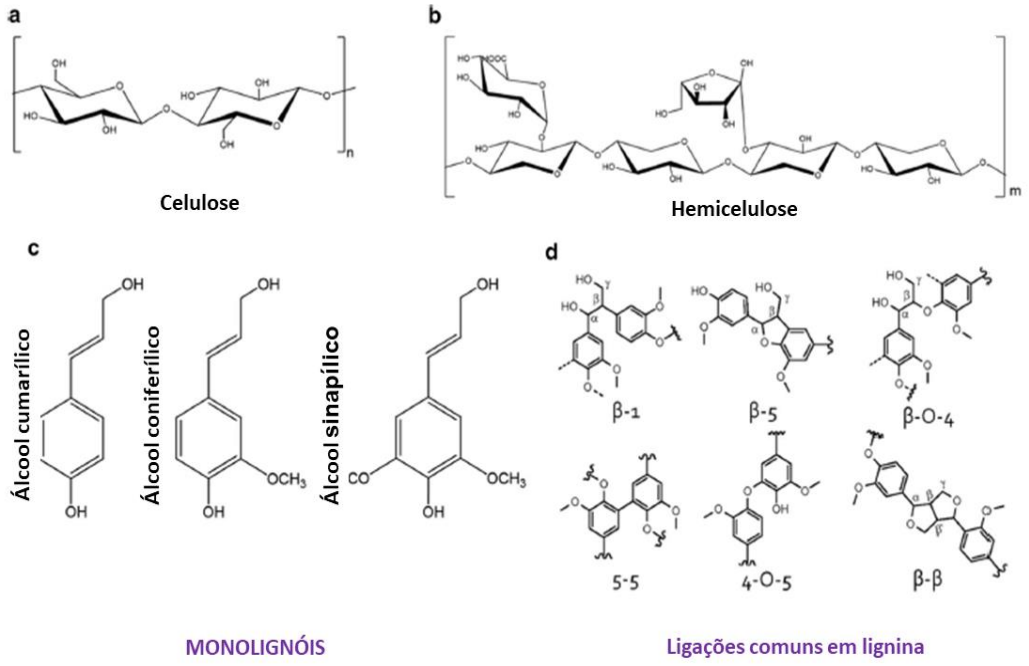

Figura 1: Principais biomoléculas que compõe a biomassa lignoceluloticas. a) Celulose; b) hemicelulose; c) monolignóis; d) ligações químicas comuns entre os monômero de lignina. **Fonte:** Imagem adaptada de Ning, et al.2021.

Tabela 1: Derivados lignocelulósicos de valor agregado

Macromolécula	Moléculas derivadas de baixo peso molecular	Produto final
Celulose e Hemicelulose	Glicose; xilose; arabinose sorbitol, manitol, frutose e sacarose.	Álcoois (etanol, butanol, xilitol, glicerol); Furanos (Furfural, 5-hidroxi-metil-furfural) Ácidos orgânicos (ácido láctico, ácido acético, ácido butílico); Polímeros (PHA, PHB, ácido poliláctico); Alcanos líquidos (hexano e pentano); Aminoácidos (glicina, aspartato, lisina).
Lignina	Compostos aromáticos com diferentes estruturas químicas	Biochar, bio-óleos, compostos aromáticos; biogás, gás de síntese.

Atualmente pesquisas voltadas para celulose em nanoescala tem demonstrado que as nanopartículas de celulose apresentam vantagens tecnológicas, e potencial para aplicações de alta performance em engenharia e biotecnologia. A nanocelulose tem características físico-química que garantem a essas partículas vantagens tecnológicas quando comparada a celulose fibrilar (Aziz, et al., 2022). Essas nanopartículas apresentam maior cristalinidade, alto módulo de elasticidade quando comparado ao Kevlar e outros polímeros de reforço, baixa densidade, maior área de superfície e alta reatividade química devido a presença dos grupamentos -OH livres (Aziz, et al., 2022). Essas nanopartículas tem sido empregadas na fabricação de embalagens para alimentos; no tratamento de água; em dispositivos eletrônicos e óptico, na biomedicina e em muitos outros campos (Ghasemlou, et al., 2021). Por exemplo, Zhong et al, 2020., produziu nanocristais de celulose a partir da reciclagem de tecido denim tingido com corante índigo, quando esses nanocristais de celulose de denim (CNC-denim) foram usados como agentes de reforço em filme de álcool polivinílico (PVA), os compósitos com até 5% m/m (CNC-denim/PVA) obtiveram maior resistência a tração quando comparados aos filmes de PVA puro, e também apresentaram uma maior barreira de proteção contra a luz ultravioleta (UV). Já Abouzeid e colaboradores, 2018., fabricaram scaffolds biomédicos usando hidrogel de nanofibrila de celulose/alginato reticulado com cálcio, os scaffolds demonstraram estabilidade, resistência e biocompatibilidade para serem aplicados como " andaimes" na engenharia óssea.

No contexto atual, as principais vantagens do uso de nanocelulose são suas propriedades mecânicas, comportamento óptico, sua hidrofilicidade e biocompatibilidade, seu baixo custo e renovabilidade. Além disso, a nanocelulose pode ser derivatizada quimicamente para que adquira as características necessárias para sua aplicação, alguns exemplos de modificações químicas de nanocelulose são: esterificação, aminação, oxidação, sililação, sulfonação e fosforilação (Ghasemlou, et al., 2021).

O mercado de nanocelulose se mostra economicamente viável e com projeções positiva de crescimento. Até 2032 espera-se que esse o mercado de nanocelulose alcance cerca de 1,45 milhões de dólares. A **figura 2** resume o crescimento econômico do setor de nanocelulose, e a **figura 3** apresenta os principais investidores e seguimentos de mercado para essa nanopartícula.

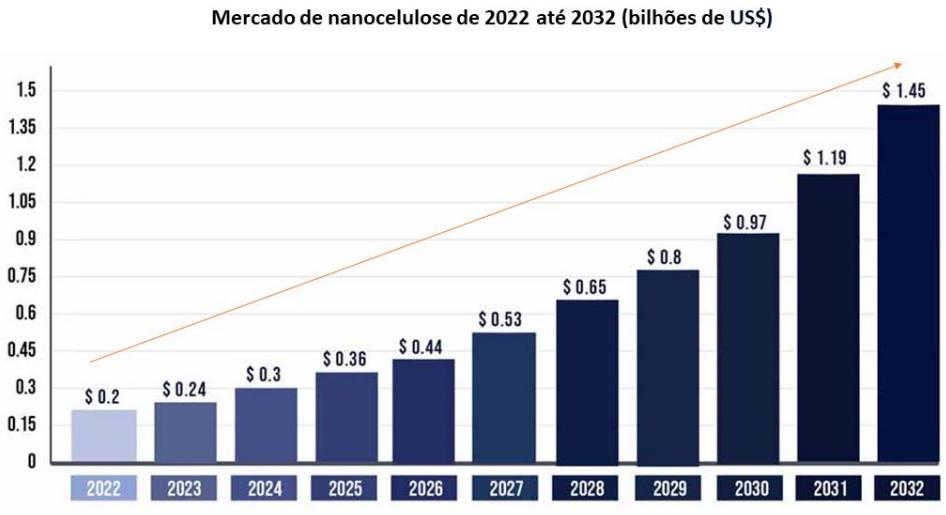

Figura 2: Crescimento em bilhões de dólar do mercado de nanocelulose, projetado de 2022 a 2023. **Fonte:** Gráfico adaptado da companhia "Precedence Research" site: <https://www.precedenceresearch.com/nanocellulose-market>.

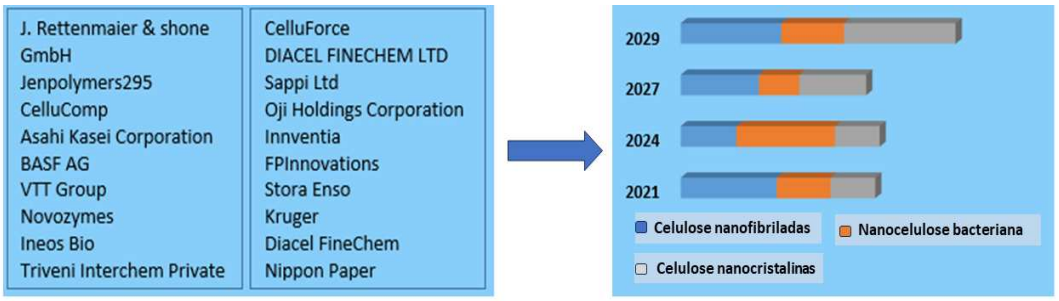

Empresas atuante no mercado de nanocelulose

Principais segmentos do mercado de nanocelulose

Figura 3: Empresas envolvidas no mercado de nanocelulose e seus segmentos de atuação. **Fonte:** Imagem adaptada de "Maximize market research" site:< https://www.maximizemarketresearch.com/market-report/global-nanocellulose market/16711/>.

1.1 Estrutura química e organização da celulose

A celulose é o polímero de carboidrato natural não ramificado mais abundante na terra, é formada pela ligação glicosídica β1-4 entre monômeros de glicose, rotacionadas em 180°, sua unidade básica é a molécula de celobiose (**Figura 4**). O seu grau de polimerização (número de unidades de glicose anidra ligadas entre si) em espécies vegetais, normalmente se encontra dentro da faixa de 300 a 15.000 unidades (Zhang et al., 2021).

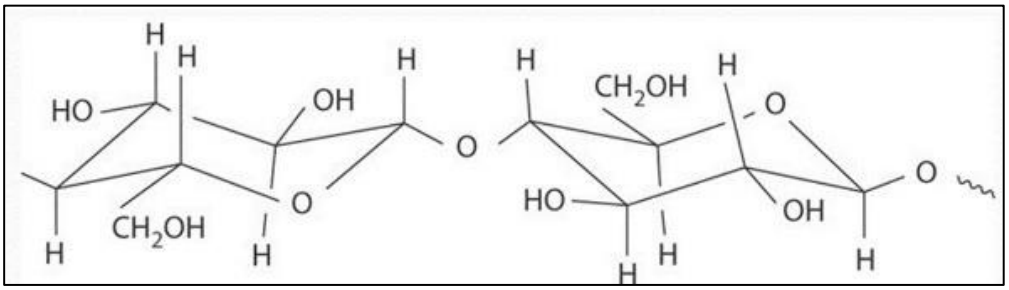

Figura 4: Unidade repetitiva da celulose (celobiose). **Fonte:** Imagem livre.

Sua organização macromolecular (**Figura 5)** se origina a partir de unidades fibrilares, as unidades fibrilares são filamentos lineares de celulose, essas estruturas são organizadas em feixes paralelos, conectados por múltiplas ligações cruzadas intermolecular e intramolecular de hidrogênio, o que confere um arranjo semi-cristalino a essa estrutura. Cada feixe contém em médias 36 unidades paralelas, esse conjunto é denominado microfibrilas que também estão associadas a polímeros não celulósicos como hemicelulose, lignina, pectina, glicoproteínas, ceras e óleos (Seddiqi, et al., 2021; Lindman, et al., 2017; Blanco et al., 2018).

A organização em microfibrilas e a sua associação com moléculas de hemicelulose e lignina, confere a celulose uma alta resistência mecânica, sendo que, a proporção de moléculas não-celulósicas associados a estrutura depende da fonte vegetal. O grau cristalinidade é dependente tanto da fonte de origem, como dos tratamentos que a celulose é submetida. Em madeiras o grau de cristalinidade varia entre 40-60%, em contraste, a celulose bacteriana pode apresentar um grau de cristalinidade de até 100% (Djafari Petroudy,2017; Nishiyama, 2009).

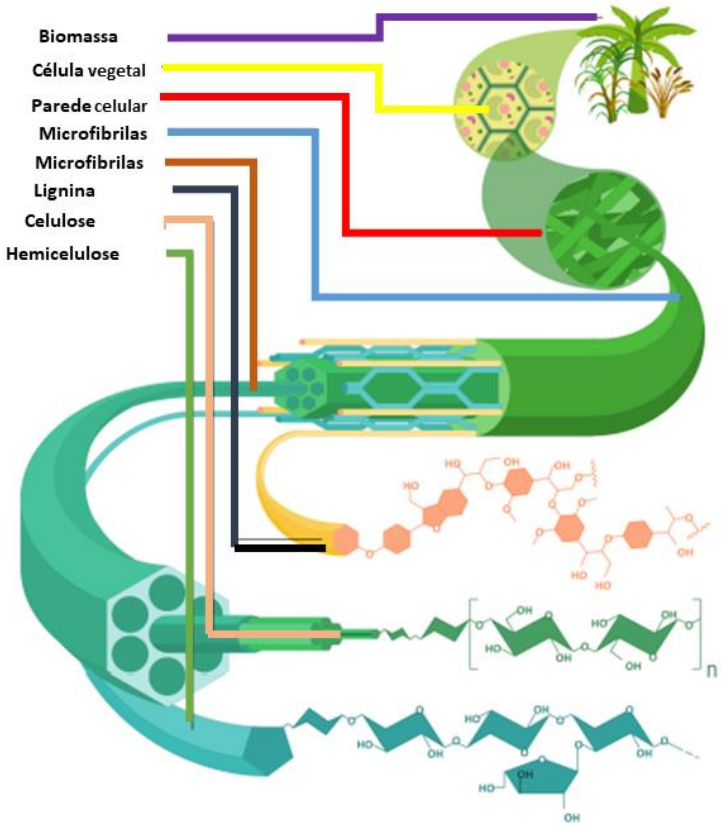

Figura 5: Organização macromolecular das fibras lignocelulóticas. **Fonte:** Imagem adaptada de Magalhães Jr, et al., 2019.

Por ser semi-cristalina, a celulose apresenta duas regiões, uma cristalina e uma amorfa que se diferenciam de forma gradual ao longo das microfibrilas, essas duas regiões são importantes para as propriedades físico-química e biológica da celulose, a região amorfa apresenta moléculas de celulose com estrutura desorganizada, resultado das quebras de ligação de hidrogênios entre as moléculas de celulose, e maior proporção de hemicelulose e lignina. Já a região cristalina, tem alta organização entre as moléculas de celulose e é menos hidratada que a região amorfa, e menor é a proporção de moléculas não celulósicas, ou seja, hemicelulose e lignina (Blake et al., 2006; Ruel et al., 2012, 2019; Seddiqi, et al, 2021).

A proporção dessas duas regiões dentro da estrutura microfibrilar da celulose, influência diretamente em seu comportamento físico-químico e mecânico, por exemplo, celulose com grande porção amorfa absorve mais água e umidade e são mais sensíveis a degradação térmica, efeito contrário acontece em celulose com maiores porções de regiões cristalinas, essas celuloses apresentam resistência maior ao elongamento e a reações químicas e possuem menor grau de hidratação, além disso, em procariotos, várias famílias de hidrólases glicosídicas são capazes de diferenciar entre a região amorfa e a região cristalina da celulose para realizar a clivagem. (Gröndahl et al., 2021; Ergun, et al.,

2016).

Segundo De Avila Delucis, e colaboradores (2021), a celulose é classificada em quatro polimorfismos estruturais: Celulose I, Celulose II, Celulose III e Celulose IV, como descritos em seguida:

Celulose tipo I: Encontrada em diversas espécies de plantas como em madeiras e algas, é organizada com folhas paralelas de celulose. Sua estrutura cristalina é composta por dois tipos metaestável de cristais Iα e Iβ. Quando tratada com soluções alcalinas a celulose tipo I é convertida em celulose tipo II (**Figura 6**).

Celulose tipo II: É a morfologia encontrada na maioria das plantas e organismos, sendo ponderada como a estrutura química mais estável. Suas microfibrilas são arranjadas de forma antiparalela que confere maior estabilidade nas interações químicas.

Celulose tipo III: A celulose tipo III pode ser dividida em dois subgrupos: Celulose tipo III_1 e Celulose tipo III_2. Essa estrutura existe apenas quando as celuloses do tipo I e II são submetidas a tratamentos com amônia líquida.

Celulose tipo IV: É derivada do tratamento térmico a partir de 260°C em uma solução de glicerol da celulose tipo III independente dos seus subgrupos.

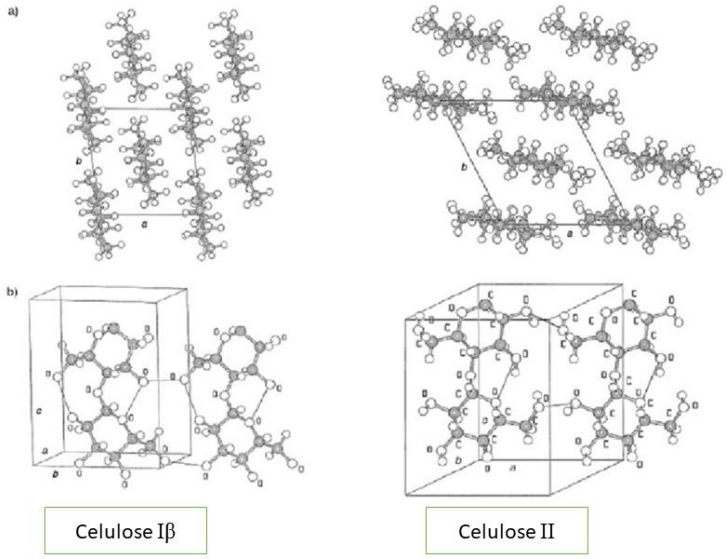

Figura 6: Polimorfismo da celulose (Celulose Iβ e Celulose II). **Fonte:** Imagem adaptada de Goyal, et al., 2008 apud Klemm et al., 2005.

1.2 Nanocristais de celulose

A celulose é um polímero abundante, quimicamente versátil e biodegradável. Essas características despertam interesses da comunidade científica, especialmente, devido a sua biodegrabilidade, e por ser derivada de fontes renováveis, incluindo resíduos agroindustriais. Pesquisa com nanocristais tiveram um aumento considerável ao longo dos anos, saltando de 77 artigos científicos em 2011 para 1469 artigos científicos em 2021 (Peter et al., 2022; Owoyokun et al., 2021).

Quando submetida a tratamentos mecânicos, enzimáticos e químicos, como, a hidrólise ácida, a celulose é capaz de ser quebrada em unidades nanoméricas. Uma vez com dimensões de nanopartículas, as microfibrilas de celulose apresentam características físico-químicas que se diferem das macromoléculas e apresentam uma gama variada de aplicabilidade (Shojaeiarani et al., 2021; S. Xie et al., 2018).

As nanopartículas de celulose, também denominadas como celulose nanofribiladas e nanocristais de celulose (**Figura 7**), apresentam dimensões variadas e a literatura científica não possuí um consenso sobre quais são as dimensões limites para nanocristais de celulose. No entanto, ao menos uma das dimensões desses partículas deve ser nanoméricas, tendo valores entre 1 e 100 nm de diâmetro ou a largura.

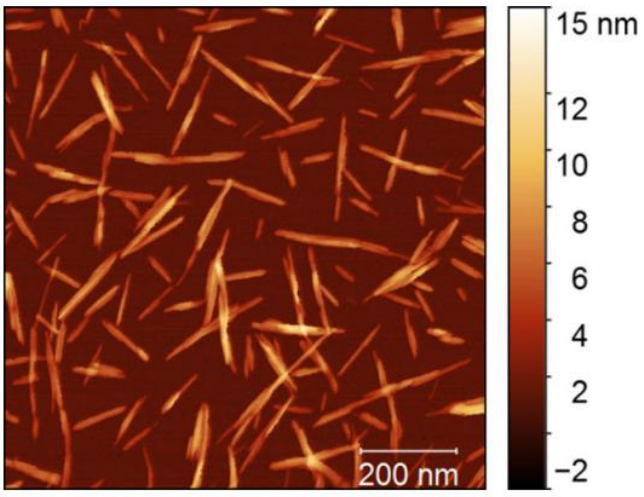

Figura 7: Microscopia de força atômica (AFM) de nanocristais de celulose de polpa de madeira maciça. **Fonte:** Imagem extraída de Chen e colaboradores, 2021.

Em média a nanocelulose produzida de fontes vegetais, tem largura ou diâmetro entre 3-50 nm e o cumprimento de 100 – 300 nm. Vale ressaltar, que essas dimensões dependem da fonte vegetal, método de extração celulose e método de produção de

nanocelulose, a morfologia mais comum dessas nanopartículas é a de bastão ou agulha (Trache et al., 2020; Owoyokun et al., 2021; Mariano et al., 2014). A **tabela 2** descreve as dimensões de nanocristais de celulose, extraída de diversas fontes vegetais.

Os nanocristais de celulose são classificados como semi-cristalino, o que lhe confere simultaneamente, resistência mecânica e maleabilidade. Podemos discutir as propriedades dos nanocristais de celulose usando dois eixos principais: Propriedade mecânica e química.

Medir essas variáveis em nanocristais de celulose, não é uma tarefa simples, especialmente devido ao seu tamanho e a sua anisotropia, além disso, diferentes técnicas de medição resultam em resultados distintos. No geral, as pesquisas apontam que a resistência a tração de nanocristais de celulose podem variar de acordo com a fonte vegetal e o seu processamento, no entanto, em média a nanocelulose possui módulo de resistência a tração em torno de 7.5-7.7 GPa e alto grau de elasticidade entre 110-220 GPa. Seu grau de elasticidade é comparável com os graus de elasticidade de materiais com o vidro e a poliamida, com módulos de elasticidade entre 63-110 GPa e 63-67 GPa respectivamente (Rowell et al., 2012; Tingaut et al., 2012; Grishkewich et al., 2017; Kim et al., 2015).

Outras características importantes das nanopartículas são a sua razão de aspecto e sua cristalinidade. Quanto menor a nanopartícula, maior é o número de átomos em sua superfície, isso permite que as nanopartículas, como os nanocristais de celulose, tenham uma maior razão de aspecto, o que resulta em um maior número de interações químicas com outras moléculas, estabelecendo dessa forma interações químicas de longo e curto alcance. No que diz respeito ao grau de cristalinidade de nanocelulose, estudos demonstram que a cristalinidade afeta diretamente o comportamento físico-químico dessas partículas, tais como, propriedade mecânica, ópticas, reológica, reatividade química, resistência térmica. Em conjunto, a razão de aspecto e a cristalinidade dos nanocristais de celulose, influenciam em sua aplicação tecnológica, por exemplo, quanto maior a razão de aspecto e a cristalinidade, melhor é resistência mecânica de diversos compósitos contendo nanocristais de celulose, pois, há um aumento do módulo de Young. (Yang et al., 2023 Wu et al., 2019, Daicho et al., 2018; Quadros & Marr, 2010).

Tabela 2: Dimensões de nanocristais de celulose extraída de diversas fontes vegetais

Biomassa vegetal	Largura/diâmetro (nm)	Comprimento (nm)	Método de produção	Referência
Casca de jaca	130	346	Clorito de sódio e ultrassom	Trilokesh & Uppuluri, 2019
Polpa de madeira	6-11	116-210	Hidrolise com ácido sulfúrico	Korolovych et al., 2018
Grãos de café	NA	120	Hidrolise ácida com ácido sulfúrico	Deb Dutta et al., 2021
Resíduos de tomate	4.7-10.2	367-510	Hidrólise ácida com ácido sulfúrico ou fosfórico ou cítrico	Kassab et al., 2020

Os nanocristais de celulose possuem vários grupamentos -OH livres em sua superfície, o que a torna uma partícula extremamente versátil em termos de modificações químicas, sejam elas covalentes ou não. Uns dos objetivos mais comuns dessas modificações dos grupamentos -OH da superfície dos nanocristais de celulose é aumentar a sua dispersão em matrizes poliméricas, substâncias ou solventes não-hidrofílicos, normalmente, a maioria dessas modificações para tal fim, visam aumentar a carga iônica na superfície dos nanocristais de celulose e promover a repulsão entre essas nanopartículas. No entanto, a maior dispersão dos nanocristais de celulose em matrizes hidrofóbicas não é o único objetivo da modificação química dessas partículas. Muitas modificações químicas dos grupamentos -OH lives da superfície dos nanocristais de celulose, promovem a funcionalização dessas nanopartículas, que objetivam por exemplo, facilitar a entrega de fármacos dentro das células, promover a ancoragem de moléculas a substratos específicos para serem utilizados como catalisadores mais eficientes, insertos poliméricos para a melhoria de filmes plásticos, entre inúmeras outras modificações. Atualmente muita metodologia tem sido estudadas para promover a derivatização dos nanocristais de celulose, sem afetar a sua estrutura primária, no entanto, as metodologias tradicionais tais como, esterificação, aminação. oxidação, sililacão, epoxidação, sulfonação, substituição nucleofílica e carboxilmetilação são as mais estudadas e as mais empregadas na derivatização desses nanocristais (Habibi et al., 2010; Hasan et al., 2021; Heise et al., 2021; Gomri et al., 2022; Abushammala & Mao, 2019). A **Tabela 3** sumariza algumas modificações químicas de nanocristais de celulose e suas aplicações

Tabela 3: Derivatização de nanocristais de celulose

Molécula adicionada	Aplicação/objetivo	Referência
Éster metílico de óleo de canola	Revestimento hidrofóbico e reforço para nanocompósitos hidrofóbicos	Wei et al., 2017
Acilação com ácidos graxos e anidrido trifluoroacético	Diminuir a umidade em nano papéis de nanocelulose	Huang et al., 2017
4-acetamido-2,2,6,6-tetrametil-1-piperinidiloxi (TEMPO)/sal quarternário de amônio	Aplicação de nanocristais como emulsificante	Saidane et al.2016
Dianidetilenodiaminotetracético (EDTAD)	Dectecção de Cu^{2+}	Zhang et al., 2018
Acetilação	Fabricação de adesivos compósitos	Eslah et al., 2018

1.3 Obtenção de nanocristais de celulose e sua aplicação em bioplástico

Os nanocristais de celulose são excelentes agentes de reforço térmico e mecânico e uma das suas aplicações mais conhecidas é como nanopartícula de reforço de materiais poliméricos, como por exemplo, os bioplásticos. Os bioplásticos são umas das classes de biomateriais que ganham cada vez mais destaque na pesquisa e na indústria de embalagens, devido a sua potencial aplicabilidade em diversas áreas, desde embalagens de alimentos a dispositivos médicos(Arikan & Ozsoy, 2015; Di Bartolo et al., 2021). E podem ser definidos como polímeros plásticos criados a partir de fontes renováveis, como as biomassas vegetais, síntese química, microorganismos naturais ou geneticamente modificados (Tokiwa et al., 2009).

Apesar de serem ecologicamente mais benéfico para a natureza, nem todo bioplástico é biodegradável. A biodegradabilidade de um bioplástico é originada de sua composição química e não da sua matéria-prima de origem, por isso, os bioplásticos são divididos em dois grandes grupos, os não-biodegradáveis e os biodegradáveis (Tokiwa et al., 2009; Rosenboom et al., 2022; Fojt et al., 2020). Abaixo segue as subclassificações dos bioplástico:

Bioplásticos "bio-based" biodegradável: O termo bio-based refere-se aos bioplásticos construídos a partir de polímeros naturais renováveis de espécies vegetais ou microbianas, tais como, celulose, amido, polihidroxialcanoato, óleos vegetais, açúcares, proteínas e outros, que são biodegradáveis por compostagem ou por decomposição espontânea no

ambiente. Exemplos são: o Poli(hidroxibutirato) (PHB), poli(lactídeo) (PLA).

Bioplásticos "bio-based" não–biodegradável: Esses bioplásticos também são baseados em moléculas de fontes renováveis, mas não são biodegradáveis. Por exemplo, o a acetato de celulose, cuja biodegradabilidade depende do grau de polimerização. Normalmente esses bioplásticos são compósitos (uma mistura de um ou mais tipos de polímeros distintos) ou são moléculas naturais que sofrem variações químicas em laboratório, com o objetivo de conferir aos mesmos característica tecnológicas desejadas. Outros exemplos são: Polietileno (PE) e o Nylon 11 (NY11) que mesmo quando obtidos de biomassa vegetal, não são biodegradáveis.

Bioplásticos "petrochemical-based" biodegradável: Como o próprio termo sugere, esses são bioplásticos biodegradáveis de origem petroquímica. A matéria-prima desses bioplásticos são resultantes dos processos da indústria petroquímica, por exemplo, dos ácidos carboxílicos ou até mesmo da utilização do óleo cru. Esses bioplásticos possuem boas características tecnológicas e quando expostos aos ambientes são degradados com facilidade. Exemplos são: a Policaprolactona (PCL) e poli (succinato de butileno) (PBS).

Os bioplásticos são uma alternativa promissora para a adoção de materiais verdes, biodegradáveis e livres de moléculas de origem petroquímica. No entanto, muitas das suas características físico-químicas como resistência mecânica e permeabilidade a vapor e gases, não corroboram para o seu uso em grande escala em substituição aos plásticos petroquímicos (). Umas das alternativas utilizadas para melhorar essas características negativas é a inserção de nanocristais de celulose na matriz polimérica ().

A maior parte dos nanocristais de celulose é extraída de polpa de madeira maciça, no entanto, o interesse em utilizar biomassa alternativas tem se mostrado promissor e desafiador. Os resíduos de biomassa advinda do cultivo de alimentos, tais como, casca de arroz, bagaço de cana-de-açúcar, sisal, casca de café, palha de milho, e diversos outros alimentos, são fontes ricas e abundante de moléculas lignocelulósicos e podem ser aproveitadas tanto para a extração de nanocristais de celulose, quanto para a produção de outras substâncias de valor agregado, como o biodiesel e o álcool (Abdullah et al., 2021; Chaka, 2022).

Uma biomassa ainda pouca explorada para esse fim, é a biomassa descartada da produção de café. O Brasil é o líder mundial na produção de café, seguido do Vietnam, Colômbia e Indonésia (Nishijima, et a.,2012).Os principais estados produtores de café no Brasil são Minas gerais, Espírito do Santo, São Paulo, Bahia, Paraná e Rondônia. Com destaque para o estado de Minas Gerais, que sozinho detém 50% da produção nacional

desse fruto (Ministério da Agricultura e pecuária,2022) Segundo a Embrapa em 2022 a produção anual de café no Brasil chegou a 50,3 milhões de sacas de 60 kg de café, sendo que cerca de 64% dessas sacas foram de café arábica e cerca de 36% de robusta. Boa parte da produção nacional é destinada à exportação e em 2022 foi responsável 9,23 bilhão de dólares (Embrapa,2022; Volsi, et al., 2019).

O café usado na alimentação passa por dois tipos de processamento antes de seus grãos serem empregados no preparo de bebidas e alimentos. São eles: I) via úmida e II) via seca. Em torno de 50% de todo o café processado se torna subprodutos, dentre eles se destacam, os grãos de baixa qualidade, como os grãos verdes e "boia", a palha de café (mistura da casca, mucilagem, endocarpo, película prateada e pergaminho) e a água de lavagem, esta última composta de substâncias químicas presente nos frutos (Arya et al., 2022).

Toda essa biomassa residual é rica em substâncias e moléculas que podem ser aplicadas em diversos setores, como na produção de combustíveis, insumos alimentícios ricos em vitaminas, materiais poliméricos, biogás, bio-óleos e extrativos incluindo a cafeína e compostos antioxidantes (Janissen & Huynh, 2018).Apesar de toda essa aplicabilidade essa biomassa residual do café não é reaproveitada de uma maneira sustentável. A maioria dos agricultores queimam esse material a céu aberto e descartam as águas residuais do processo de lavagem em rios e em cursos de águas naturais. Essas atividades impactam negativamente o meio ambiente, emitindo gases tóxicos como CO_2, metano, ou ainda, causando acidificação de águas, entre outros danos (Minuta & Jini, 2017; Mussatto, et al., 2011).

Os estudos relacionados a extração de nanocristais de celulose de café a partir de biomassa residual desse fruto, ainda é insipiente. A maioria dos trabalhos focam no uso da casca do café como matéria-prima para produção de nanocristais de celulose. Como é o caso de Collazo-Bigliardi, e colaboradores, que extraíram nanocristais de celulose a partir da casca de café, usando ácido sulfúrico como solvente de extração. Os pesquisadores observaram que os nanocristais de café possuíam uma razão de aspecto maior que 10 e quando foram adicionados como agente de reforço em filmes poliméricos de amido termoplástico, esses nanocristais de celulose acrescidos na proporção de 1% m/m nanocristais de celulose/amido, aumentaram a resistência a tensão dos filmes.

Em outro estudo, Tesfaye e demais pesquisadores 2021, isolaram nanocristais de celulose de diferentes biomassas agrícolas, dentre elas, a casca de café.O resultado desse trabalho demonstrou que os nanocristais de celulose extraídos da casca de café possuíam

alto grau de cristalinidade (77%). A alta cristalinidade é uma característica interessante para nanocristais de celulose usados como agente de reforço ou em dispositivos ópticos.

Já Frost & Foster, 2020, isolaram nanocristais de celulose a partir de grãos de café, usando ácido fosfórico e obtiveram nanocristais de celulose com 74% de cristalinidade e 12 de razão de aspecto, o que os tornam nanopartículas com potencial para ser usadas como agente de reforço polimérico.

Como demonstrado nos exemplos citados acima, a maioria dos estudos focam na extração de nanocristais da casca de café, que representa uma parte da biomassa residual. Logo, se faz necessário mais estudos sobre a extração e aplicabilidade em matrizes poliméricas de nanocristais de celulose a partir dos grãos de café que são descartados durante o processamento do café.

1.4 Tratamento de efluentes e membrana filtrante

A água é um bem essencial para a vida, por isso, sua qualidade é um ponto crucial para a manutenção da saúde humana. O tratamento de esgoto e efluentes é uma etapa extremamente importante para manter o grau de pureza química e biológica, tanto da água usada para consumo humano quanto para água usada em atividades diárias e industriais. A baixa qualidade da água acarreta doenças e prejudica processos industriais, podemos observar isso, especialmente em países pobres, onde o tratamento de esgoto e efluentes são insipientes (Bijekar et al., 2022).

As membranas filtrantes são comumente usadas como tratamento secundários e terciários de água para consumo, efluentes e esgoto, atualmente no mercado existe cerca de 500 tipos de membranas filtrantes para esse fim. Essas membranas podem ser empregadas em substituição a algumas etapas de tratamento de água, como nos processos de floculação e destilação, ou ainda, ser utilizada como uma etapa adicional para aumentar a eficiência dos tratamentos de água e esgoto já estabelecidos (Bodzek et al., 2019; Henrik Tækker,2016).

As membranas filtrantes possuem larga aplicabilidade, uma delas é a remoção de agentes biológicos, tais como vírus e bactérias. Estudos em pequena e larga escala já provaram a capacidade de inúmeras membranas de diminuir o número de células viáveis de vírus e bactérias encontrados em esgoto e efluentes, entre esses agentes, destacam-se os vírus patogênicos mais comuns, como os adenovírus, norovírus e enterovírus (Hai, et al., 2014; Zhang, et al., 2016). Uma das vantagens da utilização de membranas filtrantes aplicada na eliminação de patógenos, é a diminuição do uso de reagentes químicos, isso diminui o custo total do processo e elimina possíveis danos à saúde ocasionada pela

ingestão e/ou contato com excesso de reagentes químicos, como as substâncias cloradas. Os patógenos biológicos podem ser excluídos por tamanho e/ou eliminados por afinidade eletroestática, associada aos outros métodos como esterilização por luz ultravioleta e agentes químicos desinfetantes, como os sais de amônios quaternários (ya, 2018)

Segundo Zhang e colaboradores (2016), no geral, o processo de filtração por membranas pode envolver substâncias químicas ou não. As membranas são agrupadas em dois grandes grupos e quatro subgrupos. A primeira divisão classifica as membranas em membranas pressurizadas, ou seja, que são aplicadas em sistema com pressão e membranas não pressurizadas, que são usadas sem a ação de pressão externa ou interna. A segunda classificação é de acordo com a tecnologia de separação da própria membrana filtrante e são agrupadas em:

Osmose reversa (RO): essas membranas têm tamanhos de poros capazes de reter sais e moléculas orgânicas de pequenas dimensões.

***Nanofiltração (NF*)**: São membranas cujos poros são capazes de reter macromoléculas, vírus, pequenos coloides e alguns tipos de ácidos.

Microfiltração (MF): São membranas com poros capazes de reter bactérias, polímeros e partículas coloidais grandes.

Ultrafiltração (UF): Os poros dessas membranas retêm moléculas extremamente pequenas como vírus e compostos de 1 nm a 100 nm.

Essas membranas podem ser confecionadas a partir de uma vasta gama de materiais, a escolha do material irá depender do objetivo do processo de filtração e suas particularidades. Alguns aspectos básicos devem ser observados para a escolha da membrana, são eles: Hidrofilicidade ou hidrofobicidade, faixa de pH suportado, resistência a antioxidantes, carga superficial, flexibilidade, resistência mecânica e porosidade (Zhang et al., 2016; Chen, et al.,2021; Yang et al., 2019).

2. OBJETIVOS GERAIS

O objetivo do primeiro capítulo deste trabalho foi desenvolver bioplásticos compósitos de metil celulose, acrescidos de nanocristais de celulose produzidos a partir de grãos de café de baixa qualidade. E avaliar a sua resistência térmica.

No segundo capítulo deste trabalho pretendeu-se desenvolver e validar um prótipo de filtro de águas residuárias usando como agente ativo membranas de celulose modificada com sais quarternário de amônio, associada com luz ultravioleta, e avaliar o seu potencial de degradação de material genético de vírus

3. REFERÊNCIAS BIBLIOGRÁFICAS

1. Abdullah, N. A., Rani, M. S. A., Mohammad, M., Sainorudin, M. H., Asim, N., Yaakob, Z., Razali, H., & Emdadi, Z. (2021). Nanocellulose from agricultural waste as an emerging nanotechnology material for nanotechnology applications - An overview. In *Polimery/Polymers* (Vol. 66, Issue 3, pp. 157–168). Industrial Chemistry Research Institute. https://doi.org/10.14314/POLIMERY.2021.3.1.
2. Abouzeid, R. E., Khiari, R., Beneventi, D., & Dufresne, A. (2018). Biomimetic Mineralization of Three-Dimensional Printed Alginate/TEMPO-Oxidized Cellulose Nanofibril Scaffolds for Bone Tissue Engineering. Biomacromolecules, 19(11), 4442–4452. https://doi.org/10.1021/acs.biomac.8b01325.
3. Abushammala, H., & Mao, J. (2019). A review of the surface modification of cellulose and nanocellulose using aliphatic and aromatic mono- And di- isocyanates. In Molecules (Vol. 24, Issue 15). MDPI AG. https://doi.org/10.3390/molecules24152782.
4. Akinjokun, A. I., Petrik, L. F., Ogunfowokan, A. O., Ajao, J., & Ojumu, T. V. (2021). Isolation and characterization of nanocrystalline cellulose from cocoa pod husk (CPH) biomass wastes. Heliyon, 7(4). https://doi.org/10.1016/j.heliyon.2021.e06680.
5. Arya, S. S., Venkatram, R., More, P. R., & Vijayan, P. (2022). The wastes of coffee bean processing for utilization in food: a review. In Journal of Food Science and Technology (Vol. 59, Issue 2, pp. 429–444). Springer. https://doi.org/10.1007/s13197-021-05032-5
6. Aziz, T., Farid, A., Haq, F., Kiran, M., Ullah, A., Zhang, K., Li, C., Ghazanfar, S., Sun, H., Ullah, R., Ali, A., Muzammal, M., Shah, M., Akhtar, N., Selim, S., Hagagy, N., Samy, M., & al Jaouni, S. K. (2022). A Review on the Modification of Cellulose and Its Applications. In Polymers (Vol. 14, Issue 15). MDPI. https://doi.org/10.3390/polym14153206.
7. Bijekar, S., Padariya, H. D., Yadav, V. K., Gacem, A., Hasan, M. A., Awwad, N. S., Yadav, K. K., Islam, S., Park, S., & Jeon, B. H. (2022). The State of the Art and Emerging Trends in the Wastewater Treatment in Developing Nations. In Water (Switzerland) (Vol. 14, Issue 16). MDPI. https://doi.org/10.3390/w14162537.
8. Blake, A. W., McCartney, L., Flint, J. E., Bolam, D. N., Boraston, A. B., Gilbert, H. J., & Knox, J. P. (2006). Understanding the biological rationale for the diversity of cellulose-directed carbohydrate-binding modules in prokaryotic enzymes. Journal of Biological Chemistry, 281(39), 29321–29329. https://doi.org/10.1074/jbc.M605903200.
9. Blanco, A., Monte, M. C., Campano, C., Balea, A., Merayo, N., & Negro, C. (2018). Nanocellulose for industrial use: Cellulose nanofibers (CNF), cellulose nanocrystals (CNC), and bacterial cellulose (BC). In Handbook of Nanomaterials for Industrial Applications (pp. 74–126). Elsevier. https://doi.org/10.1016/B978-0-12-813351-4.00005-5.
10. Bodzek, M., Konieczny, K., & Rajca, M. (2019). Membranes in water and wastewater disinfection – review. January. https://doi.org/10.24425/aep.2019.126419.
11. Boina, A. (2008). Quantificação De Estoques De Biomassa E De Carbono Em Floresta Estacional Semidecidual, Vale Do Rio Doce, Minas Gerais. 89.
12. Bozell, J. J. (2021). Chemicals and Materials from Renewable Resources (Vol. 15). UTC. https://pubs.acs.org/sharingguidelines.
13. Chaka, K. T. (2022). Extraction of cellulose nanocrystals from agricultural by-products: a review. In

Green Chemistry Letters and Reviews (Vol. 15, Issue 3, pp. 582–597). Taylor and Francis Ltd. https://doi.org/10.1080/17518253.2022.2121183.

14. Chen, M., Parot, J., Hackley, V. A., Zou, S., & Johnston, L. J. (2021). AFM characterization of cellulose nanocrystal height and width using internal calibration standards. Cellulose, 28(4), 1933–1946. https://doi.org/10.1007/s10570-021-03678-0
15. Cherubini, F. (2010). The biorefinery concept: Using biomass instead of oil for producing energy and chemicals. Energy Conversion and Management, 51(7), 1412–1421. https://doi.org/10.1016/j.enconman.2010.01.015.
16. Collazo-Bigliardi, S., Ortega-Toro, R., & Chiralt Boix, A. (2018). Isolation and characterisation of microcrystalline cellulose and cellulose nanocrystals from coffee husk and comparative study with rice husk. Carbohydrate Polymers, 191, 205–215. https://doi.org/10.1016/j.carbpol.2018.03.022.
17. D'Adamo, I., Gastaldi, M., Morone, P., Rosa, P., Sassanelli, C., Settembre-Blundo, D., & Shen, Y. (2022). Bioeconomy of Sustainability: Drivers, Opportunities and Policy Implications. Sustainability (Switzerland), 14(1). https://doi.org/10.3390/su14010200.
18. Daicho, K., Saito, T., Fujisawa, S., & Isogai, A. (2018). The Crystallinity of Nanocellulose: Dispersion-Induced Disordering of the Grain Boundary in Biologically Structured Cellulose. ACS Applied Nano Materials, 1(10), 5774– 5785. https://doi.org/10.1021/acsanm.8b01438.
19. de Avila Delucis, R., de Cademartori, P.H.G., Fajardo, A.R. and Amico, S.C. (2021). Cellulose and its Derivatives: Properties and Applications. In Polysaccharides (eds Inamuddin, M.I. Ahamed, R. Boddula and T. Altalhi). https://doi.org/10.1002/9781119711414.ch11.
20. Deb Dutta, S., Patel, D. K., Ganguly, K., & Lim, K. T. (2021). Isolation and characterization of cellulose nanocrystals from coffee grounds for tissue engineering. Materials Letters, 287. https://doi.org/10.1016/j.matlet.2021.129311.
21. Di Bartolo, A., Infurna, G., & Dintcheva, N. T. (2021). A review of bioplastics and their adoption in the circular economy. In Polymers (Vol. 13, Issue 8). MDPI AG. https://doi.org/10.3390/polym13081229.
22. Djafari Petroudy, S. R. (2017). Physical and mechanical properties of natural fibers. In Advanced High Strength Natural Fibre Composites in Construction (pp. 59–83). Elsevier Inc. https://doi.org/10.1016/B978-0-08-100411- 1.00003-0.
23. Doh, H., Lee, M. H., & Whiteside, W. S. (2020). Physicochemical characteristics of cellulose nanocrystals isolated from seaweed biomass. Food Hydrocolloids, 102. https://doi.org/10.1016/j.foodhyd.2019.105542.
24. Embrapa (2022). Produção de café arábica corresponde a 64% e café conilon a 36% da safra total dos Cafés do Brasil em 2022. Acess:< https://www.embrapa.br/busca-de-noticias/-/noticia/73940564/producao-de-cafe-arabica-corresponde-a-64-e-cafe-conilon-a-36-da-safra-total-dos-cafes-do-brasil-em-2022>.
25. Endres, H. J. (2019). Bioplastics. In Advances in Biochemical Engineering/Biotechnology (Vol. 166, pp. 427–468). Springer Science and Business Media Deutschland GmbH. https://doi.org/10.1007/10_2016_75.
26. Ergun, R., Guo, J., & Huebner-Keese, B. (2015). Cellulose. In Encyclopedia of Food and Health (pp. 694–702). Elsevier Inc. https://doi.org/10.1016/B978- 0-12-384947-2.001276.
27. Eslah, F., Jonoobi, M., Faezipour, M., & Ashori, A. (2018). Chemical modification of soybean flour-

based adhesives using acetylated cellulose nanocrystals. Polymer Composites, 39(10), 3618–3625. https://doi.org/10.1002/pc.24389.

28. Ezgi Bezirhan Arikan, & Havva Duygu Ozsoy. (2015). A Review: Investigation of Bioplastics. Journal of Civil Engineering and Architecture, 9(2). https://doi.org/10.17265/1934-7359/2015.02.007.
29. Fojt, J., David, J., Přikryl, R., Řezáčová, V., & Kučerík, J. (2020). A critical review of the overlooked challenge of determining micro-bioplastics in soil. In Science of the Total Environment (Vol. 745). Elsevier B.V. https://doi.org/10.1016/j.scitotenv.2020.14.
30. Frost, B. A., & Johan Foster, E. (2020). Isolation of thermally stable cellulose nanocrystals from spent coffee grounds via phosphoric acid hydrolysis. Journal of Renewable Materials, 8(2), 187–203. https://doi.org/10.32604/jrm.2020.07940.
31. Ghasemlou, M., Daver, F., Ivanova, E. P., Habibi, Y., & Adhikari, B. (2021). Surface modifications of nanocellulose: From synthesis to high-performance nanocomposites. In Progress in Polymer Science (Vol. 119). Elsevier Ltd. https://doi.org/10.1016/j.progpolymsci.2021.101418.
32. Gomri, C., Cretin, M., & Semsarilar, M. (2022). Recent progress on chemical modification of cellulose nanocrystal (CNC) and its application in nanocomposite films and membranes-A comprehensive review. Carbohydrate Polymers, 294. https://doi.org/10.1016/j.carbpol.2022.119790
33. Goyal, Amita & Rumaiz, Abdul & Miao, Y. & Hazra, Sukti & Ni, Chaoying & Shah, Syed. (2008). Synthesis and characterization of TiO2–Ge nanocomposites. Journal of Vacuum Science & Technology B: Microelectronics and Nanometer Structures. 26. 1315 - 1320. 10.1116/1.2939262.
34. Grishkewich, N., Mohammed, N., Tang, J., & Tam, K. C. (2017). Recent advances in the application of cellulose nanocrystals. In Current Opinion in Colloid and Interface Science (Vol. 29, pp. 32–45). Elsevier Ltd. https://doi.org/10.1016/j.cocis.2017.01.005.
35. Gröndahl, J., Karisalmi, K., & Vapaavuori, J. (2021). Micro- And nanocelluloses from non-wood waste sources; Processes and use in industrial applications. In Soft Matter (Vol. 17, Issue 43, pp. 9842–9858). Royal Society of Chemistry. https://doi.org/10.1039/d1sm00958c.
36. Habibi, Y., Lucia, L. A., & Rojas, O. J. (2010). Cellulose nanocrystals: Chemistry, self-assembly, and applications. Chemical Reviews, 110(6), 3479– 3500. https://doi.org/10.1021/cr900339w.
37. Hai, F. I., Riley, T., Shawkat, S., Magram, S. F., & Yamamoto, K. (2014). Removal of Pathogens by Membrane Bioreactors: A Review of the Mechanisms, Influencing Factors and Reduction in Chemical Disinfectant Dosing. 3603–3630. https://doi.org/10.3390/w6123603.
38. Hasan, M. J., Johnson, A. E., & Ureña-Benavides, E. E. (2021). “Greener” chemical modification of cellulose nanocrystals via oxa-Michael addition with N-Benzylmaleimide. Current Research in Green and Sustainable Chemistry, 4. https://doi.org/10.1016/j.crgsc.2021.100081.
39. Hasan, M. J., Johnson, A. E., & Ureña-Benavides, E. E. (2021). “Greener” chemical modification of cellulose nanocrystals via oxa-Michael addition with N-Benzylmaleimide. Current Research in Green and Sustainable Chemistry, 4. https://doi.org/10.1016/j.crgsc.2021.100081.
40. Heise, K., Delepierre, G., King, A. W. T., Kostiainen, M. A., Zoppe, J., Weder, C., & Kontturi, E. (2021). Chemical Modification of Reducing End-Groups in Cellulose Nanocrystals. In *Angewandte Chemie - International Edition* (Vol. 60, Issue 1, pp. 66–87). Wiley-VCH Verlag. https://doi.org/10.1002/anie.202002433.
41. Henrik Tækker Madsen, Chapter 6 - Membrane Filtration in Water Treatment – Removal of

Micropollutants, Editor(s): Erik G. Søgaard, Chemistry of Advanced Environmental Purification Processes of Water, Elsevier, 2014 ,Pages 199-248, ISBN 9780444531780,https://doi.org/10.1016/B978-0-444-53178-0.00006-7.

42. Huang, F., Wu, X., Yu, Y., Lu, Y., & Chen, Q. (2017). Acylation of cellulose nanocrystals with acids/trifluoroacetic anhydride and properties of films from esters of CNCs. Carbohydrate Polymers, 155, 525–534. https://doi.org/10.1016/j.carbpol.2016.09.010.
43. Isikgor, F. H., & Becer, C. R. (2015). Lignocellulosic biomass: a sustainable platform for the production of bio-based chemicals and polymers. Polymer Chemistry, 6(25), 4497–4559. https://doi.org/10.1039/c5py00263j.
44. Janissen, B., & Huynh, T. (2018). Chemical composition and value-adding applications of coffee industry by-products: A review. In Resources, Conservation and Recycling (Vol. 128, pp. 110–117). Elsevier B.V. https://doi.org/10.1016/j.resconrec.2017.10.001.
45. Kim, J. H., Shim, B. S., Kim, H. S., Lee, Y. J., Min, S. K., Jang, D., Abas, Z.,& Kim, J. (2015). Review of nanocellulose for sustainable future materials. In International Journal of Precision Engineering and Manufacturing - Green Technology (Vol. 2, Issue 2, pp. 197–213). Korean Society for Precision Engineering. https://doi.org/10.1007/s40684-015-0024-9.
46. Korolovych, V. F., Cherpak, V., Nepal, D., Ng, A., Shaikh, N. R., Grant, A., Xiong, R., Bunning, T. J., & Tsukruk, V. V. (2018). Cellulose nanocrystals with different morphologies and chiral properties. Polymer, 145, 334–347. https://doi.org/10.1016/j.polymer.2018.04.064.
47. Lindman, B., Medronho, B., Alves, L., Costa, C., Edlund, H., & Norgren, M. (2017). The relevance of structural features of cellulose and its interactions to dissolution, regeneration, gelation and plasticization phenomena. In Physical Chemistry Chemical Physics (Vol. 19, Issue 35, pp. 23704–23718). Royal Society of Chemistry. https://doi.org/10.1039/c7cp02409f.
48. Magalhães, A. I., de Carvalho, J. C., de Melo Pereira, G. V., Karp, S. G., Câmara, M. C., Medina, J. D. C., & Soccol, C. R. (2019). Lignocellulosic biomass from agro-industrial residues in South America: current developments and perspectives. In Biofuels, Bioproducts and Biorefining (Vol. 13, Issue 6, pp. 1505–1519). John Wiley and Sons Ltd. https://doi.org/10.1002/bbb.2048.
49. Mariano, M., El Kissi, N., & Dufresne, A. (2014). Cellulose nanocrystals and related nanocomposites: Review of some properties and challenges. In Journal of Polymer Science, Part B: Polymer Physics (Vol. 52, Issue 12, pp. 791–806). John Wiley and Sons Inc. https://doi.org/10.1002/polb.23490.
50. Ministério da agricultura e pecuária (2022). Conheça a história do café no mundo e como o Brasil se tornou o maior produtor e exportador da bebida. Acess: < https://www.gov.br/agricultura/pt-br/assuntos/noticias/conheca-a-historia-do-cafe-no-mundo-e-como-o-brasil-se-tornou-o-maior-produtor-e-exportador-da-bebida>.
51. Minuta, T., & Jini, D. (2017). Impact of Effluents from Wet Coffee Processing Plants on the Walleme River of Southern Ethiopia. Research Journal of Environmental Toxicology, 11(3), 90–96. https://doi.org/10.3923/rjet.2017.90.96.
52. Mussatto, S. I., Machado, E. M. S., Martins, S., & Teixeira, J. A. (2011). Production, Composition, and Application of Coffee and Its Industrial Residues. In Food and Bioprocess Technology (Vol. 4, Issue 5, pp. 661–672). https://doi.org/10.1007/s11947-011-0565-z.
53. Nanocellulose market. Acess:<https://www.precedenceresearch.com/nanocellulose-market>.

54. Nanocellulose Market: Industry Analysis and Forecast (2022-2029). Acess: https://www.maximizemarketresearch.com/market-report/global-nanocellulose-market/16711/.
55. Ning, P., Yang, G., Hu, L., Sun, J., Shi, L., Zhou, Y., Wang, Z., & Yang, J. (2021a). Recent advances in the valorization of plant biomass. In Biotechnology for Biofuels (Vol. 14, Issue 1). BioMed Central Ltd. https://doi.org/10.1186/s13068-021-01949-3.
56. Nishijima, M., Sylvia, M., Saes, M., Antonio, F., & Postali, S. (2012). Análise de Concorrência no Mercado Mundial de Café Verde. https://www.scielo.br/j/resr/a/8gxLdFCXx4LyzyXz4J9rBcL/?format=pdf&lang=pt.
57. Nishiyama, Y. (2009). Structure and properties of the cellulose microfibril. In Journal of Wood Science (Vol. 55, Issue 4, pp. 241–249). Springer Japan. https://doi.org/10.1007/s10086-009-1029-1.
58. Owoyokun, T., Pérez Berumen, C. M., Luévanos, A. M., Cantú, L., & Lara Ceniceros, A. C. (2021). Cellulose nanocrystals: Obtaining and sources of a promising bionanomaterial for advanced applications. In Biointerface Research in Applied Chemistry (Vol. 11, Issue 4, pp. 11797–11816). AMG Transcend Association. https://doi.org/10.33263/BRIAC114.1179711816.
59. Peter, S., Lyczko, N., Gopakumar, D., Maria, H. J., Nzihou, A., & Thomas, S. (2022). Nanocellulose and its derivative materials for energy and environmental applications. In Journal of Materials Science (Vol. 57, Issue 13, pp. 6835–6880). Springer. https://doi.org/10.1007/s10853-022-07070-6 .
60. Quadros, M. E., & Marr, L. C. (2010). Environmental and human health risks of aerosolized silver nanoparticles. In Journal of the Air and Waste Management Association (Vol. 60, Issue 7, pp. 770–781). Taylor and Francis Inc. https://doi.org/10.3155/1047-3289.60.7.770.
61. Rasheed, M., Jawaid, M., Parveez, B., Zuriyati, A., & Khan, A. (2020). Morphological, chemical and thermal analysis of cellulose nanocrystals extracted from bamboo fibre. International Journal of Biological Macromolecules, 160, 183–191. https://doi.org/10.1016/j.ijbiomac.2020.05.170.
62. Reshmy, R., Philip, E., Madhavan, A., Sindhu, R., Pugazhendhi, A., Binod, P., Sirohi, R., Awasthi, M. K., Tarafdar, A., & Pandey, A. (2021). Advanced biomaterials for sustainable applications in the food industry: Updates and challenges. Environmental Pollution, 283.
63. Rosenboom, J. G., Langer, R., & Traverso, G. (2022). Bioplastics for a circular economy. In Nature Reviews Materials (Vol. 7, Issue 2, pp. 117–137). Nature Research. https://doi.org/10.1038/s41578-021-00407-8.
64. Rowell, R., Pettersen, R., & Tshabalala, M. (2012). Cell Wall Chemistry. In Handbook of Wood Chemistry and Wood Composites, Second Edition (pp. 33–72). CRC Press. https://doi.org/10.1201/b12487-5.
65. Ruel, K., Nishiyama, Y., & Joseleau, J. P. (2012). Crystalline and amorphous cellulose in the secondary walls of Arabidopsis. Plant Science, 193–194, 48–61. https://doi.org/10.1016/j.plantsci.2012.05.008
66. Saidane, D., Perrin, E., Cherhal, F., Guellec, F., & Capron, I. (2016). Some modification of cellulose nanocrystals for functional Pickering emulsions. Philosophical Transactions of the Royal Society A: Mathematical, Physical and Engineering Sciences, 374(2072). https://doi.org/10.1098/rsta.2015.0139.
67. Seddiqi, H., Oliaei, E., Honarkar, H., Jin, J., Geonzon, L. C., Bacabac, R. G., & Klein-Nulend, J. (2021). Cellulose and its derivatives: towards biomedical applications. In Cellulose (Vol. 28, Issue 4, pp. 1893–1931). Springer Science and Business Media B.V. https://doi.org/10.1007/s10570-020-03674-w.
68. Shojaeiarani, J., Bajwa, D. S., & Chanda, S. (2021). Cellulose nanocrystal based composites: A review.

In Composites Part C: Open Access (Vol. 5). Elsevier B.V. https://doi.org/10.1016/j.jcomc.2021.100164 Southern Ethiopia. Research Journal of Environmental Toxicology, v. 11, n. 3, p. 90–96, 1 mar. 2017.

69. Tesfaye, G., Belete, A., Hause, G., Neubert, R. H. H., & Gebre-Mariam, T. (2021). Isolation and Characterization of Cellulose Nanocrystals from Different Lignocellulosic Residues: A Comparative Study. Journal of Polymers and the Environment, 29(9), 2964–2977. https://doi.org/10.1007/s10924-021-02089-3.
70. Thakur, S., Chaudhary, J., Sharma, B., Verma, A., Tamulevicius, S., & Thakur,V. K. (2018). Sustainability of bioplastics: Opportunities and challenges. In Current Opinion in Green and Sustainable Chemistry (Vol. 13, pp. 68–75). Elsevier B.V. https://doi.org/10.1016/j.cogsc.2018.04.013.
71. Tingaut, P., Zimmermann, T., & Sèbe, G. (2012). Cellulose nanocrystals and microfibrillated cellulose as building blocks for the design of hierarchical functional materials. Journal of Materials Chemistry, 22(38), 20105–20111. https://doi.org/10.1039/c2jm32956e.
72. Tokiwa, Y., Calabia, B. P., Ugwu, C. U., & Aiba, S. (2009). Biodegradability of plastics. In International Journal of Molecular Sciences (Vol. 10, Issue 9, pp. 3722–3742). https://doi.org/10.3390/ijms10093722.
73. Trache, D., Tarchoun, A. F., Derradji, M., Hamidon, T. S., Masruchin, N., Brosse, N., & Hussin, M. H. (2020). Nanocellulose: From Fundamentals to Advanced Applications. In Frontiers in Chemistry (Vol.8). Frontiers Media S.A. https://doi.org/10.3389/fchem.2020.00392.
74. Trilokesh, C., & Uppuluri, K. B. (2019). Isolation and characterization of cellulose nanocrystals from jackfruit peel. Scientific Reports, 9(1). https://doi.org/10.1038/s41598-019-53412-x.
75. Volsi, B., Telles, T. S., Caldarelli, C. E., & da Camara, M. R. G. (2019). The dynamics of coffee production in Brazil. PLoS ONE, 14(7). https://doi.org/10.1371/journal.pone.0219742.
76. Wei, L., Agarwal, U. P., Hirth, K. C., Matuana, L. M., Sabo, R. C., & Stark, N. M. (2017). Chemical modification of nanocellulose with canola oil fatty acid methyl ester. Carbohydrate Polymers, 169, 108–116. https://doi.org/10.1016/j.carbpol.2017.04.008
77. Xie, H., Du, H., Yang, X., & Si, C. (2018). Recent Strategies in Preparation of Cellulose Nanocrystals and Cellulose Nanofibrils Derived from Raw Cellulose Materials. In International Journal of Polymer Science (Vol. 2018). Hindawi Limited. https://doi.org/10.1155/2018/7923068.
78. Xie, S., Zhang, X., Walcott, M. P., & Lin, H. (2018b). Applications of cellulose nanocrystals: A review. In Engineered Science (Vol. 2, pp. 4–16). Engineered Science Publisher. https://doi.org/10.30919/es.1803302.
79. Xu, C. Z. L. X. P. (2018). Elimination of viruses from domestic wastewater : requirements and technologies. World Journal of Microbiology and Biotechnology, 2016. https://doi.org/10.1007/s11274-016-2018-3.
80. Yang, J., Saqib, M. N., Liu, F., & Zhong, F. (2023). Bacterial cellulose nanocrystals with a great difference in aspect ratios: A comparison study of their reinforcing effects on properties of the sodium alginate film. Food Hydrocolloids, 108676. https://doi.org/10.1016/j.foodhyd.2023.108676.
81. Yang, Z., Zhou, Y., Feng, Z., Rui, X., Zhang, T., & Zhang, Z. (2019). A review on reverse osmosis and nanofiltration membranes for water purification. In Polymers (Vol. 11, Issue 8). MDPI AG. https://doi.org/10.3390/polym11081252.
82. Zhang, B., Gao, Y., Zhang, L., & Zhou, Y. (2021). The plant cell wall: Biosynthesis, construction, and functions. In Journal of Integrative Plant Biology (Vol. 63, Issue 1, pp. 251–272). Blackwell Publishing

Ltd. https://doi.org/10.1111/jipb.13055.

83. Zhang, R., Liu, Y., He, M., Su, Y., Zhao, X., Elimelech, M., & Jiang, Z. (2016). Antifouling membranes for sustainable water purification: Strategies and mechanisms. In Chemical Society Reviews (Vol. 45, Issue 21, pp. 5888–5924). Royal Society of Chemistry. https://doi.org/10.1039/c5cs00579e.
84. Zhang, Y. J., Ma, X. Z., Gan, L., Xia, T., Shen, J., & Huang, J. (2018).Fabrication of fluorescent cellulose nanocrystal via controllable chemical modification towards selective and quantitative detection of Cu(II) ion. Cellulose, 25(10), 5831–5842. https://doi.org/10.1007/s10570-018-19959.
85. Zhong, T., Dhandapani, R., Liang, D., Wang, J., Wolcott, M. P., Van Fossen, D., & Liu, H. (2020). Nanocellulose from recycled indigo-dyed denim fabric and its application in composite films. Carbohydrate Polymers, 240. https://doi.org/10.1016/j.carbpol.2020.116283.

4. CAPÍTULO 1: Low-quality coffee beans as a novel biomass source of cellulose nanocrystals: extraction and application in packaging

Paulino, G. S[a]; Santos, J.P[b]; Aguilar, A.P[a].; Marques, C.S[d]; Vitalino, K.V.R[a]; Moura, E.T.C[c]; Almeida,L.F[a]; Fereira, S.O[a]; Oliveira, T.V[d]; Soares, N.F.F[a]; Ribon, A.O.B[a]; Silva, D.J[e]; Mendes, T.A.O.[a]

[a]Department of Biochemistry and Molecular Biology, Federal University of Viçosa Av. Peter Henry Rolfs, Viçosa, Brazil

[b] Department of Biological Sciences the Federal University of Minas Gerais, Av. Presidente Antônio Carlos, Pampulha, Belo Horizonte, Brazil.

[c]Embrapa Café, Parque Estação Biológica, PqEB s/nº. Brasília, DF - Brazil

[d]Departamet of Food Science and Tecnology Federal University of Viçosa, Av. Peter Henry Rolfs, Viçosa, Brazil.

[e]Department of Chemistry and Molecular Biology, Federal University of Viçosa Av. Peter Henry Rolfs, Viçosa, Brazil

Abstract: In recent decades, there has been an increased number of research works related to the reuse of plant biomass and its technological applications. Plant residues generated from various industrial or agro-industrial processes can have added value, due to the presence of functional compounds with great technological potential, such as cellulose, lignin, hemicellulose, and secondary metabolites, among others. In addition, the reuse of biomass contributes to the creation of green alternatives for the disposal of the large volume of biomass generated. In this work, we produced cellulose nanocrystals from low-quality Arabica coffee beans discarded during the processing of coffee beans in the agroindustry. Arabica coffee beans were collected, sanitized, crushed, clarified by alkaline treatment, and subjected to acid hydrolysis with 65% wt./v sulfuric acid. The cellulose nanocrystals extracted from low-quality coffee beans had needle-shape, with average height and length of 7.27 nm and 221.34 nm, respectively. These nanocrystals were stable in an aqueous medium with pH 7-8, the electrical potential module of 22.5 mV and 20.5 mV, in that order, and a crystallinity index of 67.75% and a thermal degradation of just 8% by mass Finally, the coffee cellulose nanocrystals extracted were added to methylcellulose bioplastics to evaluate their capacity effect as thermal reinforcement in methylcellulose film. The joint analysis of the results demonstrates that cellulose nanocrystals extracted from low-quality coffee beans have dimensional and crystalline characteristics compatible with data found in scientific literature, thus, they are good candidates for use in various technological applications, especially as agents of mechanical reinforcement in polymeric matrices. Among the physical-chemical characteristics of these cellulose nanocrystals extracted in this work, their low thermal

degradation stands out, which makes these cellulose nanocrystals suitable for use in processes that require greater thermal resistance. In addition to this important characteristic, when applied to a methyl cellulose matrix, cellulose nanocrystals were able to reduce the percentage of moisture in the films, reduce UV-vis absorption and did not interfere with the transparency or color of the composites produced.

Keywords: cellulose nanocrystals, coffee, waste reuse, crystallinity, acid hydrolysis, bioplastics, methylcellulose.

Abstract graphic

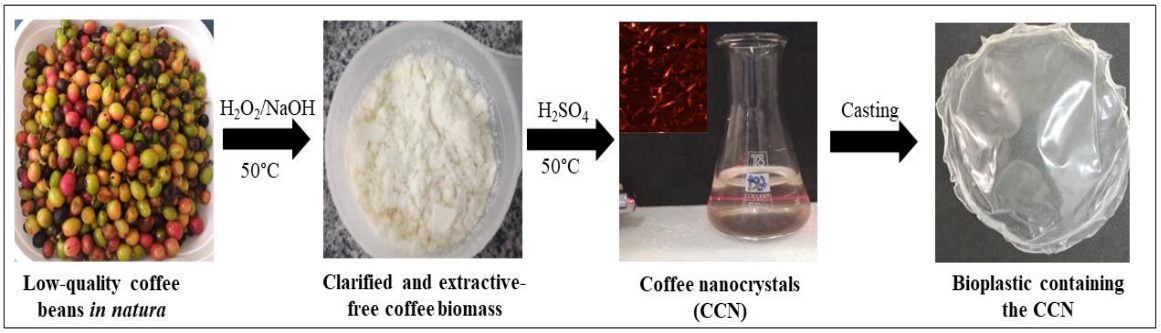

4.1 Introduction

Cellulose is the most abundant natural polymer available in nature. It is present in plant cells and some species of bacteria, such as *Komagataeibacter xylinus*, and even in animals of the phylum *Chordata* (Brigham, 2017; Saxena & Brown, 2001). Biochemically, it is a polymer composed of glucose monomers linked together by a β-1,4 glycosidic bond rotated at 180 °C around the central axis, and its basic unit is cellobiose (1-β-D-Glucopyranosyl-4-β -D-glucopyranose). Cellulose type I is the polymorphism found naturally in the cell wall of plants and can be divided into two main allomorphisms: Cellulose Iα and Iβ. The Iα allomorphism is mainly found in the primary plant wall of higher plants, while the Iβ allomorphism is found especially inside the secondary plant wall, and both types of cellulose play an important role in the mechanical strength of this structure (Paukszta & Borysiak, 2013; Wang et al., 2016).

In addition to its excellent natural function, cellulose has great technological and biotechnological applications when in the form of cellulose nanocrystals (CNC), which can be used, for example, as a reinforcement and barrier agent for a variety of plastic and bioplastic films (George & Sabapathi, 2015; Razali et al., 2019; Lin & Dufresne, 2014; Omran et al., 2021). The physical properties of cellulose nanocrystals that most contribute to such application are their high tensile strength and high Young's modulus, which result

in their reinforcing function when associated with other polymers. In the literature, theoretical calculations indicate that the tensile strength of cellulose nanocrystals varies from 50 to 220 GPa, a value similar to that of glasses and metals, and is closely linked to characteristics such as degree of crystallinity, geometry, dimensions and aspect ratio. When inserted into a polymeric matrix, mechanical reinforcement is a result especially of the increase in the number of weak chemical interactions between the cellulose nanocrystals and the polymeric matrix used, such as interaction bonding, van der Waals interactions, induced dipole, ionic interactions. This increase in mechanical resistance increases linearly the smaller the size of the cellulose nanoparticle, as the “empty spaces” between the polymer molecules tend to be filled by dispersed cellulose nanocrystals. In addition to mechanical reinforcement capacity, cellulose nanocrystals are also an excellent nanoparticle for chemical modification due to their free -OH groups (Kádár et al., 2021; Lagerwall et al., 2014; Aziz et al., 2022; Gomri et al., 2022; Perdoch et al., 2022)

Currently, the principal sources used for CNC extraction are short-fiber cellulosic pulps originating from wood processing. However, agro-industrial residues, such as corn straw, coffee, barley, rice, fruit husks, and sugar cane, have been explored as potential sources of low-cost CNC, which results in the possibility of adding value to agricultural production and raw materials, expanding the market, generating jobs and income, stimulating innovation and technology development, and contributing to stimulate the concept of “circular economy”.

In this scenario, Brazil has great potential for reusing waste from raw material processing since it is the agricultural country and food producer. Moreover, Brazil stands out in the world as the largest producer and exporter of coffee in the world. According to studies by the Brazilian Ministry of Agriculture and Agriculture estimate that 55 million 60 kg bags of coffee were processed in Brazil in 2023, and projections indicate that around 59 million bags (60 kg bag) will be produced in 2023/2024. And between 2032/2033 production should reach around 63 million processed bags, and 36 million of these bags will be exported.

During the production of high-quality coffee, defective or low-quality beans (black, sour, and green), and the husk are separated and discarded or mixed to be used in the Brazilian domestic market (Skorupa et al., 2023). These residues can represent about 50% of the production and are rich in carbohydrates, secondary metabolites, proteins and

lignocellulosic fibers (Cavaton Thiago Farah, 2023, Almeida-Couto et al., 2022; Alarcon et al., 2021, Sadh et al. al., 2018).

In this sense, in the present work, we performed CNC extraction from low-quality coffee beans, and characterized the CNCs in terms of their size and morphology (Atomic Force Microscopy (AFM)), zeta potential, functional groups (Fourier transform infrared spectroscopy (FTIR)), crystallinity (X-ray diffraction) and thermal properties (thermogravimetry (TGA)). And subsequently, evaluation of waste cellulose nanocrystals as a thermal reinforcing agent in methylcellulose polymeric films

4.2 Materials and methods

a. Plant biomass processing

Low-quality Arabica coffee beans (LQCB) were collected from coffee grown at the University of Federal of Viçosa (UFV), in São José do Triunfo, Viçosa, Minas Gerais, Brazil. In the first stage, the beans were washed thrice under running water and emerged for 15 min in sodium hypochlorite solution, at 0.5% wt/v. Then, the coffee grains were rewashed under running water until the complete removal of the sanitizing solution. The LQCB were dried in a 45 °C air circulation greenhouse, for the period of 48 h, ground in a Model TE-631 knife mill (Tecnal, Piracicaba, Brazil), at 22,500 rpm, and sieved (Ø = 35 mesh). After grinding and sieving, the secondary metabolites were extracted from the coffee beans by the exhaustive percolation method, gradually increasing the polarities of the solvent. Soluble fractions containing secondary metabolites were reserved for further studies of their antioxidant and bactericidal activities. Solid coffee lignocellulosic biomass, free of secondary metabolites (CFX) was used for the extraction of cellulose nanocrystals.

b. Alkaline treatment of plant biomass

CFX was submitted to alkaline hydrolysis to remove hemicellulose, lignin, oils, and waxes surrounding plant fibers. In this sense, 50 g of CFX was added to NaOH solution at 4% wt/v in a ratio of 1:18 (CFX:NaOH). The mixture was heated to 70 °C (± 2 °C), under stirring at 145 rpm, for 1 h. After time elapsed, the plant biomass was filtered using a vacuum filtration system, with the aid of a Büchner Funnel with a 35 mesh aperture. This coffee biomass was washed with distilled water (until the washing water reached the pH 7,0) and dried at 60 °C (± 2 °C) for 12 h in a greenhouse.

The second stage of the alkaline treatment aimed to remove lignin from plant fibers to purify the pulp content of plant biomass. At this stage, 50 g of biomass previously treated

were added to H_2O_2/NaOH, at 24% v/v and 4% wt/v, respectively, totaling a volume of 450 mL. Then, the solution was heated to 50 °C for 2 h, under constant stirring at 145 rpm. Extractive-free and clarified coffee biomass (CFXC) was washed in a filtration funnel vacuum with an opening of 35 mesh, until washing water reached pH 7,0 and then dried at 60 °C (± 2 °C), for 12 h, in the greenhouse.

c. Quantification of lignocellulosic biomolecules in fresh and clarified coffee fibers

The quantification of cellulose, hemicellulose, lignin, and ash was performed as described in "Documento 236/2010 (EMBRAPA) - Procedimento para Análise Lignocelulósica" (Morais, et al., 2010). The methods used are based on a review of the literature and methodologies by TAPPI and ANSI (American National Standards Institute).

d. Cellulose nanocrystal extraction

The CFXC biomass was crushed in a knife mill (TE-631-Tecnal) until 325 mesh (0.044 mm diameter). Then, 1 g of coffee biomass was added to 13 mL sulfuric acid at 65% wt/v (Sigma Adrich®), at 50 °C (± 2 °C), for 20 min. The acid hydrolysis reaction was terminated with the addition of 300 mL of refrigerated distilled water. Coffee cellulose nanocrystals (CCN) were resuspended after 20 cycles of centrifugation at 12,000 rpm, at 4°C (± 1°C). The supernatant containing the CCN was collected, and its pH was adjusted to pH = 5 using NaOH at 0.5 M.

e. Characterization Atomic Force Microscopy

CCN was suspended in distilled water, at a ratio of 1:20, sonicated for 5 min, and drops of it were placed on mica sheets, followed by drying in an oven at 100 °C (± 5 °C) for 5 min. The mica sheet containing the CCN was coupled to the Atomic Force Electron Microscope (AFM) (NT-MDT/Ntegra Prima - Amsterdam, Netherlands) operating in probe scanning mode. The analyses were measured using Nova NT-MDT SPM software version 1.0.

f. Fourier transform infrared spectroscopy

The coffee cellulose nanocrystal suspensions were dried at 72 °C (± 2 °C), for 24 h, and 1 mg of CCN particles was evaluated regarding their functional groups in a Fourier transform infrared-attenuated total reflectance (ATR-FTIR), using the Varian 660-IR equipment coupled to the GLadiATR accessory, with diamond crystal, operating in the

sweep transmittance mode, in the range of 4000 - 400 cm^{-1} (Thermo Fisher Scientific – USA).

g. Zeta Potential and Dynamic scattering of light

Different aliquots of CCN suspensions had their pH adjusted to values from 2 to 12, using 0.5 M NaOH or 0.5 M HCl. The zeta potential of CCN suspensions at different pH values was analyzed with the aid of the Zetasizer Malvern Nano ZS (United Kingdom). The analyses were performed at 25 °C (± 2 °C), using a detection angle of 173° operating at a wavelength of 633 nm.

h. X-Ray Diffractometry

The X-ray diffractometry (XRD) was performed to determine the crystalline index (CI) of CCN, using a BRUKER X-ray diffractometer (D8-Discover, USA), with Ni filter and Cu-Kα radiation (λ= 1.5406 Å), angular variation of 10º to 40º (2Θ;) and 3 min^{-1} speed, 40 kV voltage and 40 mA current. The CI was calculated using the following equation (Eq 1):

$$\% \, CI = \frac{(A_C - A_a)}{A_t} \times 100 \qquad \textbf{(Eq. 1)}$$

In which A_c is the area of the crystalline peaks, A_a is an amorphous area of the amorphous pattern, and A_t is the total area. The identification of the crystalline peaks was calculated using the X Powder X 2021 program (Martin, J.D, 2016). The Full Crystallographic Open Database (COD) was used to identify the type of cellulose present in crystalline structures.

i. Thermogravimetry

Thermogravimetry (TGA) was used to evaluate the thermal decomposition of CCN through the TGA analyzer, model Model DTG-60 H (Shimadzu, Japan). A sample of 3 mg of nanocrystals was heated in alumina crucibles up to 1000 °C (± 5 °C), with a heating rate of 10 °C.min^{-1} in an inert nitrogen atmosphere with a flow rate of 50 mL.min^{-1}.

j. Bioplastics Production

Firstly, 1.5 g of methyl cellulose (cP 4,000, Sigma Aldrich, USA) was gradually dispersed in 100 mL of a 50% wt/wt solution of ethanol/distilled water at 0 °C (± 2 °C) totaling a 1.5% (wt/wt) solution of methyl celulose (MC). Subsequently, the mixture was heated at a rate of 5 °C.min^{-1} to a temperature of 70 °C (± 2 °C), under constant stirring at 100 rpm. Once the temperature reached 70 °C (± 2 °C), 500 µL of glycerin (Sigma

Aldrich, USA) and 50 µL of Tween 80 (Sigma Aldrich, usa) were added, corresponding to 33.33% and 3.33% of the polymer mass, respectively. The dispersion was maintained at 70 °C for 15 min under stirring.

The amounts of CCN added to MC dispersions were calculated in relation to the polymer mass: 0, 0.6, 1, 3, and 5% (wt/wt). The weighted CCN was dispersed in 5 mL of Dimethyl sulfoxide (DMSO) and added to 95 mL of the MC dispersion previously cooled in an ice bath to 35°C (± 2 °C). The filmogenic dispersions containing cellulose nanocrystals (MCNC) were stirred for 30 min at 100 rpm, and approximately 25 g were poured into 10 cm Petri dishes and dried in an oven for 72 h at 37°C (± 2 °C) to solvent evaporation.

Characterization of the bioplastic

a. Moisture content

The bioplastics of MC and MCNC bioplastics (Ø = 10 cm) were initially weighed and then placed in an oven at 105 °C for 2 h. After, dried films were weighed again. Then moisture content was quantified by the difference of the initial and final mass of the films sur the initial mass.

b. Fourier transform infrared

The Fourier transform infrared (FTIR) of MC and MCNC bioplastics were carried out at the Multivariate Chemical Data Analysis Laboratory (MCDALab) of the Department of Chemistry at UFV. For this, a small section of MC and MCNC films were subjected to the attenuated reflectance technique (ATR) using the Varian 660-IR equipment coupled to the GLadiATR accessory with diamond crystal, operating in transmittance mode with scanning in the wavelength range of 400 - 4000 cm^{-1}.

c. Color Analysis

MC and MCNC bioplastics with 25 cm^2 were subjected to color analysis using the L*, a*, b* color coordinates of the CIELAB color scale. The instrument was the Colorquest XE Colorimeter (Hunter Lab, Reston, USA) by reflectance, with spherical geometry d/8º, illuminant D65 and observation angle of 10°. The equations below were used for the calculation of the Hue angle (Eq. 2) (McLELLAN, 1994)

$$Hue^{o} = 180 + arctang() \frac{b}{a} \quad \textbf{(Eq. 2)}$$

d. UV-vis analysis

The MC and MCNC bioplastics transparency and UV protection were assessed using a UV-Vis spectrophotometer, model UV 1800 (Shimadzu, Japan) with scanning in the range of 200-700 nm. The films samples 25 cm^2 were placed directly in the test cell for the scanning ranging from 200 to 700 nm.

e. Scanning electron microscopy analysis

Micrographs of the bioplastics were obtained using a Scanning electron microscope (SEM) with a secondary electron detector operating under low vacuum, model TM3000 (Hitachi High Technologies America, Inc. Schaumburg, IL, USA). The electron accelerating voltage used was 15 kV with a magnification of 500x.

f. Thermogravimetry

Termogravimetry (TGA) was used to evaluate the thermal decomposition of methylcellulose bioplastics containing or not low-quality coffee cellulose nanocrystals. For this purpose, a TGA analyzer, model DTG-60 H (Shimadzu, Japan), was used. Samples of 3 mg of bioplastic film were heated in alumina crucibles up to 1000 °C (± 5 °C), with a heating rate of 10 °C.min-1 in an inert nitrogen atmosphere with a flow rate of 50 mL. min^{-1}

4.3 Results and Discussion

a. Quantification of biomolecules

Cellulose, hemicellulose, lignin, ash content, and moisture were quantified in CFX and clarified CFXC biomass, and the results are presented in **Table 1**. The coffee biomass clarification process was able to halve the relative lignin content, from 36.3% to 17%. Furthermore, the process increased the relative cellulose and hemicellulose content of CFXC by 1.6x and 1.5x, respectively. The clarification process did not obtain 100% efficiency, which can be noticed by the result of lignin reduction of only 50%. Many external factors can influence the removal of lignin, and at the same time result in the loss of cellulose during the purification and clarification process. Among these factors, the concentration $NaOH/H_2O_2$, temperature, alkaline hydrolysis time, the combination of these factors can act either as bleaching agents, modifying only the structure of the lignin chromophore groups, which results in an apparent loss of lignin, or as catalytic agents resulting in the total loss of the chemical structure of lignin and the release of this biomolecule from the vegetable fiber. Regarding the yield of the acid hydrolysis reaction with 65% w/t sulfuric acid for extraction of cellulose nanocrystals, the calculated results indicate that the reaction had a yield of 21% by mass for every 1 g CFXC hydrolyzed.

Table 1: Biomolecule contents of coffee biomass

Coffe Biomass	% Celullose	%Hemicellulose	% Lignin	%Ash	%Moisture
[1]CFX	22.7	35.8	36.3	9.3	1
[2]CFXC	36.7	52.7	17	10.55	1.8

[1] CFX = coffee lignocellulosic biomass, free of secondary metabolites

[2] CFXC = Extractive-free and clarified coffee biomass

b. Fourier Transform Infrared Spectrometry and Zeta Potential

Spectrum A **(Figure 1)** compares the FTIR profile between the CFX and CFXC samples. The band at 3200 cm^{-1} refers to the OH stretching presented in cellulose, lignin and hemicellulose molecules. The absorption at 1024 cm^{-1} characterizes the vibration of the C-O-C bond, a relative decrease in the transmittance intensity value of this wavelength in CFXC in relation to the transmittance value at the same wavelength for CFX, indicates that the clarification process has increased the number of molecules that have glycosidic bonds (cellulose and hemicellulose), this conclusion is supported by the relative increase in cellulose and hemicellulose that were quantified in the CFXC fibers in **Table 1**. For the CFX and CFXC samples, the peaks at 2800 and 2883 cm^{-1} are characteristic of CH_2 stretching and the peaks at 1316 cm^{-1} are attributed to the deformation of the CH bond of the methylene groups, both chemical groups feature cellulose, hemicellulose and lignin molecules. An increase in the transmission intensity is noted at the wavelengths mentioned above, and it is observed a decrease in the transmission intensity at the wavelength of 1024 cm^{-1}, which refers to the vibration of the glycosidic bond. These observations indicate a structural change caused by the occurrence of oxidation with hydrogen peroxide in an alkaline medium, which possibly led to the demethylation of lignin molecules and consequently the relative increase of lignin and hemicellulose. (Alghooneh et al., 2017; Cardoso et al., 2016; Mancera et al., 2020; Santos, 2020).

The absorption at 1234 cm^{-1} is related to the stretching of the C-O bond, the increase in the transmittance intensity of this band in CFXC indicates a loss/modification in the phenolic -OH groups. At 1583 cm^{-1}, it is the region of deformation of the C=C aromatic bond and the increase in transmittance at this wavelength indicates the loss of the aromatic structure existing in the lignin molecules. The CFX spectrum has a small jump at 1713 cm^{-1} that is associated with the ester absorption region, which is abundant in hemicellulose and lignin compounds. The absence of this transmittance in the CFXC

spectrum corroborates the hypothesis that there was oxidation of lignin and hemicellulose (Cardoso et al., 2016).

In spectrum B **(Figure 1)**, there is an increase in transmittance intensity at all wavelengths of the CCN sample when compared to the spectrum of commercial microcrystalline cellulose (MCC). The transmittance at 3.200 cm^{-1} and 1.633 cm^{-1} refers to the stretching movement of the OH group of cellulose. The band centered in the 2860 cm^{-1} region is related to the symmetric and asymmetric stretching of the methyl and methylene groups (Matebie et al., 2021; Doh et al., 2020).The peak at 1420 cm^{-1} is attributed to the C6's rocking movement of the CH_2 groups of the cellulose's ring (Rasheed et al., 2020; Aguayo et al., 2018b). The increase in transmittance intensity of these peaks in the nanocrystals' spectrum indicates organization of hydrogen bonds in the structure of the celulose, which reduced the rocking movement of this group, which indicates the presence of a crystalline structure (cellulose nanocrystals). Finally, the peak at 1022 cm^{-1} can be related to the stretching motion of the C-O-C group of the cellulose glucose hexagonal rings (Deb Dutta et al., 2021; Akinjokun et al., 2021; Rasheed

et al., 2020). The quantification of glucose from the cellulose nanocrystals via HPLC supports the cellulose spectrum data obtained by the FTIR, and the amount of glucose present in the sample of nanocrystals was 0.212 mg/g.

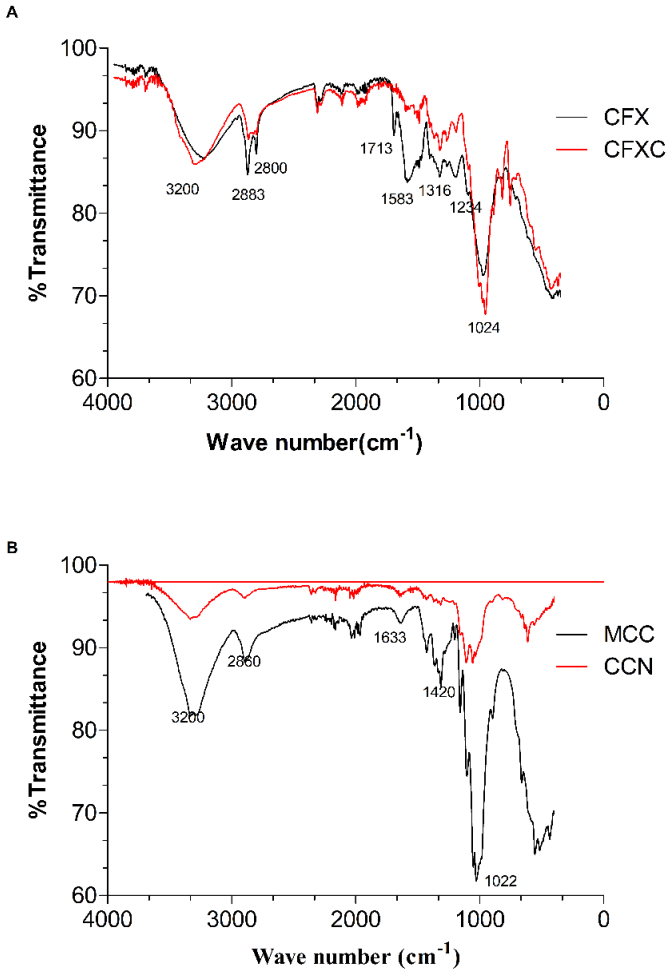

Figure 1: Fourier transforms infrared. A) FTIR of low-quality extractive free (CFX) and low-quality extractive-free-clarified coffee beans(CFXC). B) FTIR of low-quality coffee bean celulose nanocrystals (CCN) and commercial Microcrystalline Cellulose (MCC).

c. Atomic Force Microscopy and Dynamic ligth mirroring

Atomic force microscopy and Dynamic Light Scattering are one of the techniques commonly used to characterize nanoparticles. Using these techniques **(Figure 2)**, it was possible to observe the dimensions and morphology of the cellulose nanocrystals extracted. The CCN had a rodshape, average height of 7.27 nm and an average length of 221.34 nm, which is in agreement with the values reported in the literature for cellulose nanocrystals. Based on the length, width, and height of cellulose nanocrystals' values, it is possible to calculate their aspect ratio and obtain information about their surface area, which plays an important role in their applications. Studies on the morphology of cellulose nanocrystals proved that the higher the aspect ratio, the better the tensile strength of the compounds reinforced with these nanoparticles, and the greater their chemical reactivity and optical transmittance (Lahiji, 2010; Wu, et al 2019; Shrestha, et al, 2018; Babaei-Ghazvini & Acharya 2022; Panchal, et al 2019). In this study, the aspect ratio of

the cellulose nanocrystals was equal to 30.45, which can be considered an average aspect ratio value, when compared to those found in the literature.

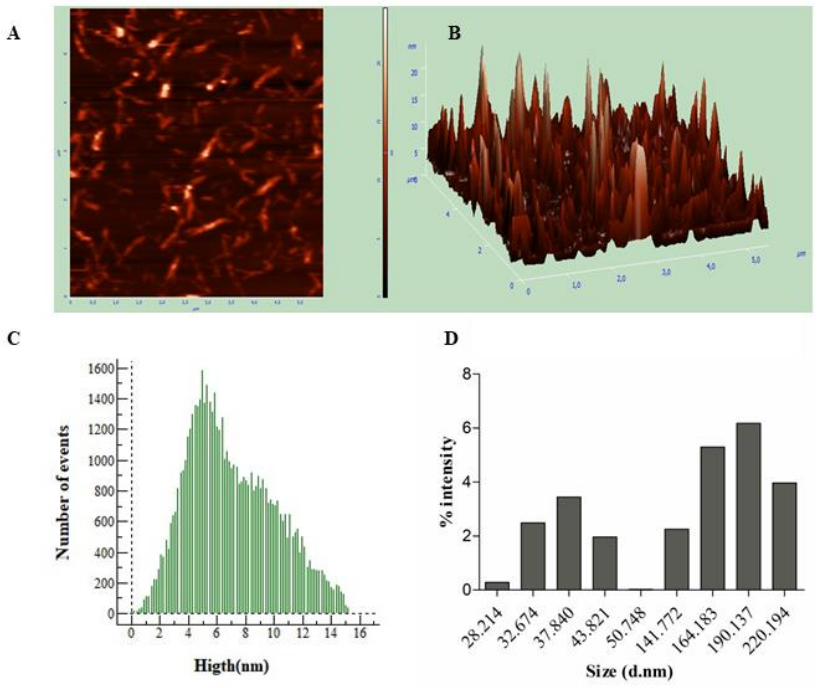

Figure 2: Micrographs from Atomic Force Microscopy (AFM) and data from Dynamic Light Scattering (DLS). A) CCN AFM-1D B) CCN AFM-3D C) CCN height distribution using AFM D) CCN width bimodal distribution using DLS.

e. Zeta Potential

Stability in aqueous solutions is an important feature of cellulose nanocrystals. In general, dispersions with Zeta Potential in module values greater than 30 mV are more stable, with a low tendency to agglomeration since molecular forces of electrical repulsion are predominant. Suspensions with Zeta Potential in module less than 15mV tend to agglomerate, forming clusters. The stability of the coffee cellulose nanocrystals extracted in this work was through their dispersion in aqueous solutions with pH ranging from 2 to 12 and measuring the zeta potential of these solutions. Coffee cellulose were stable in the pH range between 7-8, with potential Zeta Potential in module values 22.5mV and 20.5mV, respectively. The values found are consistent with the literature data for the Zeta potential of cellulose nanocrystals (Kassab et al., 2020; Tesfaye et al., 2021).

f. X-Ray Diffractometry

The **Figure 3** shows the X-ray diffractogram of the NCC and **Table 2** explains the peaks present in the diffractogram, the sample showed crystalline peaks at 18°- 45°, and peaks with less intensity between 45° and 75°. The peak centered at 18° 2θ is typical of

the crystalline portion of cellulose nanocrystals. Other characteristic peaks centered at 22° 2θ were less intense. Peaks in the regions of 50° ≤ 2θ ≤ 70° are less common in the diffraction pattern of cellulose nanocrystals, probably due to impurities, different shapes and sizes, or the occurrence of more than one type of crystal (Holder & Schaak, 2019). The crystallinity index was 67.75%, thus corroborating the literature data, which values range from 54% to 90%. According to the data from Crystallography Open Database (Gražulis et al., 2012), the cellulose of coffee nanocrystals is Iβ type, characteristic of plant biomasses, with triclinic as the main crystallite type. The crystallinity of cellulose nanocrystals is an important factor for their technological application, because of their physicochemical properties, such as tensile strength, stiffness, melting point, gas, and vapor permeability, besides the optical properties. The cellulose nanocrystals extracted in this study have a medium crystallinity index, which allows them to be used as a reinforcing composite in various biodegradable and synthetic polymeric matrices.

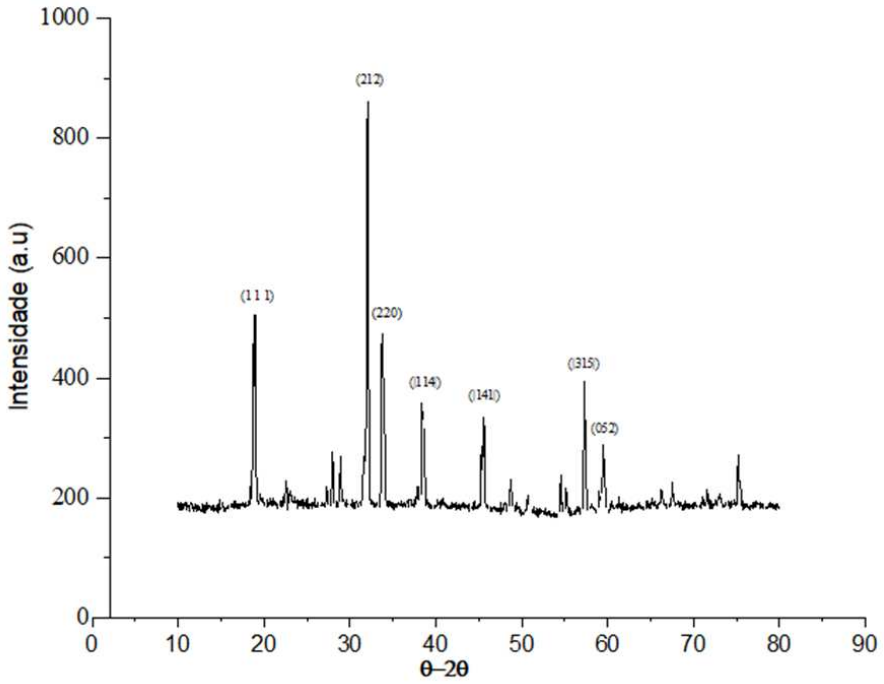

Figure 3: CCN X-Ray diffraction pattern.

Table 2: Main crystalline peaks of cellulose nanocrystals

2θ	d-spacing	2θ	d-spacing	2θ	d-spacing

18.9	4.704	32.0	2.795	54.654	1.678
22.57	3.926	33.8	2.649	55.27	1.661
27.29	3.270	38.53	2.339	57.323	1.606
28.0	3.182	45.53	1.988	59.492	1.552
28.9	3.086	48.815	1.864	75.339	1.260

g. Thermogravimetry

Figure 4 compares the mass loss between the CFXC and CCN samples. Graph A is related to the linear loss of mass with the gradual increase in temperature and graph B represents the first derivative of mass loss in relation to time, during the gradual increase in temperature. The profile of both samples has significant differences in the amount of mass loss and also in relation to the degradation profile. The CFXC sample presents a degradation profile characteristic of cellulosic or lignocellulosic fibers, for this sample the total degradation rate is 97.75% with maximum loss at 315°C. The loss of water molecules through dehydration, the evaporation of volatile organic molecules, as well as the degradation of low molecular weight organic molecules occurred between 100 and 200 ºC, as can be seen by the presence of the first degradation peak in **Figure 4 B**. Cellulose degradation in the CFXC sample occurred at 311°C and the physicochemical events involved in this stage are especially the breaking of hydrogen bonds between parallel cellulose chains and oxidation of carboxylic groups, leading to the complete degradation of cellulose into CO_2 and water. The red curve in **Figure 4 A** is the thermogravimetric curve for cellulose nanocrystals (CCN). These nanocrystals have high thermal stability, as the total mass loss during the gradual increase in temperature was only 8%. The amplification of the thermogravimetric curve shows that there are two initial events of thermal degradation, the first event occurs between 100°C and 200°C, and corresponds to the loss of water molecules, evaporation of volatile molecules and breakdown of low-weight organic molecules. The second thermal degradation event occurs at 311°C, and corresponds to the degradation of cellulose molecules or ligncocellulosic molecules. Several factors can explain the low mass loss rate of nanocrystals (CCN), mainly the chemical composition of the biomass, clarification process, nature of hydrolysis, degree of crystallinity of the nanocrystals and size of the crystallite (Akinjokun et al, 2021; Farooq Adil et al., 2020a; Frost & Johan Foster, 2020;

Tesfaye et al., 2021; Gong et al., 2017; de Carvalho Benini et al., 2017). In this work, the main hypothesis that explains the low rate of thermal degradation is the interaction of residual lignin from the clarification process with the extracted cellulose nanocrystals. Lignin has a slow degradation rate that can vary from 60° C to 950° C, which is justified especially by the complexity of the oxygen groups present in its structure, each of these functional groups has a degradation temperature, resulting in an extensive thermal range for complete lignin degradation. Furthermore, oxygenated groups frequently undergo rearrangements during an increase in temperature, which generates secondary compounds with high thermal resistance. Another important factor is the presence of inorganic salts, which enhance the natural flame retardant effect of lignin, increasing resistance to thermal degradation (Brebu, 2014; Brebu & Vasile, 2010; López-Beceiro et al., 2021). Results similar to those found in this work were also reported in experiments carried out by collaborators Farooq (2020 a) and also by Sabaruddin & Paridah,2018.

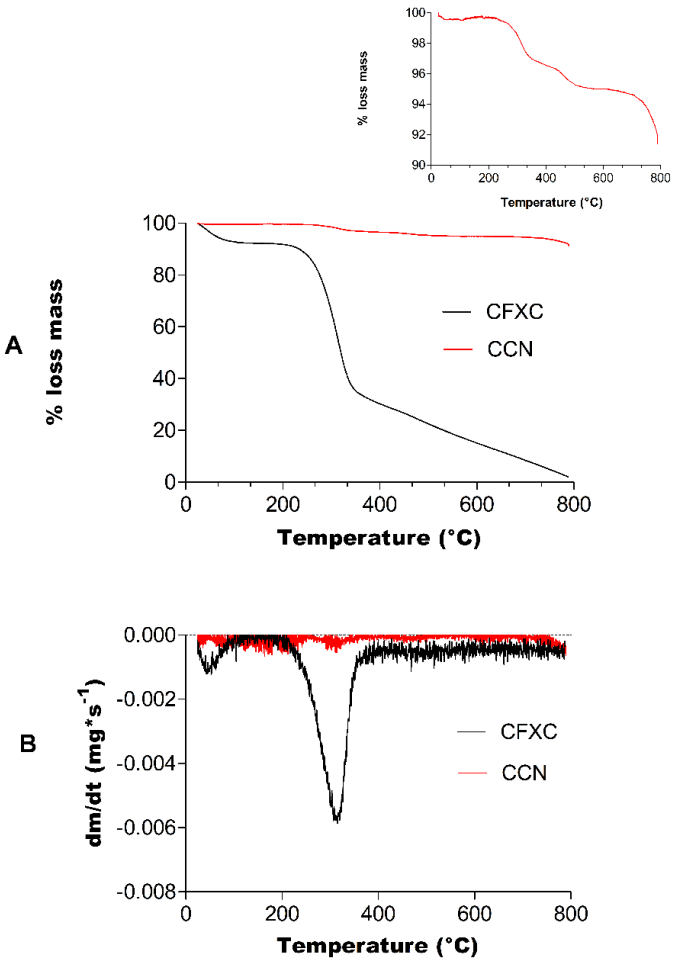

Figure 4: Thermogravimetry of CFXC and CCN. A) Comparison between the TGA of CFXC and CCN. B) Comparison between the DTG of the CCN sample and the CFXC sample.

g. Characterization of bioplastics by Fourier Transform Infrared Spectrometry and Scanning electron microscopy analysis

Pure methylcellulose (MC) films had an average moisture content of 10.76 % and methylcellulose films added with cellulose nanocrystals had an average moisture content of 1.40%. Photographs of produced bioplastics containing different concentrations of low-quality coffee celulose nanocrystals are shown in **figure 5**. The increase in CCN concentration made the bioplastics more opaque and rigid to the touch. Furthermore, is possible observe that the bioplastics containing CCN were not homogeneous.

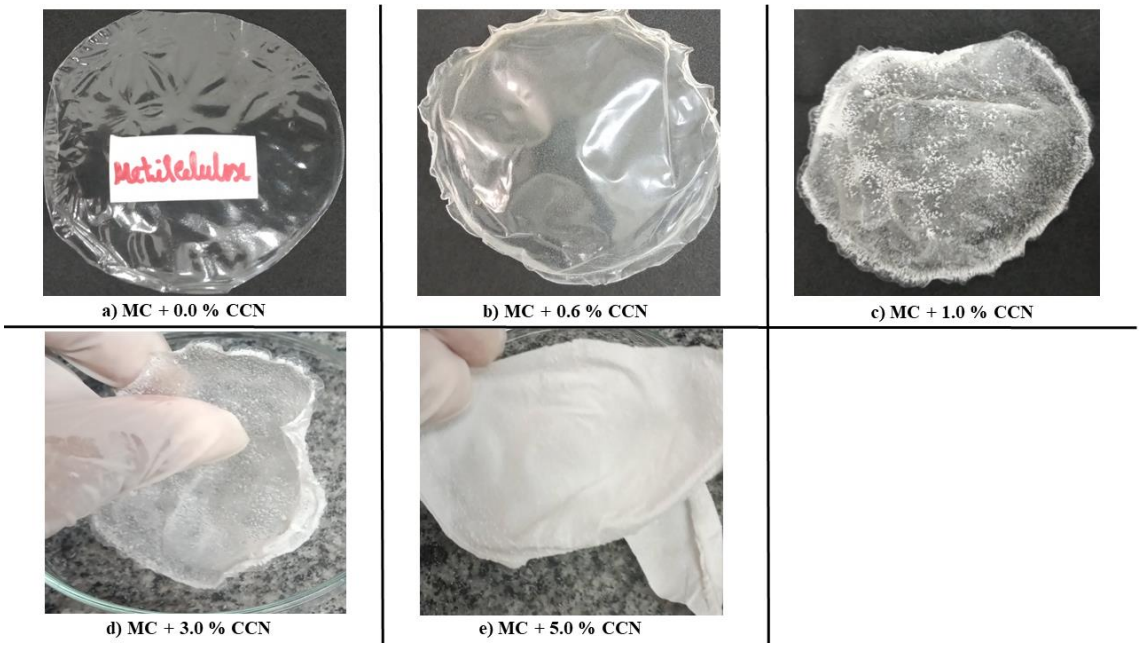

Figure 5: Photographs methyl cellulose bioplastics containing low quality coffee cellulose nanocrystals: (a) pure methyl cellulose bioplastic (control); (b) methyl cellulose bioplastic with 0.6% wt/wt of CCN; (c) methyl cellulose bioplastic with 1.0 % wt/wt of CCN; (d) methyl cellulose bioplastic with 3.0 % wt/wt of CCN; and (e) methyl cellulose bioplastic with 5.0 % wt/wt of CCN.

In **Figure 6**, the SEM images are presented,showing the surface morphology of the produced bioplastics. For the methyl cellulose bioplastic without the addition of CCN (**Fig.6a**) a smooth surface with some whitish spots can be observed, which are probably lumps of non-gelatinized methyl cellulose, causing a small irregularity in the produced bioplastic. Shallow tears, which may result from occasional abrasion of bioplastics with hard surfaces during film handling can also be seen.

Images **Fig.6b to Fig.6e** refer to methyl cellulose bioplastics with increasing concentrations of coffee cellulose nanocrystals. In all micrographs, the presence of CCN agglomerates with different morphologies can be seen, in addition to an irregular

dispersion of CCN in the films. In some points, clusters of cellulose nanocrystals can be seen, with a needle-like morphology, characteristic of CCN extracted by acid hydrolysis with sulfuric acid.

Several factors can cause the agglomeration of cellulose nanocrystals, such as chemical compatibility with the polymeric matrix, shear force, surface energy increase, drying process, temperature, interactions with plasticizers and other components.

Methyl cellulose is a cellulose derivative with uncontrolled replacement of the free -OH groups by the $-CH_3$ methyl group. Thus it is a less hydrophilic derivative than cellulose. Cellulose nanocrystals, on the other hand, are hydrophilic nanoparticles because they have free -OH groups. Additionally, in the case through acid hydrolysis, CCN extracted with sulfuric acid, have negative charges on their surface, derived from the replacement of some free -OH by $–SO_4^{3-}$ groups, contributing even more to its hydrophilicity. Therefore, the CCN tends to agglomerate and escape from the polymeric matrix, physically observed in bioplastics with concentrations of CCN greater than 0.6%. These films expelled the nanocrystals from the polymeric matrix, causing that the dry bioplastic to contain a thin layer of whitish and shiny powder on its surface, possibly the coffee cellulose nanocrystals added to the filmogenic dispersion.

When cellulose nanocrystals are agglomerated, they can acquire different morphologies, as observed by several authors (Fitriani et al., 2021; Pereira et al., 2020; Wei et al., 2017; Zhu et al., 2022), the most common morphologies found in groups of cellulose nanocrystals are spherical, cylindrical and sheet-shaped, the films produced here have spherical agglomeration and cylindrical cellulose nanocrystals.

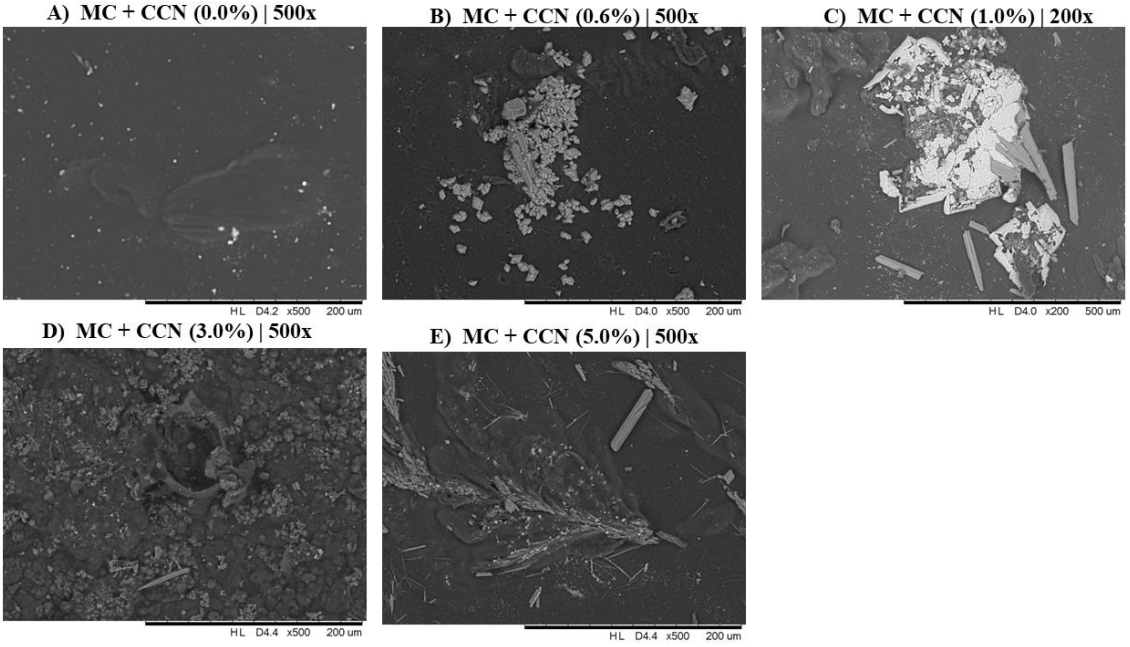

Figure 6: Scanning electron microscopy (SEM) of methyl cellulose bioplastics containing low quality coffee cellulose nanocrystals with magnifications of 200x or 500x: **(a)** pure methyl cellulose bioplastic; **(b)** methyl cellulose bioplastic with 0.6% wt/wt of CCN; **(c)** methyl cellulose bioplastic with 1.0 % wt/wt of CCN; **(d)** methyl cellulose bioplastic with 3.0 % wt/wt of CCN; **(e)** methyl cellulose bioplastic with 5.0 % wt/wt of CCN.

The FTIR spectra of methyl cellulose (MC) and methylcellulose bioplastics containing coffee cellulose nanocrystals (MCNC) in general exhibited a typical cellulose spectrum **(Figure 7).** The peak at 2950 cm^{-1} is the result of symmetric and asymmetric stretching of the C-H bond. Peaks around 1350 – 1650 cm^{-1} related to the deformation in the plane of the δ(C-H) bond, whereas the peak at 1068 cm^{-1} is characteristic of stretching of the C-O-C glycosidic bond. The band at 3400 cm^{-1} is the result of stretching vibration of the ν(O-H) bond. The peak identifies methyl cellulose is 950 cm^{-1}, corresponding to the -OCH_3 radical of methyl cellulose.

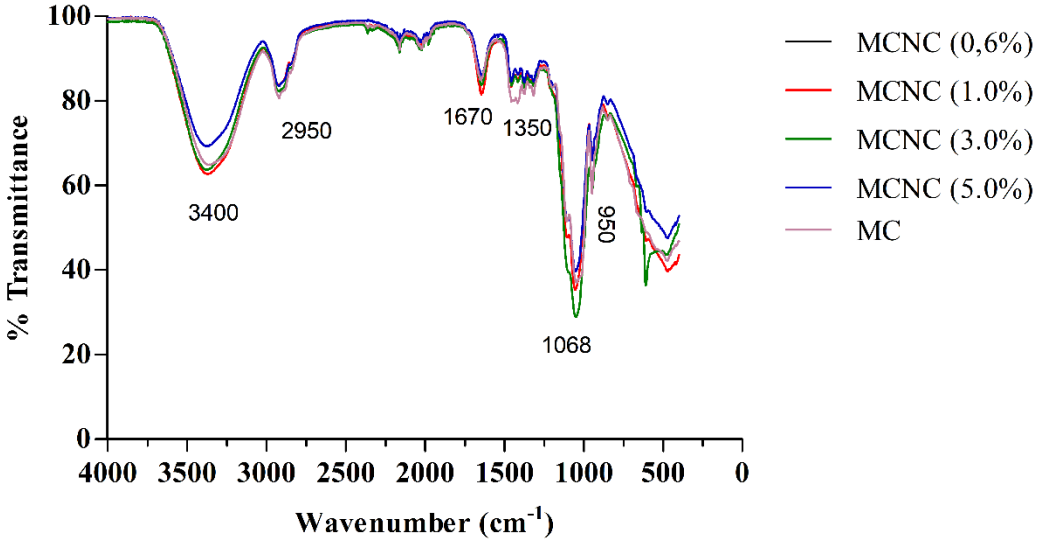

Figure 7: Fourier transform infrared of the produced bioplastics: pure methyl cellulose film (MC) and films containing different concentrations of low-quality coffee cellulose nanocrystals (MCNC).

After evaluation by SEM and FTIR, the chosen concentration of cellulose nanocrystals for application in methyl cellulose bioplastics was 0.6% (wt/wt), % due to the homogeneous distribution of cellulose nanoparticles. Besides, there was no expulsion of cellulose nanocrystals to the surface of the films produced. In this film presented good malleability during touch. Therefore, the following characterizations refer to MCNC 0.6% films.

h. Color and ultraviolet analysis

Color analysis was performed using the CIELAB system. MC and MCNC bioplastics do not differ significantly for luminosity index (L). MCNC 0.6% bioplastics emit higher intensity with L = 66.83, while MC bioplastics are slightly less luminous with L = 66.66. In relation to the color coordinates a and b, the bioplastics resulted in greenish-yellow, with the color coordinates for the MCNC bioplastic being 0.6% a= -1.79, b= 5.39 and HUE° = 108.87, and for MC bioplastic the color coordinates were a= -2.46, b= 6.42 and HUE°= 110.97.The UV analysis (**Figure 8**) demonstrated that 0.6% MCNC bioplastics had a UV protection range between 225-375 nm greater than MC bioplastics.

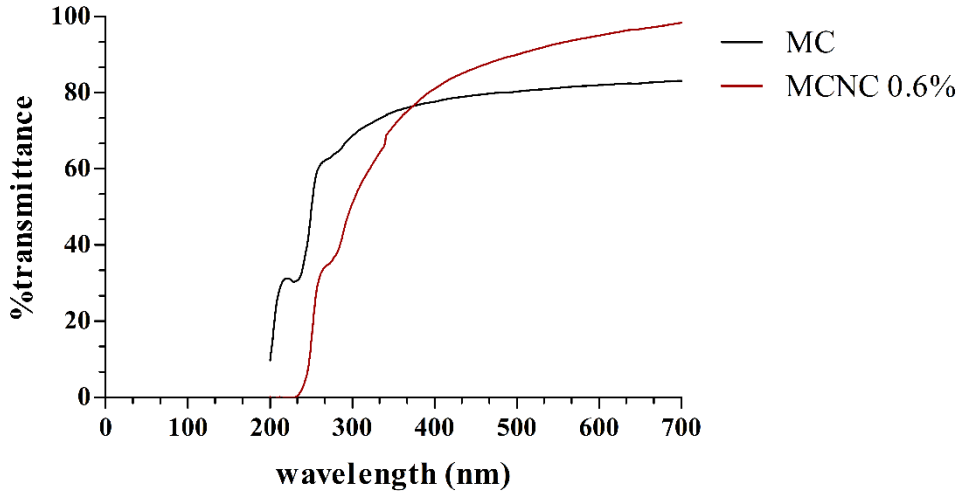

Figure 8: UV-Vis transmittance of MC bioplastics (blac color curve) and MCNC (red color curve).

i. Thermogravimetric

No significant difference in the degradation temperature between MCC (Tonset=179 °C Tmax. = 359 °C) and MCNC (Tonset= 181 °C and Tmax = 359°C) bioplastics was observed when the thermogravimetric results were evaluated. In other words, the presence of nanocrystals did not affect the thermal resistance of the film.

Based on the profile of mass loss between 100 ºC and 200 °C, MCNC films have less moisture than the MCC films, corroborating with the humidity test carried out previously. This behavior can be explained by the capacity of cellulose nanocrystals to establish bonds with the MCC polymeric matrix, preventing water molecules absorption and interaction with the MCC matrix and increasing the , humidity. Other studies with

cellulose nanocrystals have also shown that there is no increase in the thermal resistance of the studied bioplastics when adding cellulose nanocrystals extracted with acid hydrolysis with sulfuric acid (Agustin et al., 2014; Blilid et al., 2020).

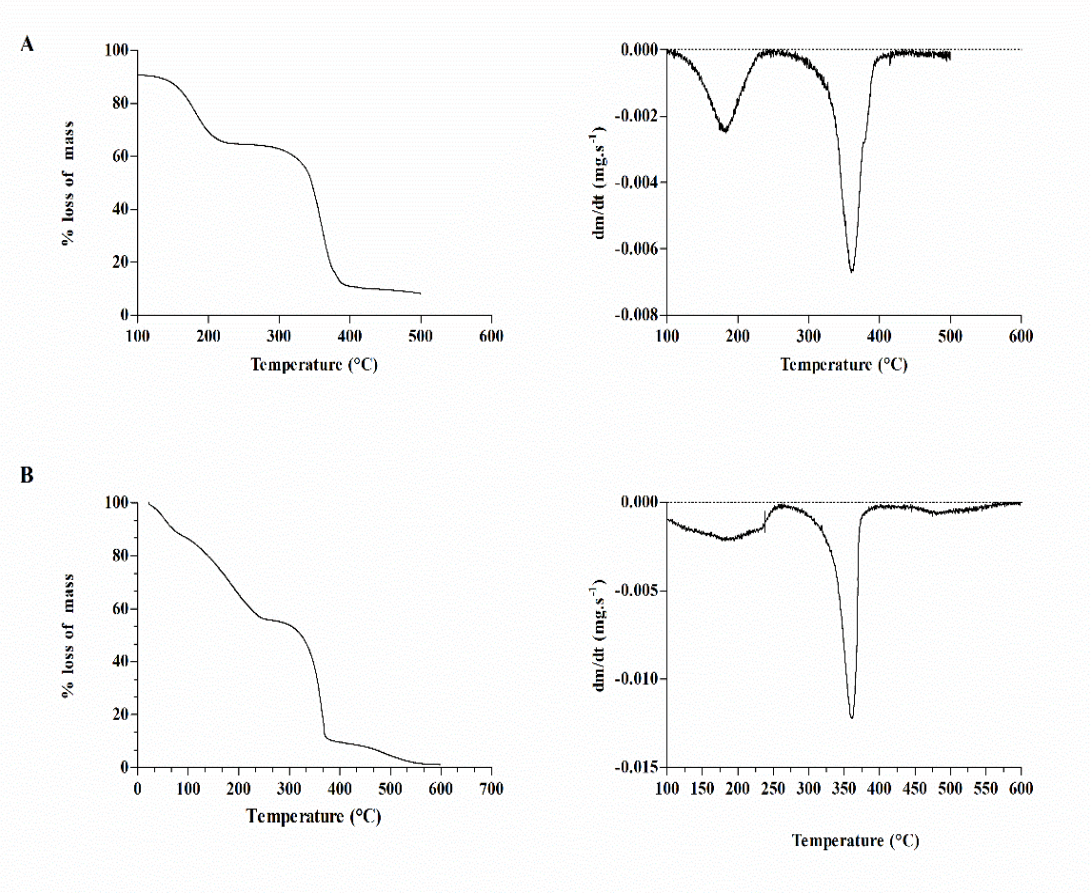

Figure 9: Thermogravimetry of bioplastics. A) TGA curve and 1° curve derived from MCC bioplastic. B) TGA curve and 1° curve derived from the MCNC (0.6%) bioplastic.

4.4 Conclusion

The results presented in this work demonstrate that cellulose nanocrystals extracted from low quality coffee beans (LQCB) have physicochemical characteristics with potential biotechnological application. Among these characteristics, the degree of crystallinity and thermal resistance of cellulose nanoparticles stand out. The crystallinity degree of the nanocrystals extracted from LQCB was 67.75% and their thermal degradation was 8% up to 800°C. In this sense, the combination of high thermal resistance and a significant degree of crystallinity of these nanoparticles makes them useful in processes that require high temperature and/or that require mechanical reinforcement, such as in food packaging. The results found for the application of these cellulose nanocrystals as a composite in methyl cellulose films demonstrate that the cellulose

nanocrystals do not alter the thermal resistance of this polymer. However, the addition of cellulose nanocrystals to the methyl cellulose matrix was able to reduce the percentage of moisture in the films, maintain the high degree of transparency of this polymer and act as a barrier against ultraviolet light. These characteristics are essential in the development of biopackaging capable of maintaining food quality, especially foods sensitive to light and humidity.

4.5 Perspectives

In the next work, we intend to evaluate films containing coffee cellulose nanocrystals, as antimicrobial and antioxidative packaging for dry foods. Furthermore, testing the chemical compatibility of coffee cellulose nanocrystals in other biodegradable polymeric matrices.

4.6 Bibliographic references

1. Aguayo, M. G., Pérez, A. F., Reyes, G., Oviedo, C., Gacitúa, W., Gonzalez, R., & Uyarte, O. (2018b). Isolation and characterization of cellulose nanocrystals from rejected fibers originated in the Kraft Pulping process. Polymers, 10(10). https://doi.org/10.3390/polym10101145

2. Agustin, M. B., Ahmmad, B., Alonzo, S. M. M., & Patriana, F. M. (2014). Bioplastic based on starch and cellulose nanocrystals from rice straw. *Journal of Reinforced Plastics and Composites*, *33*(24), 2205–2213. https://doi.org/10.1177/0731684414558325

3. Akinjokun, A. I., Petrik, L. F., Ogunfowokan, A. O., Ajao, J., & Ojumu, T. V. (2021). Isolation and characterization of nanocrystalline cellulose from cocoa pod husk (CPH) biomass wastes. Heliyon, 7(4). https://doi.org/10.1016/j.heliyon.2021.e06680

4. Alarcon, R. T., Lamb, K. J., Bannach, G., & North, M. (2021). Opportunities for the Use of Brazilian Biomass to Produce Renewable Chemicals and Materials. In ChemSusChem (Vol. 14, Issue 1, pp. 169–188). Wiley-VCH Verlag. https://doi.org/10.1002/cssc.202001726

5. Alarcon, R. T., Lamb, K. J., Bannach, G., & North, M. (2021). Opportunities for the Use of Brazilian Biomass to Produce Renewable Chemicals and Materials. In *ChemSusChem* (Vol. 14, Issue 1, pp. 169–188). Wiley-VCH Verlag. https://doi.org/10.1002/cssc.202001726

6. Alghooneh, A., Mohammad Amini, A., Behrouzian, F., & Razavi, S. M. A. (2017). Characterization of cellulose from coffee silverskin. International Journal of Food Properties, 20(11), 2830–2843. https://doi.org/10.1080/10942912.2016.1253097

7. Almeida-Couto, J.M.F.; Abrantes, K.K.B. ; Stevanato, N.; Silva, W.R.; Wisniewski, A.; Silva, C.; Cabral, V.F.; Cardozo-Filho, L. Oil recovery from defective coffee beans using pressurized fluid extraction followed by pyrolysis of the residual biomass: Sustainable process with zero waste. The Journal of Supercritical Fluids, Volume 180, 2022, 105432, https://doi.org/10.1016/j.supflu.2021.105432.

8. Aparecida, M., Cardoso, P., Carvalho, G. M., & Yamashita, F. (2016). Oat fibers modification by reactive extrusion with alkaline hydrogen peroxide. 26(4), 320–326.

9. Aziz, T., Farid, A., Haq, F., Kiran, M., Ullah, A., Zhang, K., Li, C., Ghazanfar, S., Sun, H., Ullah, R., Ali, A., Muzammal, M., Shah, M., Akhtar, N., Selim, S., Hagagy, N., Samy, M., & al Jaouni, S. K. (2022). A Review on the Modification of Cellulose and Its Applications. In Polymers (Vol. 14, Issue 15). MDPI. https://doi.org/10.3390/polym14153206

10. Babaei-Ghazvini, A., & Acharya, B. (2022). Influence of cellulose nanocrystal aspect ratio on shear force aligned films: Physical and mechanical properties. Carbohydrate Polymer Technologies and Applications, 3. https://doi.org/10.1016/j.carpta.2022.100217

11. Bellotti, R., Picotto, G. B., & Ribotta, L. (2022). AFM Measurements and Tip Characterization of Nanoparticles with Different Shapes. Nanomanufacturing and Metrology. https://doi.org/10.1007/s41871-022-00125-x

12. Blilid, S., Kędzierska, M., Miłowska, K., Wrońska, N., El Achaby, M., Katir, N., Belamie, E., Alonso, B., Lisowska, K., Lahcini, M., Bryszewska, M., & El Kadib, A. (2020). Phosphorylated Micro- A nd Nanocellulose-Filled Chitosan Nanocomposites as Fully Sustainable, Biologically Active Bioplastics. *ACS Sustainable Chemistry and Engineering*, *8*(50), 18354–18365. https://doi.org/10.1021/acssuschemeng.0c04426

13. Brebu, M. (2014). *Thermal degradation of lignin-A Review*. https://www.researchgate.net/publication/237090542

14. Brigham, C. (2017). Biopolymers: Biodegradable Alternatives to Traditional Plastics. In Green Chemistry: An Inclusive Approach (pp. 753–770). Elsevier Inc. https://doi.org/10.1016/B978-0-12-809270-5.00027-3

15. Cardoso, M. A. P., Carvalho, G. M., Yamashita, F., Mali, S., Olivato, J. B., & Grossmann, M. V. E. (2016). Oat fibers modification by reactive extrusion with alkaline hydrogen peroxide. Polimeros, 26(4), 320–326. https://doi.org/10.1590/0104-1428.2316

16. Cavaton Thiago Farah. (2023, May 30). Produtividade média dos Cafés do Brasil equivale a 28,9 sacas por hectare em 2023. https://www.embrapa.br/busca-de-noticias/-/noticia/80992551/produtividade-media-dos-cafes-do-brasil-equivale-a-289-sacas-por-hectare-em-2023

17. de Carvalho Benini, K. C. C., Pereira, P. H. F., Cioffi, M. O. H., & Cornelis Voorwald, H. J. (2017). Effect of acid hydrolysis conditions on the degradation properties of cellulose from Imperata brasiliensis fibers. Procedia Engineering, 200, 244–251. https://doi.org/10.1016/j.proeng.2017.07.035

18. Deb Dutta, S., Patel, D. K., Ganguly, K., & Lim, K. T. (2021). Isolation and characterization of cellulose nanocrystals from coffee grounds for tissue engineering. Materials Letters, 287. https://doi.org/10.1016/j.matlet.2021.129311

19. Doh, H., Lee, M. H., & Whiteside, W. S. (2020). Physicochemical characteristics of cellulose nanocrystals isolated from seaweed biomass. Food Hydrocolloids, 102. https://doi.org/10.1016/j.foodhyd.2019.105542

20. Doh, H., Lee, M. H., & Whiteside, W. S. (2020). Physicochemical characteristics of cellulose nanocrystals isolated from seaweed biomass. *Food Hydrocolloids*, *102*. https://doi.org/10.1016/j.foodhyd.2019.105542.

21. Farooq Adil, S., Bhat, V. S., Batoo, K. M., Imran, A., Assal, M. E., Madhusudhan, B., Khan, M., & Al-Warthan, A. (2020a). Isolation and characterization of nanocrystalline cellulose from flaxseed Hull: A future once-drug delivery agent. Journal of Saudi Chemical Society, 24(4), 374–379. https://doi.org/10.1016/j.jscs.2020.03.002

22. Fitriani, F., Aprilia, S., Arahman, N., Bilad, M. R., Amin, A., Huda, N., & Roslan, J. (2021). Isolation and characterization of nanocrystalline cellulose isolated from pineapple crown leaf fiber agricultural wastes using acid hydrolysis. Polymers, 13(23). https://doi.org/10.3390/polym13234188

23. Frost, B. A., & Johan Foster, E. (2020). Isolation of thermally stable cellulose nanocrystals from spent coffee grounds via phosphoric acid hydrolysis. Journal of Renewable Materials, 8(2), 187–203. https://doi.org/10.32604/jrm.2020.07940

24. George, J., & Sabapathi, S. N. (2015). Cellulose nanocrystals: Synthesis, functional properties, and applications. Nanotechnology, Science and Applications, 8, 45–54. https://doi.org/10.2147/NSA.S64386

25. Gomri, C., Cretin, M., & Semsarilar, M. (2022). Recent progress on chemical modification of cellulose nanocrystal (CNC) and its application in nanocomposite films and membranes-A comprehensive review. Carbohydrate Polymers, 294. https://doi.org/10.1016/j.carbpol.2022.119790

26. Gong, J., Li, J., Xu, J., Xiang, Z., & Mo, L. (2017). Research on cellulose nanocrystals produced from cellulose sources with various polymorphs. RSC Advances, 7(53), 33486–33493. https://doi.org/10.1039/c7ra06222b

27. Gražulis, S., Daškevič, A., Merkys, A., Chateigner, D., Lutterotti, L., Quirós, M., Serebryanaya, N. R., Moeck, P., Downs, R. T., & le Bail, A. (2012). Crystallography Open Database (COD): An open-access collection of crystal structures and a platform for worldwide collaboration. Nucleic Acids Research, 40(D1). https://doi.org/10.1093/nar/gkr900

28. Gražulis, S., Daškevič, A., Merkys, A., Chateigner, D., Lutterotti, L., Quirós, M., Serebryanaya, N. R., Moeck, P., Downs, R. T., & Le Bail, A. (2012). Crystallography Open Database (COD): An open-access collection of crystal structures and platform for world-wide collaboration. *Nucleic Acids Research*, *40*(D1). https://doi.org/10.1093/nar/gkr900

29. Holder, C. F., & Schaak, R. E. (2019). Tutorial on Powder X-ray Diffraction for Characterizing Nanoscale Materials. In ACS Nano (Vol. 13, Issue 7, pp. 7359–7365). American Chemical Society. https://doi.org/10.1021/acsnano.9b05157

30. https://usdabrazil.org.br/wp-content/uploads/2022/06/Coffee-Annual_Sao-Paulo-ATO_Brazil_BR2022-0035.pdf)

31. Jin, E., Guo, J., Yang, F., Zhu, Y., Song, J., Jin, Y., & Rojas, O. J. (2016). On the polymorphic and morphological changes of cellulose nanocrystals (CNC-I) upon mercerization and conversion to CNC-II. Carbohydrate Polymers, 143, 327–335. https://doi.org/10.1016/j.carbpol.2016.01.048

32. Kádár, R., Spirk, S., & Nypelö, T. (2021). Cellulose Nanocrystal Liquid Crystal Phases: Progress and Challenges in Characterization Using Rheology Coupled to Optics, Scattering, and Spectroscopy. In ACS Nano (Vol. 15, Issue 5, pp. 7931–7945). American Chemical Society. https://doi.org/10.1021/acsnano.0c09829

33. Kassab, Z., Kassem, I., Hannache, H., Bouhfid, R., Qaiss, A. E. K., & el Achaby, M. (2020). Tomato plant residue as a new renewable source for cellulose production: extraction of cellulose nanocrystals with different surface functionalities. Cellulose, 27(8), 4287–4303. https://doi.org/10.1007/s10570-020-03097-7

34. Kumar, A., Singh Negi, Y., Choudhary, V., & Kant Bhardwaj, N. (2020). Characterization of Cellulose Nanocrystals Produced by Acid-Hydrolysis from Sugarcane Bagasse as Agro-Waste. Journal of Materials Physics and Chemistry, 2(1), 1–8. https://doi.org/10.12691/jmpc-2-1-1

35. Lagerwall, J. P. F., Schütz, C., Salajkova, M., Noh, J., Park, J. H., Scalia, G., & Bergström, L. (2014). Cellulose nanocrystal-based materials: From liquid crystal self-assembly and glass formation to multifunctional thin films. In NPG Asia Materials (Vol. 6, Issue 1). https://doi.org/10.1038/am.2013.69

36. Lahiji, R. R., Xu, X., Reifenberger, R., Raman, A., Rudie, A., & Moon, R. J. (2010). Atomic force microscopy characterization of cellulose nanocrystals. Langmuir, 26(6), 4480–4488. https://doi.org/10.1021/la903111j

37. López-Beceiro, J., Díaz-Díaz, A. M., Álvarez-García, A., Tarrío-Saavedra, J., Naya, S., & Artiaga, R. (2021). The complexity of lignin thermal degradation in the isothermal context. *Processes*, *9*(7). https://doi.org/10.3390/pr9071154

38. Mancera, A., Fierro, V., Pizzi, A., Dumarçay, S., Gérardin, P., Velásquez, J., Quintana, G., & Celzard, A. (n.d.). Physicochemical characterization of sugar cane bagasse lignin oxidized by hydrogen peroxide. Polymer Degradation and Stability, 95, 470–476. https://doi.org/10.1016/j.polymdegradstab.2010.01.012

39. Mancera, A., Fierro, V., Pizzi, A., Dumarçay, S., Gérardin, P., Velásquez, J., Quintana, G., & Celzard, A. (n.d.). Physicochemical characterisation of sugar cane bagasse lignin oxidized by hydrogen

peroxide. *Polymer Degradation and Stability*, *95*, 470–476. https://doi.org/10.1016/j.polymdegradstab.2010.01.012

40. Martin JD, 2016. XPowderX, A SOFTWARE PACKAGE FOR POWDER X-RAY DIFFRACTION ANALYSIS. Qualitative, quantitative and microtexture. XPowderX 16.01.10 version Lgl . Dp. GR 780-2016. ISBN 978-84-16478-87-3 2016 D.L. GR 1001/04.ISBN 84-609-1497-6. 10. www.xpowder.com http://www.xpowder.com/download/QuickUserGuideForXPowderX.pdf

41. Matebie, B. Y., Tizazu, B. Z., Kadhem, A. A., & Venkatesa Prabhu, S. (2021). Synthesis of Cellulose Nanocrystals (CNCs) from Brewer's Spent Grain Using Acid Hydrolysis: Characterization and Optimization. Journal of Nanomaterials, 2021. https://doi.org/10.1155/2021/7133154.

42. Mattos, B. D., Tardy, B. L., & Rojas, O. J. (2019). Accounting for Substrate Interactions in the Measurement of the Dimensions of Cellulose Nanofibrils. Biomacromolecules, 20(7), 2657–2665.

43. Ministério da agricultura e pecuária Secretaria de Política Agrícola. (n.d.). *Projeções do Agronegócio - Brasil 2022/23 a 2032/33*. Retrieved October 27, 2023, from https://www.gov.br/agricultura/pt-br/assuntos/politica-agricola/todas-publicacoes-de-politica-agricola/projecoes-do-agronegocio/projecoes-do-agronegocio-2022-2023-a-2032-2033.pdf/view.

44. Moon, R. J., Martini, A., Nairn, J., Simonsen, J., & Youngblood, J. (2011). Cellulose nanomaterials review: Structure, properties and nanocomposites. Chemical Society Reviews, 40(7), 3941–3994. https://doi.org/10.1039/c0cs00108b

45. Morais, S. P. J., De Freitas, M., José, R., & Marconcini, M. (2010). Documentos 236 Procedimentos para Análise Lignocelulósica.

46. Omran, A. A. B., Mohammed, A. A. B. A., Sapuan, S. M., Ilyas, R. A., Asyraf, M. R. M., Koloor, S. S. R., & Petrů, M. (2021). Micro-and nanocellulose in polymer composite materials: A review. In Polymers (Vol. 13, Issue 2, pp. 1–30). MDPI AG. https://doi.org/10.3390/polym13020231

47. Panchal, P., Ogunsona, E., & Mekonnen, T. (2019). Trends in advanced functional material applications of nanocellulose. In Processes (Vol. 7, Issue 1). MDPI AG. https://doi.org/10.3390/pr7010010

48. Paukszta, D., & Borysiak, S. (2013). The influence of processing and the polymorphism of lignocellulosic fillers on the structure and properties of composite materials-A review. Materials, 6(7), 2747–2767. https://doi.org/10.3390/ma6072747

49. Perdoch, W., Cao, Z., Florczak, P., Markiewicz, R., Jarek, M., Olejnik, K., & Mazela, B. (2022a). Influence of Nanocellulose Structure on Paper Reinforcement. *Molecules*, *27*(15). https://doi.org/10.3390/molecules27154696.

50. Pereira, P. H. F., Ornaghi Júnior, H. L., Coutinho, L. V., Duchemin, B., & Cioffi, M. O. H. (2020). Obtaining cellulose nanocrystals from pineapple crown fibers by free-chlorite hydrolysis with sulfuric acid: physical, chemical and structural characterization. Cellulose, 27(10), 5745–5756. https://doi.org/10.1007/s10570-020-03179-6

51. Pérez, S., & Samain, D. (2010). Structure and Engineering of Celluloses. In Advances in Carbohydrate Chemistry and Biochemistry (Vol. 64, Issue C, pp. 25–116). Academic Press Inc. https://doi.org/10.1016/S0065-2318(10)64003-6

52. Rasheed, M., Jawaid, M., Parveez, B., Zuriyati, A., & Khan, A. (2020). Morphological, Chemical, and thermal analysis of cellulose nanocrystals extracted from bamboo fiber. International Journal of Biological Macromolecules, 160, 183–191. https://doi.org/10.1016/j.ijbiomac.2020.05.170

53. Razali, S. A., Azwadi, N., Sidik, C., & Koten, H. (2019). Cellulose Nanocrystals: A Brief Review on Properties and General Applications. Journal of Advanced Research Design Journal Homepage, 60, 1–15. www.akademiabaru.com/ard.html

54. Razali, S. A., Azwadi, N., Sidik, C., & Koten, H. (2019). Cellulose Nanocrystals: A Brief Review on Properties and General Applications. *Journal of Advanced Research Design Journal Homepage*, *60*, 1–15. www.akademiabaru.com/ard.html.

55. Sabaruddin, F. A., & Paridah, M. T. (2018). Effect of lignin on the thermal properties of nanocrystalline prepared from kenaf core. *IOP Conference Series: Materials Science and Engineering*, *368*(1). https://doi.org/10.1088/1757-899X/368/1/012039.

56. Sadh, P. K., Duhan, S., & Duhan, J. S. (2018). Agro-industrial wastes and their utilization using solid-state fermentation: a review. In Bioresources and Bioprocessing (Vol. 5, Issue 1). Springer Science and Business Media Deutschland GmbH. https://doi.org/10.1186/s40643-017-0187-z

57. Sadh, P. K., Duhan, S., & Duhan, J. S. (2018). Agro-industrial wastes and their utilization using solid state fermentation: a review. In *Bioresources and Bioprocessing* (Vol. 5, Issue 1). Springer Science and Business Media Deutschland GmbH. https://doi.org/10.1186/s40643-017-0187-z

58. Saxena, I. M., & Brown, R. M. (2001). Biosynthesis of cellulose. In Progress in Biotechnology (Vol. 18, Issue C, pp. 69–76). Elsevier. https://doi.org/10.1016/S0921-0423(01)80057-5

59. Shrestha, S., Montes, F., Schueneman, G. T., Snyder, J. F., & Youngblood, J. P. (2018). Effects of aspect ratio and crystal orientation of cellulose nanocrystals on properties of poly(vinyl alcohol) composite fibers. Composites Science and Technology, 167, 482–488. https://doi.org/10.1016/j.compscitech.2018.08.032

60. Skorupa, A.; Worwąg, M.; Kowalczyk, M. Coffee Industry and Ways of Using By-Products as Bioadsorbents for Removal of Pollutants. Water 2023, 15, 112. https://doi.org/10.3390/w15010112

61. Tesfaye, G., Belete, A., Hause, G., Neubert, R. H. H., & Gebre-Mariam, T. (2021). Isolation and Characterization of Cellulose Nanocrystals from Different Lignocellulosic Residues: A Comparative Study. Journal of Polymers and the Environment, 29(9), 2964–2977. https://doi.org/10.1007/s10924-021-02089-3

62. Wang, T., Yang, H., Kubicki, J. D., & Hong, M. (2016). Cellulose Structural Polymorphism in Plant Primary Cell Walls Investigated by High-Field 2D Solid-State NMR Spectroscopy and Density Functional Theory Calculations. Biomacromolecules, 17(6), 2210–2222. https://doi.org/10.1021/acs.biomac.6b00441

63. Wei, L., Agarwal, U. P., Hirth, K. C., Matuana, L. M., Sabo, R. C., & Stark, N. M. (2017). Chemical modification of nanocellulose with canola oil fatty acid methyl ester. Carbohydrate Polymers, 169, 108–116. https://doi.org/10.1016/j.carbpol.2017.04.008

64. Wu, Q., Li, X., Li, Q., Wang, S., & Luo, Y. (2019). Estimation of the aspect ratio of cellulose nanocrystals by viscosity measurement: Influence of aspect ratio distribution and ionic strength. Polymers, 11(5). https://doi.org/10.3390/polym11050781

65. Zhu, P., Feng, L., Ding, Z., & Bai, X. (2022). Preparation of Spherical Cellulose Nanocrystals from Microcrystalline Cellulose by Mixed Acid Hydrolysis with Different Pretreatment Routes. International Journal of Molecular Sciences, 23(18). https://doi.org/10.3390/ijms231810764.

5. CAPÍTULO 2: Optimizing efficiency of SARS-CoV-2 removal from synthetic wastewaters using UVC and derivatized cellulose membranes

Thaís Viana Fialho Martins[a]*, Graziela dos Santos Paulino[a]*, Yaremis Beatriz Meriño Cabrera[a], Renato Lima Senra[a], Mônica Maria Magalhães Caetano[a], Tiago Antônio de Oliveira Mendes[a]

[a] Department of Biochemistry and Molecular Biology, Universidade Federal de Viçosa, Av. Peter Henry Rolfs, Viçosa, Brazil Corresponding author: Tiago Antônio de Oliveira Mendes E-mail address: tiagoaomendes@ufv.br

Abstrat:

The SARS-CoV-2 are mainly transmitted through respiratory droplets and aerosol particles. However, as for other CoVs, this virus can also be eliminated from symptomatic or asymptomatic patients via faeces, an excreta that is commonly disposed of in wastewater. The presence of SARS-Cov-2 RNA in wastewater can be exploited in different ways, and therefore needs to receive necessary attention. Thus, in this work was evaluated the ability to remove SARS-CoV-2 genetic material from synthetic wastewater using a low cost prototype containing a cellulose membrane functionalized with alkylammonium and alkylamine groups coupled with UVC light. The prototype used shows that a short exposure time to UVC (5 min) is already possible to degrade more than 60% of the N-SARS-CoV-2 gene. Furthemore, we observe a removal of approximately 100% of the genetic material evaluated when the cellulose membrane was derivatized with QASN+(CH2)3. Thus, our prototype can be used especially for the removal of emerging pathogenic microorganisms with potential risk for the population living in regions where basic sanitation is deficient or non-existent. In addition, its application in hospitals effluents can minimizes the risk of contamination in times of epidemic outbreaks, ensuring the safety of the population.

5.1 Introduction

Access to safe and readily available water is essential to prevent the spread of several waterborne diseases and to avoid a major problem for public health. The World Health Organization (WHO, 2014) estimated that, in low and Middle income countries, inadequate drinking water and sanitation were the reason for 502 000 and 280,000 diarrhoea deaths, respectively.

The incidence of waterborne diseases is mainly related to the quality of drinking water available for human consumption, as these infections occur from ingestion or contact with contaminated water by pathogenic microorganisms including bacteria, virus, protozoa, and parasites (Leclerc et al., 2002; WHO, 2015). Recently, the identification of SARS-CoV-2 RNA in wastewater and sewage of several countries, including Australia, Brazil, Spain, Italy, and France, drew attention to a potential new route for the spread of this new coronavirus (CoV) responsible for the global outbreak 51 of COVID-19 (Ahmed et al. 2020 ; La-Rosa et al. 2020 ; Prado et al. 2020 ; Randazzo et al. 2020 ; Wurtzer et al. 2020).

The SARS-CoV-2 are mainly transmitted through respiratory droplets and aerossol particles (Meselson 2020). However, as for other CoVs, this virus can also be eliminated from symptomatic or asymptomatic patients via faeces, excreta that is commonly disposed of in wastewater (Pan et al. 2020 ; Wölfel et al. 2020 ; Zhang et al. 2020). The presence of SARS-Cov-2 RNA in wastewater can be exploited in different ways, and therefore needs to receive necessary attention. Monitoring levels of SARS-Cov-2 RNA in wastewater, known as wastewater-based epidemiology (WBE), provides valuable information about the levels of infection as well as the transmission dynamics of COVID-19 in a community (Prado et al., 2021 ; Westhaus et al., 2021). In this way, WBE supports prevention and control plans against COVID-19 in a specific region. On the other hand, these findings indicate that wastewater and sewage can be potential sources in spreading of COVID-19 in a community, especially in regions with poor sanitation.

Tertiary treatments promote water disinfection in treatment plants commonly through the use of chemical disinfectants, such as chlorine and ozone, or ultraviolet light (Mbonimpa et al. 2018). Although these treatments effectively reduce the concentration of pathogens in wastewater and prevent disease transmission, they have some disadvantages due to their genotoxic and carcinogenic properties (Li and Mitch 2018), high operating costs (Collivignarelli et al. 2018) and their potential induction of microorganisms to antibiotic

resistance (Li et al. 2016).

In the last fifty years, the use of cellulose membranes in the water treatment area has become common (Siedenbiel & Tiller, 2012 ; kang & Jiao,2013). Three mechanisms are directly related to virus reduction by membrane - size exclusion, adsorption, and electrostatic interaction (Zhu et al. 2021). Although it does not naturally have biocidal activity, cellulose can be chemically modified by compounds covalently linked to its hydroxyl groups that provide antimicrobial activity (Tavakolian, et al, 2020 ; Shaghaleh, Xu, & wang, 2018).

Quaternary ammonium salts (QAS) are completely substituted amines that have a positive charge on the nitrogen atom that can be produced naturally or synthetically (Sun, 2011 ; Bureš, 2019). Due to their chemical reactivity, they act as biocides, inactivating or killing vegetative microorganisms, which makes them recommended for industrial use for surface asepsis. Recently its use was also recommended for the removal of SARS-CoV- 2 by the Environmental Protection Agency -US EPA (Hora, et al., 2020 ; Bureš, 2019 ; Kwasniewska, 2020). A polar region positively charged ($^{+}$NR4) and an apolar region formed by the substituting hydrocarbons (R), promote the interaction with the surface of microorganisms, especially with the plasma membrane. Upon infiltrating the plasma membrane, these compounds collapse the proteins and lipids that cover the microorganisms, what induces the formation of pores in the membrane through which the cellular material overflows (REN, et al, 2016 ; Khattak, et al, 2019).

Among the quaternary ammonium salts, trimethoxysilyl propyl trimethylammonium chloride has been applied, for example, in the functionalization of surfaces for the capture of genomic DNA sequences for the study of genetic variants of diseases, as well as surfaces antiseptic, chelating and purifying agent in water and sewage treatment Du, et al, 2017 ; Dioum & Hamoudi, 2014 ; Li, et al, 2016).

In this work we evaluated the ability to remove SARS-CoV-2 genetic material from synthetic wastewater using a low-cost prototype containing a cellulose membrane functionalized with alkylammonium and alkylamine groups coupled with UVC light. The cellulose functionalization with trimethoxysilyl propyl trimethylammonium chloride ($QASN^{+}(CH_2)_3$) showed the greatest capacity to remove the genetic material of SARS-CoV-2. When associated with exposure for a short period of time to UVC light, it is possible to ensure, in addition to the total removal of viral genetic material, the safe handling of the prototype. This prototype make way for the development of an eficiente pathogen removal system that can be applied in sewage and wastewater treatment plants.

5.2 Material and methods

a) Chemical protocol to modificat ion of the cellulose membranes with a quaternary ammonium salt

The reagents were: trimethoxysilylpropyltrimethylammonium chloride ($QASN^{+}(CH_2)_3$) 50% Alfa AesarTM, trimethoxysilyl propyl chloride octadecyldimethylammonium ($QAS\text{-}(CH_2)_{18}$), 42% Sigma Aldrich® and 3-aminopropyl-trimethoxysilane ($QASNH_2$) Aldrich®, Ethanol (Synth), Acetone (Synth), Regenerated cellulose membrane with 12000-14000 Da (Spectrum® Laboratories). The protocol for cellulose modification membranes with quaternary ammonium salts was based on Menge et al., 2015. The regenerated cellulose membrane was cut with an area of 3.9 cm^2, and washed with distilled water for 30 minutes. These membranes were dried in an air oven at 35 °C for 2 hours and weighed. Three solutions were used for immobilization of quaternary ammonium salts. (A) Aqueous solution of $QASN^{+}(CH_2)_3$ at 6.72 mmol in 10 ml of deionized water; (B) Aqueous solution of QAS- $(CH_2)_{18}$ at 4.23 mmol in a total volume of 10 ml and; (C) $QAS\text{-}NH_2$ at 27 mmol in 40 ml of acetone. After drying, the regenerated cellulose membranes were immersed in solutions A, B and C under suspension at room temperature for 3.5 h. The membranes were dried at room temperature for 12 hours. In the next step, $QASN^{+}(CH_2)_3$ and $QAS\text{-}(CH_2)_{18}$ membranes were washed vigorously in 250 ml of 95% ethanol for 30 min at 25°C and the $QAS\text{-}NH_2$ membrane was washed in 250 ml acetone for 30 min at 25 °C. All membranes were dried at 35 °C overnight and then weighed. The calculation of the yield of the ammonium salt graft was given in mg/cm^2 and converted to $mmol/cm^2$.

b) Characterization by the Infra-Red Technique with Fourier transform

The Infra-Red Technique with Fourier Transform (FTIR) analysis was carried out at the Multivariate Chemical Data Analysis Laboratory (MCDALab) of the Chemistry Department of the Universidade Federal de Viçosa (UFV). For this, small horizontal

sections of cellulose modified membranes with quaternary ammonium salts, QAS-$(CH_2)_{18}$, QAS-NH_2, QAS$N^+(CH_2)_3$ and control membrane, were subjected to theattenuated reflectance technique (ATR) using the Varian 660-IR equipment coupled to the GLadiATR accessory with diamond crystal, operating in transmittance mode wit scanning in the wavelength range of 400 - 4000 cm^{-1}.

c) Evaluation of the surface load of the Zeta Potential

The surface load of the QAS$N^+(CH_2)_3$ membrane was evaluated using the potential streaming method. For this, 0.5 g of the QAS$N^+(CH_2)_3$ membrane was frozen in liquid nitrogen and later macerated. The resulting powder was dispersed in deionized water pH = 7, this dispersion was homogenized by inversion and equilibrated at 10 °C for 24 hours. After this period, the dispersion was again agitated and submitted to Zeta Potential analysis on the Zetasizer equipment, Nano Series by Malvern Instruments, from the Laboratório de Embalagens (LABEM-UFV), at 25 °C, with a fixed angle of 173° and with a length of 633 nm wave. The analyzes were performed in triplicates.

d) Production and quantificaion of N SARS-CoV-2 gene

The gene sequence encoding structural protein N from SARS-Cov-2 (nucleocapsid phosphoprotein_SARS-COV-2) was synthesized by Biomatik Corporation (Kitchener, Ontario - Canada) (Gene ID: 43740575). The gene was cloned into the NheI and NotI restrictions site placed at 5' and 3' ends, respectively, in cloning vector pET28a (+). Then the transformation experiments were performed with chemically competent cells Escherichia coli DH5α using the heat shock method (Panja et al., 2006), briefly described by the addiction in ice for 30 min, followed by water bath at 42°C for 1 min, plus ice for 2 min and in the sequence shaking at 37°C for 1 h. After centrifugation at 2,500 x g for 10 min, the transformed cells were plated on LB/agar plates containing 50 mg/ml kanamycin and the plates were inverted and incubated at 37°C overnight. The resistant single colony was picked and amplified in LB medium. The plasmid extraction was performed using the commercial QIAGEN Plasmid Kit (Germantown, MD - USA). The quantification of the genetic material was performed in a Qubit ™ 4 Fluorometer equipment (Invitrogen, California - USA).

e) Synthetic wastewater

The synthetic wastewater used to perform the experiments was prepared from a 10X solution containing 160 mg/L peptone, 110 mg/L meat extract, 30 mg/L urea, 28 mg/L K_2HPO_4, 7 mg/L NaCl, 4 mg/L $CaCl_2.2H_2O$, 2 mg/L $MgSO_4.7H_2O$, dissolving in distilled water, previously described by (Giannakis et al., 2014). The initial pH of the synthetic wastewater obtained with this composition was pH 6.6. The N Sars-CoV-2 synthetic gene was diluted according the required experiment.

f) Removal of N-SARS-CoV-2 gene from synthet ic wastewater by ultraviolet -C light

A simulated prototype of a treatment plant was built using two aquariums interconnected by hoses, containing between them an 9 watt ultravioleta - C (UVC) lamp filter, in a closed circuit. Inside the aquariums, pumps circulated the liquid volume at a constant speed of 2L/min. The experiment was carried out in two phases: the first with the UVC lamp off and the second with the UVC lamp on. A final volume of 7 L of synthetic wastewater containing $1x10^5$ copies/L of the N SARS-CoV-2 gene was added to the system and 5 mL aliquots were collected from the entrance aquarium, after circulation in the filter system, at the times 0 min, 5 min, 10 min, 15 min, and 30 min.The samples were processed immediately after collection, following the subsequente methodologies described here.

g) Quantification of N-SARS-CoV-2 gene by real time PCR

N-SARS-CoV-2 gene was extracted from the samples of synthetic wastewater by precipitation. Five hundred µL of each sample was precipitated with 300 µL phenol, 300 µL chloroform/isoamyl alcohol (24:1). The supernatant was recovered and incubated with ethanol on ice for 10 min and in the centrifuged sequence. The pellets were washed with 70% ethanol and later resuspended in RNAse free dH_2O.N SARSCoV- 2 gene was detected by TaqMan real-time RT-PCR (RT-qPCR) on StepOnePlus Real-Time PCR System thermocycler (Applied Biosystems) conducted in two replicates using the following cycling parameters established by CDC (Centers for Diseas Control and Prevention, Georgia, USA): a final reaction volume of 10 µL in MicroAmp Fast Optical 48 Well Reaction Plates (Thermo Fisher Scientific) containing 1X GoTaq qPCR Master

Mix (Promega Corporation), 300 nM CXR Reference Dye, a final concentration of 200 nM. The cycling parameters were at 50°C for 15 min, preheating at 95°C for 2 min and 45 cycles of amplification at 95°C for 3 s, 55°C for 30 s. Ct values generated by the equipment were interpolated in a standard curve Ct x DNA concentration (ng) and subsequently transformed into a percentage reduction of NSARS- Cov-2 gene from the value found for the zero-time controls.

h) Removal of N-SARS-CoV-2 gene by derivatized membranes

Derivatized membranes of dimensions 35 mm x 10 mm were added to 5 ml of synthetic wastewater solution containing $1x10^9$ copies/L of the N-SARS-CoV-2 gene or synthetic wastewater without gene. The untreated membranes, 3- aminopropyltrimethoxysilane (QAS-NH_2), trimethoxysilylpropyl octadecyldimethyl ammonium chloride (QAS-$(CH_2)_{18}$) and trimethoxysilyl propyl trimethylammonium chloride ($QASN^+(CH_2)_3$) treated membranes were under agitation in contact with the solutions for 30 min. In the end, 1 ml of each sample was collected and the gene was extracted by precipitation. Wastewater control without N-SARS-CoV-2 was also precipitated to verify the influence of membranes on the solution. The material was evaluated by real time PCR.

i) Removal of N-SARS-CoV-2 gene from synthet ic wastewater by association between derivatized membranes and UVC

Cellulose derivatized membrane with trimethoxysilyl propyl trimethylammonium chloride ($QASN^+(CH_2)_3$) or untreated membrane of dimensions 500 mm x 40 mm were inserted into the prototype filter and were subjected to the capture test under the same conditions described in point “d". The tests were carried out under the incidence of UVC light or not. Aliquots of 5 mL were collected from the entrance aquarium, after circulation in the filter system, at the times 0 min, 5 min, 10 min, 15 min, and 30 min. The samples were processed immediately after collection.

Statistical analysis

The performance of the biosensor was evaluated by the unpaired *T-Student* test used to compare the means of reducing the samples genetic material collected before and at different times after coming into contact with the decontamination prototype. The differences were considered statistically significant when $p < 0.05$. The One-way ANOVA test was applied for multiple comparisons between the different evaluated derivatized membranes. P values <0.0001 were considered statistically different. All analyzes were performed using the GraphPad Prism 6.0 softwares (https://www.graphpad.com/scientific-software/prism/).

5.3 Results

Modified and Characterization of cellulose membranes

The different quaternary ammonium salts resulted in different reaction yields. Following an increasing order, we have QAS-$(CH_2)_{18}$ ($5.17x10^{-9}$ mol/cm^2); QAS-NH_2 ($2,86 \times 10^{-8}$ mol/cm^2) and $QASN^+(CH_2)_3$ ($5x10^{-8}$mol/cm^2) **Figure 1**.

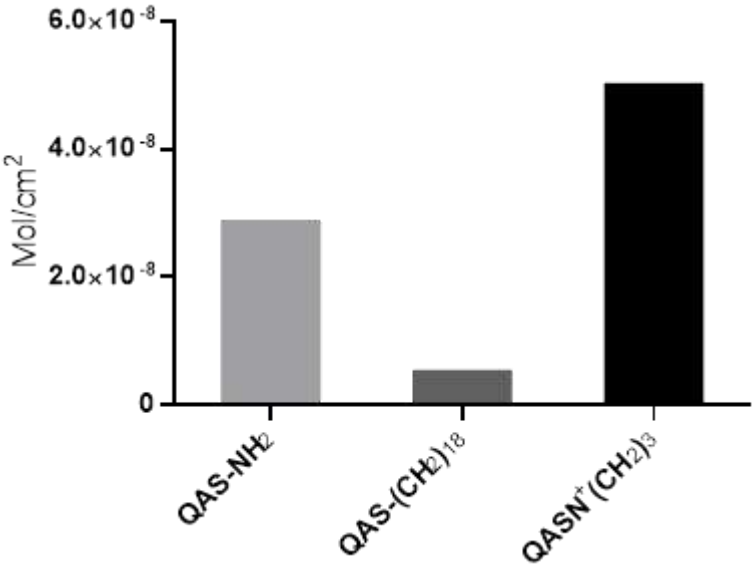

Figure 1: Yield of modification reaction with ammonium salts of cellulose membranes. Yield given in mol/cm^2.

Infrared spectroscopy with ATR is useful in identifying chemical groups characteristic of organic compounds, so it can be applied to confirmation of Chemical modification of cellulose membranes, functionalized with quaternary ammonium salts. We can notice in

the FTIR spectrum functionalized cellulose and non-functionalized cellulose membrane (control membrane) the appearance of new absorption peaks in modified cellulose membranes when compared to the control membrane **(Figure 2).** The peak at 2885 cm^{-1} is characteristic of C-H stretching of glycosidic molecules. The stretch of cellulose molecule group OH is the wide peak at 3315 cm^{-1} and at 898 cm^{-1} we can notice the characteristic peak of the C-O stretch of the glycosidic cellulose bond. The infrared spectrum of the modified membranes shows the appearance of two new bands, a 1345 cm^{-1} which is characteristic of a C-N stretch in a tertiary amine and peak at 1545 cm^{-1} which refers to the N-H stretch of primary amine (Makarem,2019; Paiva,2010).

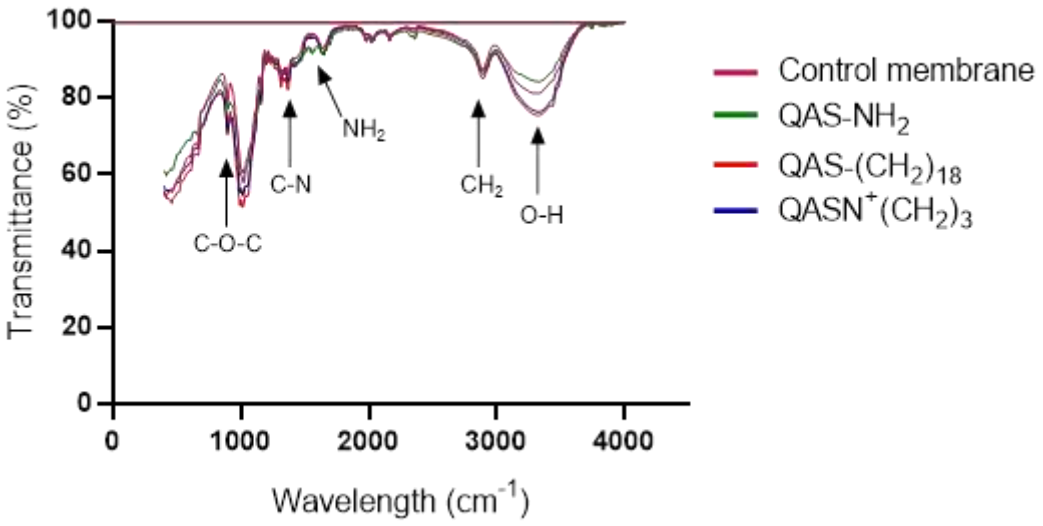

Figure 2: Fourier transform infrared spectrum (FTIR) of cellulose membranes modified with quaternary ammonium salts. Attenuated reflectance technique (ATR), operating in transmittance mode with scanning in the wavelength range of 400 - 4000 cm^{-1}.

The zeta potential preset in the **figure 3** the unmodified membrane has a high zeta potential value (-27.5mV), counter-starting, the modified membrane ($QASN^{+}CH_2)_3$ has a lower zeta potential.) As we can see from the **figure 3** the unmodified membrane has a high zeta potential value (-27.5mV) this is probably the result of the higher concentration of OH ions that binds to cellulose forming hydrogen bridges, counter-starting, the modified membrane $QASN^{+}(CH_2)_3$ has a lower Zeta Potential, this can be explained by the lower formation of hydrogen bridges, since quaternary amine induces a higher concentration of H_3O^{+} ions in the shear layer. Zeta potential of the modified membrane enhances efficiency in the chemical membrane modification process by

trimethoxysilylpropyl trimethyl ammonium chloride.

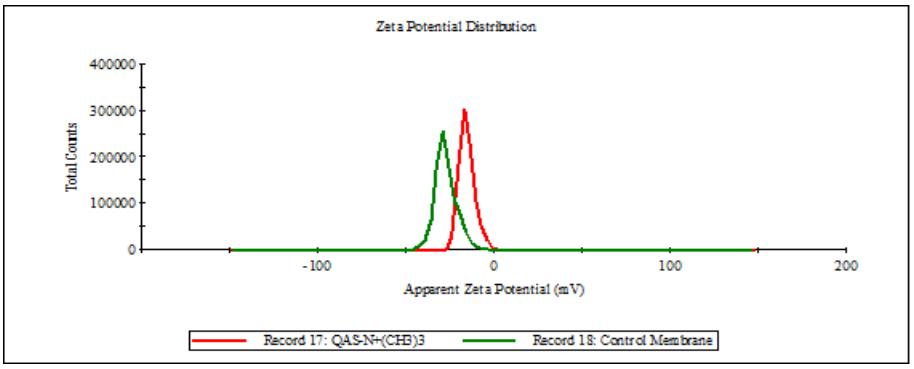

Figure 3: Apparent Zeta Potential. In red $QASN^{+}(CH_3)_3$ derivatized membrane, in green the membrane control.

Avaliation N-SARS-CoV-2 gene removal of the wastewater

The ability to remove the N-SARS-Cov-2 gene by the prototype based on the use of UVC light is shown in figure 4. We observed that there was a spontaneous N-SARS-Cov- 2 gene degradation in the developed prototype observed in the UV- group, in the four evaluated times **(figure 4)**. This spontaneous degradation ranged from 14.2% at 5 min of system operation to 39.2%, after 30 min. However, when the UVC light was activated in the system, the emission of light degraded the genetic material more quickly (UV+), where we were able to verify a 62.7% reduction in the DNA evaluated in the initial time of 5 min. This removal pattern was maintained, reaching 66.3% removalat 15 min, and remained until the end of the trial, which occurred after 30 min of exposu to UVC light.

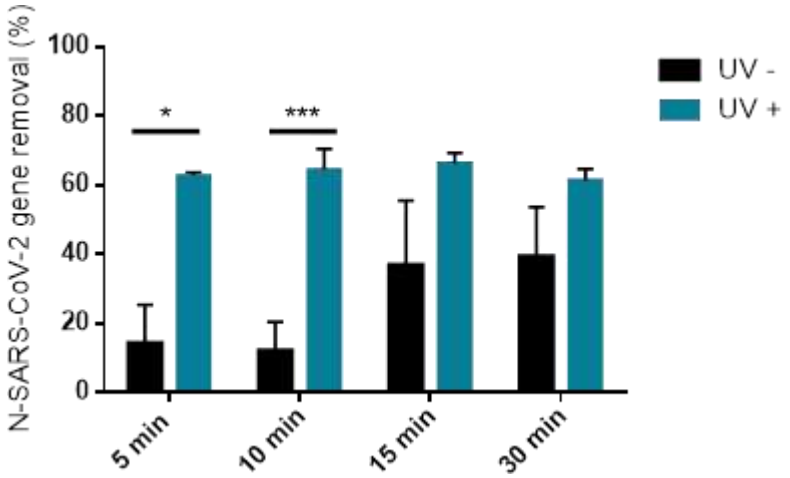

Figure 4: Percentage of N-SARS-CoV-2 gene removal by UVC light in 5', 10', 15' and 30'. UV^{-}: light off, UV^{+}: light on. The symbol * represents a significant statistical

difference with $p < 0.05$ by nonparametric Student t test.

The use of functionalized membranes can favor removal by immobilization and capture of several charged particles. Membranes functionalized with 3-aminopropyltrimethoxysilane (QAS-NH_2), trimethoxysilylpropyl octadecyldimethyl ammonium chloride (QAS-$(CH_2)_{18}$) and trimethoxysilyl propyl trimethylammonium chloride ($QASN^+(CH_2)_3$) were evaluated for their ability to remove the N-SARS-CoV- 2 gene and it was possible to verify that the $QASN^+(CH_2)_3$ membrane removed 99.0% of the synthetic genetic material **(figure 5).** The untreated cellulose membrane removed 58.2% of the N-SARS-CoV-2 gene after 30 min of contact with the solution and the removal potential was optimized with treatment by the quaternary amine $QASN^+(CH_2)_3$. The other quaternary amines evaluated, QAS-NH_2 and QAS-$(CH_2)_{18}$, did not show potential for immobilization and capture of genetic material, presenting worse results when compared to the membrane without treatment.

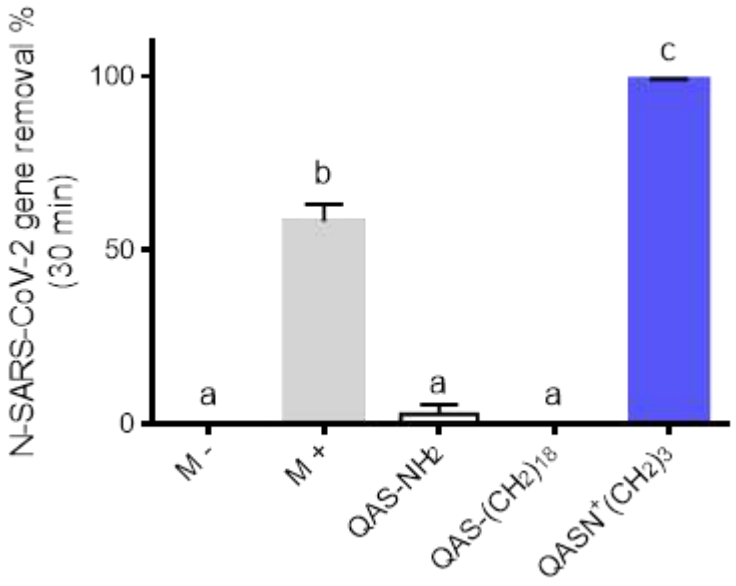

Figure 5: Percentage of N-SARS-CoV-2 gene removal by cellulose membranes in 30'. M^-, control; M^+, untreated membrane; 3-aminopropyltrimethoxysilane (QAS-NH_2), QAS- NH_2 treated membrane; trimethoxysilylpropyl octadecyldimethyl ammonium chloride (QAS-$(CH_3)_{18}$), QAS-$(CH_3)_{18}$ treated membrane; trimethoxysilyl propyl trimethylammonium chloride ($QASN^+(CH_3)_3$), $QASN^+(CH_3)_3$ treated membrane. Diferent letters represents a significant statistical difference with $p<0.0001$ by nonparametric one-way analysis of variance (ANOVA) test with Bonferroni correction.

After verifying the potential for removal of synthetic gene material by membranes, the association of potential membranes in the UVC light system was performed to verify the

removal efficiency in the prototype. When the non-functionalized cellulose membrane was added to the system, it came into contact with the synthetic wastewater flow and did not receive direct action of UVC light, it was possible to verify the removing capacity the genetic material, which varied from 16.3% at 5 min to 61.8% at the end, in 30 min test (figure 6A). When the $QASN^{+}(CH_3)_3$ functionalized membrane was evaluated in the system under the same conditions, it showed a higher removal efficiency since the initial stages of the experiment. The removal efficiency of the $QASN_{+}(CH_3)_3$ functionalized membrane reached 55.6% removal within 5 min of the assay, gradually increasing until reaching 91.3% removal of the N-SARS-CoV-2 gene at 30 min of the assay **(figure 6A)**.

When the UVC light was activated in the system in association with the membranes, a worsening in the efficiency of the functionalized membrane in promotingthe removal of the N-SARS-CoV-2 gene was observed. In 5 min of evaluation, the control membrane removed 29.0% of the genetic material while the functionalized $QASN^{+}(CH_3)_3$ membrane removed 17.9% **(figure 6B)**. The capacity of both increased gradually over the 10 and 15 min times, however, there was a drop in the percentage of genetic material captured by the $QASN^{+}(CH_3)_3$ functionalized membrane at the end of the experiment **(figure 6B).**

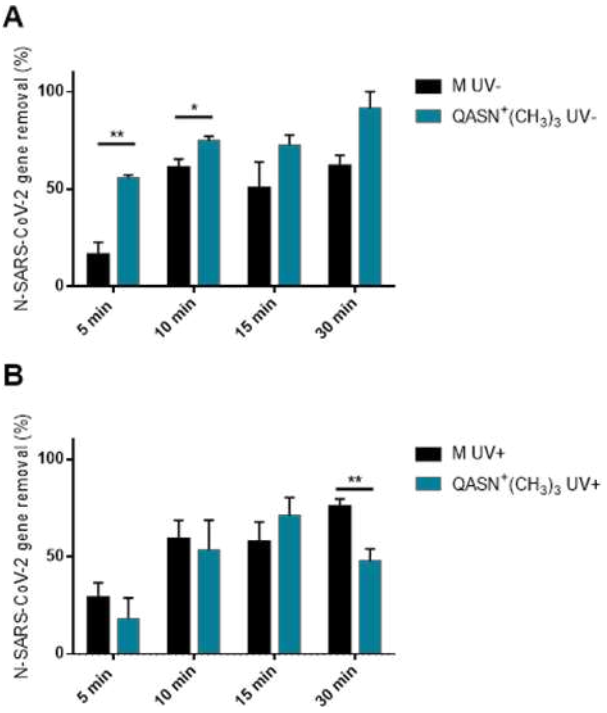

Figure 6: Percentage of N-SARS-CoV-2 gene removal by membranes and UVC light in 5', 10', 15' and 30'. M UV -: control membrane with light off, $QASN^{+}(CH_3)_3$ UV -: $QASN^{+}(CH_3)_3$ funcionalized membrane with light off, M UV +: control membrane with light on and, $QASN^{+}(CH_3)_3$ UV +: $QASN^{+}(CH_3)_3$ funcionalized membrane with light on.

The symbol * represents a significant statistical difference with $p < 0.05$ by nonparametric *Student t test*.

5.4 Discussion and Conclusion

Hospitals are important sources of pollutants resulting from the release of excretafrom patients that may contain from pathogenic microorganisms to residues of pharmaceutical products and their metabolites, radioactive markers, iodinated contrast media, etc., which in a way may represent a potential risk of contamination of the population, when the discharge of hospital waste is not subjected to adequate treatment (Wang et al, 2020). In this context, some emerging pathogens, such as Ebola virus and SARS-CoV-2, pose a significant health threat and their exposure in an unsanitary sewage system can have potentially serious consequences for public health (Lahrich et al., 2021).

The SARS-CoV-2 virus has the characteristic of being an enveloped virus. Although enveloped viruses are predisposed to inactivation in water, the survival time of thes viruses can still be very long, depending on environmental conditions. This is explaine by the fact that the S proteins on the viral surface are deeply anchored and only pass through the envelope. Thus, if the envelope is altered, but surface S proteins are preserved, viral infectivity is maintained (Lahrich et al. 2021), which leads us to think about the increased risk of infections by wastewater. In this context, the use of highly efficient sanitation methods in sewage treatment plants or at exits from places with a high rate of water contamination, such as hospitals, become important interventions to reduce the risk of transmitting emerging diseases. With this intention, a low-cost prototype containing a cellulose membrane functionalized with alkylammonium and alkylamine groups coupled to UVC light was developed for application in the treatment and removal of viral particles from contaminated water. We evaluated the prototype's removal potential based on electrical charge interactions with the derivatized membranes, and thus we used a circular synthetic DNA containing the coding for the SARS-CoV-2 N protein as an insert, as a particle to be removed by the prototype.

The chemical structure of cellulose does not have biocidal activity, but the hydroxyl groups present in its structure allow covalent chemical modifications that, depending on the chemical nature of the modifying molecule, end up conferring biocidal activity to the cellulose. Many antimicrobial substances are used as modifying agents to create cellulose materials with biological activities of medical, industrial or technological interest

(Tavakolian, et al, 2020; Shaghaleh, Xu, & wang, 2018; Milani, France, Balieiro and Faez, 2017). The main advantages of using cellulose as a raw material for such purposes are its high abundance, low cost, low toxicity, biocompatibility, biodegradability and easy handling (Kumaran, Chopra, Oh, & Choi, 2020), opposite advantages the use of UVC light, which has been shown to have virucidal activity against SARS-CoV-2, but has limitations related to exposure that can cause adverse health effects, such as damage to the eyes, skin cancer and aging, and UVC should not be used in housing environment (Sabino, 2020). Interestingly, in our prototype, which is composed of a closed system with no risk of exposure, it was observed that a short exposure time to UVC (5 min) was already possible to degrade more than 60% of the N-SARS-CoV-2 gene. The removal rate was maintained until the end of the experimente (30 min), showing a limited ability to degrade the N-SARSCoV- 2 gene. The short exposure time to UVC light provided by the continuous flow of liquid inside the prototype may be preventing the total degradation of the genetic material after 30 min.

As shown, QAS are able to interact with DNA and even induce DNA photopolymerization (Tischer et al., 2012; Song et al., 2006; Flood et al., 2019). The interactions of QAS with DNA are not well understood, but the most accepted hypothesis is related to the ionic interaction between the positive charge of the amine nitrogen of the QAS and the negative charge of the phosphate group of the DNA. The presence of the ammonium salt on the membrane surface maximizes DNA adsorption on the membrane surface as the surface becomes positively charged, thus exerting na ionic force on the DNA. This effect is probably clear in our results, where we could observe a removal of approximately 100% of the genetic material evaluated when the

cellulose membrane was derivatized with QASN+(CH2)3 (fig. 5). Disregarding the solvation effect, we can state that the more exposed the positive charge of nitrogen, the easier and more intense the ionic interaction between DNA and QAS will be, therefore, QAS molecules that have hydrocarbon substitutes with smaller volume and/or size will adsorb a greater amount of DNA on the membrane surface, on the other hand, molecules with long and/or bulky hydrocarbons have a larger electronic cloud that shields the positive charge of the nitrogen atom and consequently minimizes the ionic interaction with the DNA, and maximizes interactions ion-dipole. This effect explains the fact that the membrane modified with QASN+(CH2)3 adsorbs more DNA than the membrane QAS-(CH2)18 (fig. 5). The lack of charge of the membrane QASNH2 explains its low efficiency

in removing DNA (fig. 5), as the only interaction it exerts electrostatic ion-dipole is that, besides the solvation effect can not significantly increase the adsorption of DNA enough (Flood et al., 2019; Lin et al., 2009; Tadrosand Tadros, 2013).

Interestingly, when the QASN+(CH2)3 membrane was added to the prototype and its adsorption capacity of the SARS-CoV-2 N gene was evaluated over time (fig. 6), a gradual increase in removal efficiency was observed in relation to the time, with a result at the end of 30 min, corroborating the previously result, shown in fig. 5. Different methodologies and different amounts of initial DNA, culminated in the same result, demonstrating the robustness and efficiency of membrane removal.

When UVC light was associated with the system containing the QASN+(CH2)3 derivatized membrane, the rate of removal of the SARS-CoV-2 N gene by the membrane continued to increase up to 15 min, but with a rate of removal lower than that observed for the untreated control membrane, at times of 5 and 10 min (Fig. 6B). After 30 min, contrary to what we expected, a somatory effect of the retention of the SARSCoV- 2 N gene by the derivatized membrane to the degradation action promoted by UVC light, an increase of genetic material in the sample was observed. In a way, the SARSCoV- 2 N gene seems to detach from the membrane and return to the synthetic effluent. UV C emits radiation in the range of 200 to 280nm and by the principle of photo equivalence the energy absorbed by 1mol of molecules at 200nm is equal to 598 kJ / mol and at 280nm is equal to 427 kJ / mol, this energy is enough to break the Si-O and CO covalent bond between QASN+(CH2)3 and the cellulose membrane, as these bonds have a formation energy equal to 368 kJ and 343 kJ respectively. Therefore, exposure of the modified membrane to UV C for 30 min is sufficient to break the bond between OH cellulose and QASN+(CH2)3 releasing this quaternary ammonium salt into the aqueous medium and, consequently, decreasing the amount of retained DNA on the membrane (Chiavari et al., 2015; Lin et al., 2009; Flood et al., 2019; Grigoras, 2021; Xue et al., 2015).

Given the above, we propose the application of the low-cost attachable prototype for the removal of negatively charged molecules, especially emerging pathogenic microorganisms with potential risk for the population living in regions where basic sanitation is deficient or non-existent. In addition, its application in hospitals effluents minimizes the risk of contamination in times of epidemic outbreaks, ensuring the safety of the population.

5.5 Bibliographic references

1. Agustin, M. B., Ahmmad, B., Alonzo, S. M. M., & Patriana, F. M. (2014). Bioplastic based on starch and cellulose nanocrystals from rice straw. Journal of Reinforced Plastics and Composites, 33(24), 2205–2213. https://doi.org/10.1177/0731684414558325
2. Ahmed, Warish et al. 2020. "First Confirmed Detection of SARS-CoV-2 in Untreated Wastewater in Australia: A Proof of Concept for the Wastewater Surveillance of COVID- 19 in the Community." Science of the Total Environment 728(January):138764.
3. Blilid, S., Kędzierska, M., Miłowska, K., Wrońska, N., El Achaby, M., Katir, N., Belamie, E., Alonso, B., Lisowska, K., Lahcini, M., Bryszewska, M., & El Kadib, A. (2020). Phosphorylated Micro- A nd Nanocellulose-Filled Chitosan Nanocomposites as Fully Sustainable, Biologically Active Bioplastics. ACS Sustainable Chemistry and Engineering, 8(50), 18354–18365. https://doi.org/10.1021/acssuschemeng.0c04426.
4. Bureš, F., 2019. Quaternary Ammonium Compounds: Simple in Structure, Complex in Application. Top. Curr. Chem. 377, 1–21. https://doi.org/10.1007/s41061- 019-0239-2
5. Chiavari, C., Balbo, A., Bernardi, E., Martini, C., Zanotto, F., Vassura, I., Bignozzi, M.C., Monticelli, C., 2015. Organosilane coatings applied on bronze: Influence of UV radiation and thermal cycles on the protectiveness. Prog. Org. Coatings 82, 91–
6. Chiavari, C., Balbo, A., Bernardi, E., Martini, C., Zanotto, F., Vassura, I., Bignozzi, M.C., Monticelli, C., 2015. Organosilane coatings applied on bronze: Influence of UV radiation and thermal cycles on the protectiveness. Prog. Org. Coatings 82, 91–
7. Collivignarelli, Maria Cristina, Alessandro Abbà, Ilaria Benigna, Sabrina Sorlini, and Vincenzo Torretta. 2018. "Overview of the Main Disinfection Processes for Wastewater and Drinking Water Treatment Plants." Sustainability "10:86.
8. Daughton, Christian G. 2020. "Wastewater Surveillance for Population-Wide Covid-19: The Present and Future." Science of the Total Environment 736:139631.
9. Dioum, A., Hamoudi, S., 2014. Mono- and quaternary-ammonium functionalized mesoporous silica materials for nitrate adsorptive removal from water and wastewaters 685–690. https://doi.org/10.1007/s10934-014-9815-6
10. Du, Y., Wang, Y., Hu, X., Liu, J., Diao, J., 2020. Single-molecule quantification of 5-methylcytosine and 5-hydroxymethylcytosine in cancer genome. https://doi.org/10.1002/viw2.9
11. durability and low toxicity antimicrobial coatings fabricated by quaternary ammonium silane copolymers. Biomater. Sci. 4, 299–309. https://doi.org/10.1039/c5bm00353a
12. European Commission, 1967. Council Directive 67/548/EEC: Appendix V: Methods for the determination of the Physicochemical Characteristics, the Toxicity and the Ecotoxicity. <http://www.umweltrecht.de>.
13. Flood, D.T., Asai, S., Zhang, X., Wang, J., Yoon, L., Adams, Z.C., Dillingham, B.C., Sanchez, B.B., Vantourout, J.C., Flanagan, M.E., Piotrowski, D.W., Richardson, P., Green, S.A., Shenvi, R.A., Chen, J.S., Baran, P.S., Dawson, P.E., 2019. Expanding
14. Flood, D.T., Asai, S., Zhang, X., Wang, J., Yoon, L., Adams, Z.C., Dillingham, B.C., Sanchez,

B.B., Vantourout, J.C., Flanagan, M.E., Piotrowski, D.W., Richardson, P., Green, S.A., Shenvi, R.A., Chen, J.S., Baran, P.S., Dawson, P.E., 2019. Expanding Reactivity in DNA-Encoded Library Synthesis via Reversible Binding of DNA to an Inert Quaternary Ammonium Support. J. Am. Chem. Soc. 141, 9998–10006. https://doi.org/10.1021/jacs.9b03774

15. Grigoras, A.G., 2021. Natural and synthetic polymeric antimicrobials with quaternary ammonium moieties: a review. Environ. Chem. Lett. https://doi.org/10.1007/s10311-021-01215
16. Hora, P.I., Pati, S.G., Mcnamara, P.J., Arnold, W.A., 2020. Increased Use of Quaternary Ammonium Compounds during the SARS-CoV-2 Pandemic and Beyond: Consideration of Environmental Implications. Cite This Environ. Sci. Technol. Lett 7, 622–631. https://doi.org/10.1021/acs.estlett.0c00437
17. WHO Coronavirus (COVID-19) Dashboard.https://covid19.who.int/ . (accessed 11.30.20).
18. Julbe A., Drobek M. (2016) Zeolite A Type. In: Drioli E., Giorno L. (eds) Encyclopedia of Membranes. Springer, Berlin, Heidelberg. https://doi.org/10.1007/978- 3-662-44324-8_604
19. Khattak, S., Wahid, F., Liu, L.-P., Jia, S.-R., Chu, L.-Q., Xie, Y.-Y., Li, Z.-X.,
20. Kwaśniewska, D., Chen, Y.-L., Wieczorek, D., 2020. Biological Activity of Quaternary Ammonium Salts and Their Derivatives. Pathogens 9, 459. https://doi.org/10.3390/pathogens9060459
21. L. M. Poon, and Quanyi Wang. 2020. “Viral Load of SARS-CoV-2 in Clinical Samples.” The Lancet 20(April):411.
22. La-Rosa, Giuseppina et al. 2020. “First Detection of SARS-CoV-2 in Untreated Wastewaters in Italy.” Science of the Total Environment Journal 736(January):139652.
23. Leclerc, H.; Schwartzbrod, L.; Dei-Cas, E. Microbial agents associated with waterborne diseases. Crit. Rev. Microbiol. 2002, 28, 371–409.
24. Lescure, Francois-Xavier et al. 2020. “Clinical and Virological Data of the First Cases of COVID-19 in Europe: A Case Series.” Lancet Infectious Diseases 20(January):697–706.
25. Li, Dan, Siyu Zeng, Miao He, and April Z. Gu. 2016. “Water Disinfection Byproducts Induce Antibiotic Resistance- Role of Environmental Pollutants in Resistance Phenomena.” Environmental Science & Technology 50(6):3193–3201.
26. Li, H., Bao, H., Bok, K.X., Lee, C.Y., Li, B., Zin, M.T., Kang, L., 2016. Hig
27. Li, Xing-fang and William A. Mitch. 2018. “Drinking Water Disinfection Byproducts (DBPs) and Human Health E Ff Ects: Multidisciplinary Challenges and Opportunities.” Environmental Science & Technology 52:1681–89.
28. Lin, X., Liao, G., Tang, Z., Shi, T., 2009. UV surface exposure for low temperature hydrophilic silicon direct bonding. Microsyst. Technol. 15, 317– 321. https://doi.org/10.1007/s00542-008-0703-3
29. Lin, X., Liao, G., Tang, Z., Shi, T., 2009. UV surface exposure for low temperature hydrophilic silicon direct bonding. Microsyst. Technol. 15, 317– 321. https://doi.org/10.1007/s00542-008-0703-3
30. Lofrano, Giusy and Jeanette Brown. 2010. “Wastewater Management through the Ages: A History of Mankind.” Science of the Total Environment 408(22):5254–64.

31. Makarem, M., Lee, C.M., Kafle, K. et al. Probing cellulose structures with vibrational spectroscopy. Cellulose 26, 35–79 (2019). https://doi.org/10.1007/s10570- 018-2199-z
32. Malvern Instruments . Zetasizer Nano Series User Manual. Malvern Instruments Ltd.; Worcestershire, UK: 2013.
33. Mbonimpa, E. G., E. R. Blatchley Iii, B. Applegate, and W. F. Harper Jr. 2018. "Ultraviolet A and B Wavelength-Dependent Inactivation of Viruses and Bacteria in the Water." Journal of Water and Health 16:796–806.
34. Meselson, Matthew. 2020. "Droplets and Aerosols in the Transmission of SARS- CoV-2." The New England Journal of medicine 382(21):2063.
35. Mishra, Sanjay Kumar and Timir Tripathi. 2021. "One Year Update on the COVID-19 Pandemic: Where Are We Now?" Acta Tropica 214:105778.
36. Naddeo, Vincenzo and Haizhou Liu. 2020. "Editorial Perspectives: 2019 Novel Coronavirus (SARS-CoV-2): What Is Its Fate in Urban Water Cycle and How Can the Water Research Community Respond?" Environmental Science Water Research & Technology 6:1213.
37. on Virus Entry and Its Immune Cross-Reactivity with SARS-CoV." Nature Communications 11:1620. 34. Paiva, D.L., Lampman, G.M., Kriz, G.S., 2001. Introduction-to-Spectroscopy, 3rd ed. USA. 35. Pan, Yang, Daitao Zhang, Peng Yang, Leo
38. Ou, Xiuyuan et al. 2020. "Characterization of Spike Glycoprotein of SARSCoV-
39. Prado T, Fumian TM, Mannarino CF, Resende PC, Motta FC, Eppinghaus ALF,Chagas do Vale VH, Braz RMS, de Andrade JDSR, Maranhão AG, Miagostovich MP. Wastewater-based epidemiology as a useful tool to track SARS-CoV-2 and support public health policies at municipal level in Brazil. Water Res. 2021 Mar 1; 191:116810. doi: 10.1016/j.watres.2021.116810. Epub 2021 Jan 5. PMID: 33434709; PMCID: PMC7832254.
40. Prado, Tatiana et al. 2020. "Preliminary Results of SARS-CoV-2 Detection in Sewerage System in Niterói Municipality, Rio de Janeiro, Brazil." Memorias Do Instituto Oswaldo Cruz 115:e200196.
41. Randazzo, Walter et al. 2020. "SARS-CoV-2 RNA in Wastewater Anticipated COVID-19 Occurrence in a Low Prevalence Area." Water Research 181:115942.
42. Reactivity in DNA-Encoded Library Synthesis via Reversible Binding of DNA to an Inert Quaternary Ammonium Support. J. Am. Chem. Soc. 141, 9998–10006. https://doi.org/10.1021/jacs.9b03774
43. Ren, X., Liang, J., 2016. Smart anti-microbial composite coatings for textiles and plastics, in: Smart Composite Coatings and Membranes: Transport, Structural, Environmental and Energy Applications. Elsevier Inc., pp. 235–259. https://doi.org/10.1016/B978-1-78242-283-9.00009-9
44. Sabino, Caetano P. et al. 2020. "UV-C (254nm) Lethal Doses for SARS-CoV- 2." Photodiagnosis and Photodynamic Therapy 32:101995.
45. Sun, G., 2011. Antibacterial textile materials for medical applications, in: Functional Textiles for Improved Performance, Protection and Health. Elsevier Ltd., pp. 360–375. https://doi.org/10.1533/9780857092878.360
46. Tadros, T., Tadros, T., 2013. Encyclopedia of Colloid and Interface Science, Encyclopedia of

Colloid and Interface Science. https://doi.org/10.1007/978-3- 642- 20665-8

47. Westhaus, S., Weber, F.-A., Schiwy, S., Linnemann, V., Brinkmann, M., Widera, M., ...Ciesek, S., 2021. Detection of SARS-CoV-2 in raw and treated wastewater in Germany–suitability for COVID-19 surveillance and potential transmission risks.
48. WHO, 2014 Preventing diarrhoea through better water, sanitation and hygiene: exposures and impacts in low- and middle-income countries, Available at.
49. WHO, 2015. Waterborne Diseases – MDGs-SDGs2015. Available online: [Accessed 02 May 2021].Acess:< https://www.who.int/gho/publications/mdgssdgs/MDGsSDGs2015_chapter5_snapshot_ waterborne_diseases.pdf?ua=1>.
50. WHO, 2020. WHO Coronavirus Disease (COVID-19) Dashboard [WWW Document] URL
51. Wölfel, Roman et al. 2020. "Virological Assessment of Hospitalized Patients with COVID-2019." Nature 581(May):465.
52. Wurtzer, S. et al. 2020. "Evaluation of Lockdown Effect on SARS-CoV-2 Dynamics through Viral Genome Quantification in Waste Water, Greater Paris, France, 5 March to 23 April 2020." Euro Surveillance 25(50):2000776.
53. Xiao, Fei et al. 2020. "Evidence for Gastrointestinal Infection of SARS-CoV- 2." Gastroenterology 158:1831–33.
54. Xue, Y., Xiao, H., Zhang, Y., 2015. Antimicrobial Polymeric Materials with Quaternary Ammonium and Phosphonium Salts. Int. J. Mol. Sci 16, 3626–3655. https://doi.org/10.3390/ijms16023626
55. Zhang, Wei et al. 2020. "Molecular and Serological Investigation of 2019-NCoV Infected Patients: Implication of Multiple Shedding Routes." Emerging Microbes & Infections 9:386.
56. Zhong, C., n.d. MINI-REVIEW Applications of cellulose and chitin/chitosan derivatives and composites as antibacterial materials: current state and perspectives. https://doi.org/10.1007/s00253-018
57. Zhu, Yifan, Rong Chen, Yu-you Li, and Daisuke Sano. 2021. "Virus Removal by Membrane Bioreactors: A Review of Mechanism Investigation and Modeling Effort S." Water Research 188:116522.